

UNIVERSITA' DEGLI STUDI DI PARMA

Dottorato di ricerca in Scienze Chimiche

Ciclo XXIV

Synthesis, Characterization and Biological
Activity of Copper and Nickel
Thiosemicarbazonates

Coordinatore:

Chiar.mo Prof. G. Predieri

Tutor:

Chiar.mo Prof. P. Tarasconi

Chiar.mo Prof. G. Pelosi

Dottorando: Matteo Tavone

Contents

Chapter 1 Introduction

1.1	Thiosemicarbazones	5
1.1.2	Thiosemicarbazones as metal chelators	8
1.2	Biological targets	11
1.2.1	Ribonucleotide reductase	11
1.2.2	Topoisomerase II	12
1.2.3	Ros generators	13
1.2.4	MDR (Multidrug resistance)	14
1.3	Perspectives	16
1.4	References	18

Chapter 2 Relationship between structure and biological activity of variously functionalized thiosemicarbazones and their copper(II) and nickel(II) metal complexes

2.1	Introduction	20
2.2	Ligands	22
2.2.1	Partition coefficient (P)	24
2.3	Complexes	25
2.4	Biological assays	25
2.4.1	Cell growth inhibition of ligands and complexes	27
2.5	Conclusions	33
2.6	Experimental	34
2.6.1	Synthesis of the ligands	35
2.6.2	Synthesis of the complexes	54

2.7	References	65
-----	------------	----

Chapter 3 Theoretical studies, synthesis and biological evaluation of glycosylated thiosemicarbazones

3.1	Ribonucleotide reductase	66
3.1.1	Allosteric regulation	67
3.1.2	Docking	68
3.2	Synthesis of glycosylated thiosemicarbazones	71
3.3	Biological assays	73
3.4	Conclusions	73
3.5	Experimental	75
3.5.1	Ligands synthesis	75
3.5.2	Complex synthesis	87
3.6	References	88

Chapter 4 Thiosemicarbazones as inhibitors of topoisomerase II α

4.1	Topoisomerase II α	89
4.1.1	Topoisomerase inhibition	90
4.2	Thiosemicarbazones and topoisomerase II α	92
4.3	Project description	96
4.3.1	Ligands and complexes	97
4.4	Proliferation inhibition assay	99
4.4.1	Cell growth inhibition of ligands and complexes	100
4.4.2	Quinolines derivatives	101
4.4.3	Quinoline metal complexes	101
4.4.4	Fluoro isatin	101

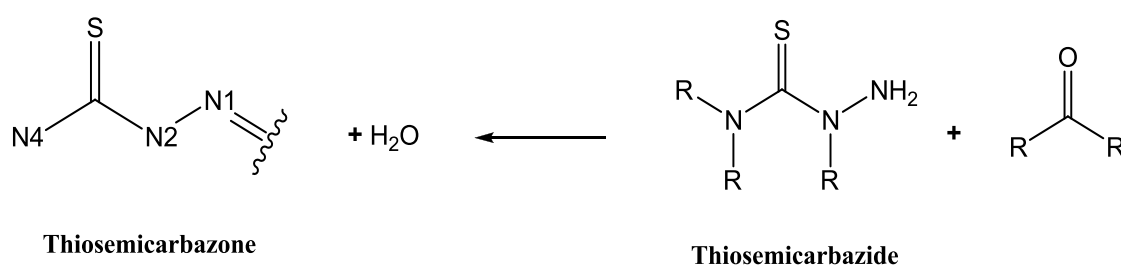
4.4.5	Sodium isatin-5-sulfonate	102
4.5	Topoisomerase II α inhibition assays	103
4.5.1	Ligands and metal complexes topoisomerase II α inhibition	103
4.5.2	Quinoline	105
4.5.3	Isatin	105
4.6	Conclusions	105
4.7	Experimental	107
4.7.1	Syntheses of the quinoline-based ligands	107
4.7.2	Syntheses of the quinoline-based complexes	116
4.7.3	Syntheses of the isatin-based ligands	129
4.7.4	Syntheses of the isatin-based complexes	136
4.8	References	141

Chapter 1

Introduction

1.1 Thiosemicarbazones

Thiosemicarbazones form an important class of organic compounds thanks to their structural, chemical and biological activities. Thiosemicarbazone derivatives are formally obtained by condensation of the terminal N of the hydrazine group of a thiosemicarbazide with a carbonyl group of a ketone or an aldehyde of aliphatic or aromatic nature (Fig. 1.1).



R = H, Alkyl, Aryl

Figure 1.1 - Synthesis of a generic thiosemicarbazone

The starting thiosemicarbazides can be prepared by a series of synthetic procedures (Fig. 1.2) such as, for instance, the reaction of amines with carbon disulphide or thiophosgene followed of the addition of hydrazine or the reaction of hydrazine with isothiocyanates¹.

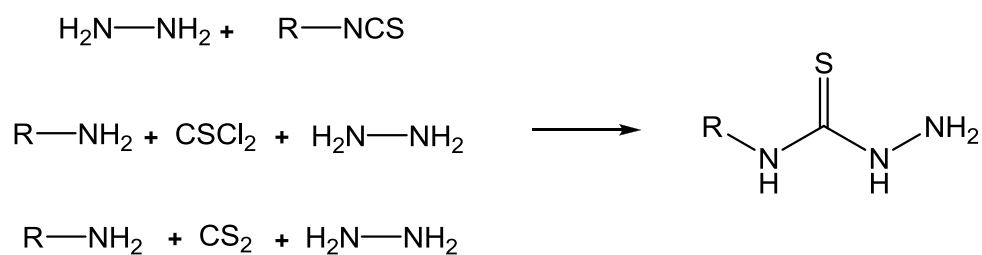


Figure 1.2 – Thiosemicarbazide synthesis

Thiosemicarbazones chemical interest dates back to the beginning of the 20th century but the first reports on their medical applications began to appear in the Fifties as drugs against tuberculosis and leprosy.

In 1946 Domagk reported the antitubercular activity *in vitro* of some thiosemicarbazones derived from cyclic ketones and aldehydes². Subsequently other tests against tuberculosis were done by Hoggart *et al.*³ using different kind of thiosemicarbazones (aliphatic and aromatic) variously substituted at N2 and N4. Tests on acute *Mycobacterium tuberculosis* in mice revealed that thiosemicarbazones obtained from aromatic aldehydes possessed marked activity. In this screening the highest activity was associated to a *para* substituent in the aromatic ring. The antileukemic effect of 2-formylpyridine thiosemicarbazone was first reported Brockman *et al.* during the Fifties³ while during the Sixties a new thiosemicarbazone was developed and commercialized, Marboran[®] (Methisazone, N-methylisatin-8-thiosemicarbazone) (Fig. 1.3). Marboran[®] was therefore used to treat smallpox thanks to its ability to inhibit the mRNA and protein synthesis especially in pox viruses² and herpes simplex virus (HSV)⁴.

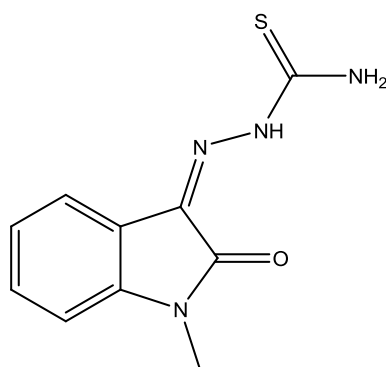


Figure 1.3 – Marboran® (Methisazone)

More recently its N4-diethyl and N4-allyl derivatives were discovered to have a significant and selective inhibition activity on structural protein synthesis in human immunodeficiency virus (HIV) infected cells⁵.

After the discovery of antitumor properties of pyridine-2-carboxyaldehyde thiosemicarbazone a large number of different ring systems (benzene, thiophene, furan, etc) have been synthesized and evaluated for antineoplastic activity. Interestingly the most active compounds revealed to be six membered heterocyclic rings carrying the thiosemicarbazone side-chain in α position to the heterocyclic nitrogen while compounds bearing the side chain in β or γ position to the ring nitrogen resulted to be inactive^{1,6}. Despite the activity of these compounds their poor solubility played a central role in the discovery of one of the most promising drugs in cancer therapy, Triapine® (Fig.1.4).

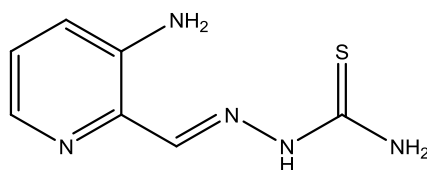


Figure 1.4 - 3-aminopyridine-2-carboxaldehyde thiosemicarbazone
(Triapine[®], Vion Pharmaceuticals)

Triapine[®] or 3-AP has been developed by Alan Sartorelli (Yale University School of Medicine) during attempts to study and to optimize isoquinoline and pyridine thiosemicarbazones solubility using as functional groups hydrophilic groups⁷. An amino group resulted to be the best option for both the heterocyclic systems. The best positions to be substituted were 5 for isoquinoline and 3 and 5 for pyridine. In particular the 3-aminopyridine-2-carboxaldehyde thiosemicarbazone (Triapine[®]) derivative appeared to be the most promising. This compound is currently used in Phase II clinical trials (Vion Pharmaceuticals)^{8,9}.

1.1.2 Thiosemicarbazones as metal chelators

Focusing on the structural characteristics, thiosemicarbazones are characterized by a N,S set of donor atoms (Fig. 1.5) which render them good metal chelating agents.

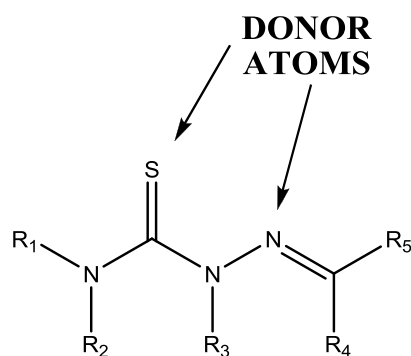


Figure 1.5 – Donor atoms of thiosemicarbazones

The coordination chemistry of thiosemicarbazones appears to be very interesting because of their versatility in coordinating metal ions and their ability to stabilize various oxidation states of metals thanks to their donor atoms^{1,10}. Also the biological activity of the organic molecules has often been ascribed to their ability to chelate endogenous metals to form metal complexes which are the active species.

In solution thiosemicarbazones exist in two tautomeric forms thione and thiol (Fig.1.6) and this has a remarkable effect on their chemical properties¹.

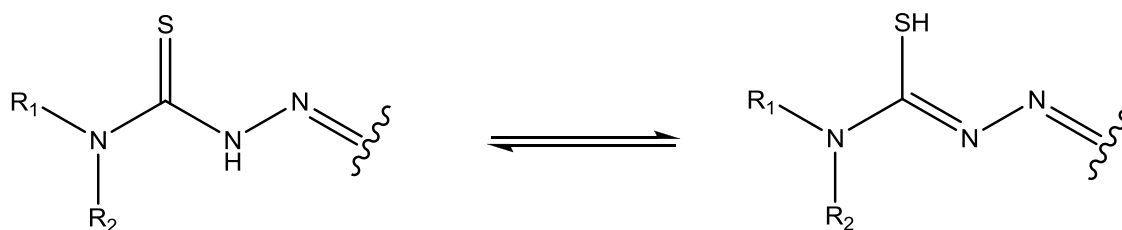


Figure 1.6 – Thione-thiol equilibrium

In the solid state, most of the thiosemicarbazones adopt a *trans* configuration in which the sulphur atom is in *trans* position to the azomethine nitrogen atom, this conformation could be adopted to favor the formation of intramolecular hydrogen bonding between N4 and N1¹.

However in most of the thiosemicarbazonic complexes the ligand binds the metal adopting a *cis* configuration. Denticity of thiosemicarbazone can also be increased if the starting aldehyde or ketone possesses a functional group in a position suitable for chelation (Fig.1.7). When the thiosemicarbazone side chain is attached in α position to a α -N-heterocyclic ring, thiosemicarbazones have shown substantial *in vitro* activity against various human tumour lines⁶.

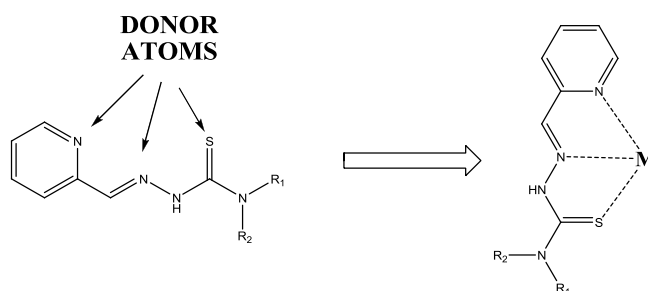


Figure 1.7 – Tridentate heterocyclic ligand

The presence of a conjugate NNS donor set favors the coordination to metal ions. Regarding the role of a metal ion, it almost systematically increases the activity or contributes to mitigate the side effects of the organic parent compounds¹¹. The reported effects related to their anticancer activity are ribonucleotide reductase (RR) inhibition, reactive oxygen species (ROS) production, topoisomerase II inhibition, mitochondria disruption and, more recently, a multidrug resistance protein (MDR1) inhibition¹¹.

1.2 Biological targets

1.2.1 Ribonucleotide Reductase

During the Sixties French *et al.*¹² formulated the hypothesis of the tridentate nature of α -N-heterocyclic thiosemicarbazones giving an insight into the mode of action of this class of compounds. Thanks to the NNS chelating system they can bind metals with high formation constants. Based on this hypothesis Sartorelli *et al.*^{11,13} proposed as target of these compounds the enzyme ribonucleotide reductase after having observed that these molecules blocked the incorporation of ³H thymidine into DNA. Ribonucleotide reductase (RR) is an iron dependent enzyme which converts ribonucleotides to 2-deoxyribonucleotides through a mechanism generated by a tyrosyl radical.

Thelander¹⁴ observed that 1-formylisoquinoline thiosemicarbazone inhibits the enzyme by destroying the free radical. The mode of action of the quinoline derivative has been ascribed to the chelation of the iron contained in the enzyme and/or its possible activation of molecular oxygen in a redox process causing the destruction of the tyrosyl radical.

Recently Kowol *et al.*¹⁵ studied iron(III) and gallium(III) complexes of Triapine[®] and its related compounds with unsubstituted or dimethylated N4. Cytotoxicity assays were performed on two human cancer cell lines (41M and SK-BR-3). Complexation of Triapine[®] and related ligands resulted in increased cytotoxicity of gallium(III) complexes while iron(III) derivatives showed reduced activity. On the contrary terminal nitrogen dimethylation was found to enhance the cytotoxicity of both metal complexes

and free ligands, unless a NH₂ functionality was present anywhere at the thiosemicarbazone backbone.

Tests on ³H-Cytidine DNA incorporation were performed on ribonucleotide reductase with Triapine[®], with dimethyl thiosemicarbazone of formyl pyridine and their iron(III) to study an hypothetical relationship between growth and ribonucleotide reductase inhibition. Results showed that the toxicity on cells due to the dimethylated compounds was only partly dependent on the ribonucleotide reductase inhibition, thus implying that other mechanisms are involved.

1.2.2 Topoisomerase II

Topoisomerase-II is a family of enzymes which disentangle double stranded DNA introducing transient breaks¹⁶. Exploiting the fact that one of the mechanisms of action of naphthoquinone with anticancer properties is the stabilization of the cleavable complex formed between topoisomerase-II and DNA, Chen *et al.*¹⁷ synthesized 1,2-naphthoquinone-2-thiosemicarbazone (Fig.1.8) and its metal complexes of copper(II), nickel(II) and palladium(II).

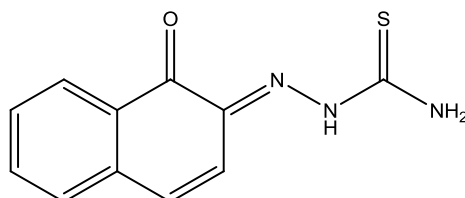


Figure 1.8 - 1,2-naphthoquinone-2-thiosemicarbazone

These compounds were tested on MCF-7 cells of human breast cancer and compared with 1,2-naphthoquinone and etoposide, an anti-cancer agent known to inhibit topoisomerase-II.

A comparison of cytotoxic activity of the compounds with 1,2-naphthoquinone showed a marked activity of the ligand and of its nickel and copper complexes while the palladium derivative had little effect. It is worth of note that the nickel complex is even more active than etoposide.

Studies on topoisomerase-II to elucidate the mechanism of action of these compounds revealed that the metal complexes stabilize the cleavable complex between DNA and enzyme. Data also indicate that the three metal complexes antagonize the enzyme action on DNA because relaxed DNA formation is completely inhibited.

1.2.3 Ros generators

ROS (Reactive Oxygen Species), highly reactive molecules containing unpaired electrons, are the by-product of oxygen metabolism. Recently Hancock *et al.*¹⁸ evaluated if the copper complex of NSC 689534 (Fig. 1.9) a derivative of formyl pyridine, could act as a ROS generator.

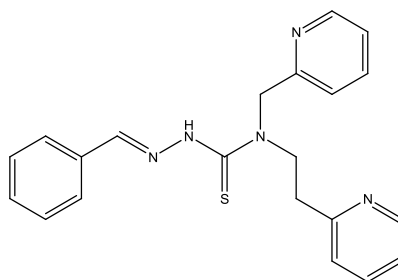


Figure 1.9 – NSC 689534

This complex induces apoptosis in HL60 cells and causes a G₂M block followed by necrosis in PC3 cells. Further tests revealed that these effects were caused as a direct consequence of ROS increase in a process which induces endoplasmic reticulum stress. To study the involvement of ROS, administration of the NSC-689534 copper complex in presence of different antioxidants, as N-acetyl-cysteine, ascorbate, diethylcarbamate (Cu/Zn superoxide dismutase inhibitor) or the antioxidant enzyme catalase, resulted in attenuated cytotoxic activity. As ROS can induce oxidative cleavages in DNA, Gomez-Saiz¹⁹ studied the nuclease activity of formyl pyridine thiosemicarbazones. Electrophoresis of supercoiled DNA pUC18 exposed to the two metal complexes, in the presence of 1-mercaptopropionic acid (a reducing agent), was used to test their nuclease activity. Both complexes produce strand breaks. The use of radical scavengers, like DMSO, tert-butyl alcohol, sodium formate and potassium iodide, as control, inhibit the DNA cleavage suggesting that these compounds act as hydroxyl radical generator.

1.2.4 MDR (Multidrug resistance)

Multidrug resistance is a condition by which many cancers develop resistance to chemotherapy drugs²⁰. This phenomenon is associated with a decrease of drug accumulation caused by the overexpression of ATP-binding cassette (ABC) transporter proteins, such as MDR-associated proteins (MRP), P-glycoprotein (P-gp) ABCB1 and ABCG2²¹. These proteins are transmembrane proteins which bind ATP to transport various molecules (ions, bile acids, organic anions) across biological membranes^{22,23}. These proteins protect also organism from accumulation of toxic compounds conferring

cytotoxic resistance, in addition they play an important role in determining absorption, distribution, and excretion of many different pharmacologic compounds by the body²⁴. Ludwig *et al.*²⁶ identified a small thiosemicarbazone (NSC73306) (Fig.1.10) as a compound that exploits, rather than suppressing, P-gp function to induce cytotoxicity.

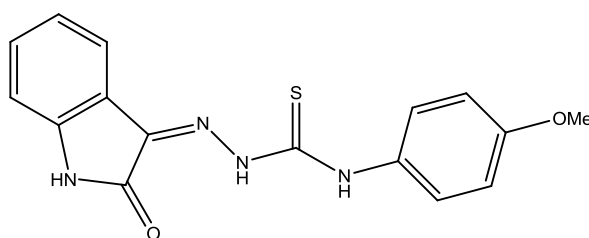


Figure 1.10 - NSC73306

NSC73306 was tested on four KB epidermoid carcinoma cell lines expressing increasing levels of P-gp. Results showed that the toxicity of NSC73306 is directly proportional to the levels of functional P-gp while no growth inhibition was observed in P-gp-negative cells when used at concentrations effective in P-gp-positive cells. It was also observed that a three-week exposure to NSC73306 caused a decrease of P-gp expression rendering cells sensitive to P-gp substrates against which they had previously shown resistance. This mechanism was further explained by Wu *et al.*²³. As the presence of MRPs and ABCG2 is well documented in literature they investigated the interaction of NSC73306 with ABCG2, MRP1, MRP4 and MRP5. No particular cytotoxicity was observed in cells expressing these proteins compared with their respective parental cells but selectivity towards ABCG2 expressing cells was observed.

NSC73306 not only resulted possessing selectivity for the substrate-binding site of ABCG2 but it is also transported by it.

Interaction between NSC73306 and ABCG2 was confirmed by an ATPase assay.

In addition, NSC73306 at non toxic concentration (0.5 $\mu\text{mol/L}$) is able to resensitize ABCG2 expressing cells to topotecan and mitoxantrone, two antineoplastic agents.

1.3 Perspectives

As can be seen from the above paragraphs the way these molecules work is still greatly unknown since the amount of information we have is spread over a limited variety of compounds and a wide range of cell lines. The same compound inhibits proliferation of a particular tumor but leaves other totally unaffected. Recently, a thiosemicarbazone with an aliphatic long chain (citronellal), instead of the usual aromatic moiety that was held for necessary for the thiosemicarbazone to be active, has been tested on leukemia cell line U937 and revealed an activity of the same order of magnitude of many of those compounds previously published in the literature and this opens new perspectives in this research.

In my doctoral work I followed three main research addresses that were carried out in parallel:

1. A study of the relationship between structure and biological activity of variously functionalized thiosemicarbazones and their copper(II) and nickel(II) metal complexes,
2. Theoretical studies, synthesis and biological evaluation of glycosylated thiosemicarbazones,

3. Quinoline and isatin thiosemicarbazone metal complexes as inhibitors of topoisomerase II α .

1.4 References

- 1) Matesanz A.I, Souza P, *Mini-Review in Medicinal Chemistry*, **2009**, 9(12), 1389-1396
- 2) Domagk, G.; Behnisch, R.; Mietzch, F.; Schmidt, H. *Naturwissenschaften*, **1946**, 33, 315.
- 3) Beraldo H, Gambino D, *Mini-Reviews in Medicinal Chemistry*, **2004**, 4(1), 31-39.
- 4) Shipman C, Smith S.H, Drach J.C, Klayman D.L, *Antiviral Research*, **1986**, 6, 197-222.
- 5) Teitz Y, Ronen D, Vansover A, Stematsky T, Riggs J.L, *Antiviral Research*, **1994**, 24, 305-314.
- 6) West D. X, Padhye B.S, Sonawane P. B, *Structure & Bonding*, **1991**, 76, 1-50.
- 7) Liu M, Lin T, Sartorelli A.C, *Prog. Med. Chem.*, **1995**, 32, 1-35.
- 8) Traynor A.M, Ju-Whei Lee, Bayer G.K, Tate J.M, Thomas S.T, Mazurczak M, Graham D.L, Kolesar J.M, and Schiller J.H, *Investigational New Drugs*, **2008**, 28(1), 91-97
- 9) Nutting C.M, van Herpen C.M.L, Miah A.B, Bhide S. A, Machiels J.P, Buter J, Kelly C, de Raucourt D. and Harrington K.J, *Annals of Oncology*, **2009**, 20(7), 1275-1279.
- 10) Pandeya SN, Dimmock JR, *Die Pharmazie*, **1993**, 48(9), 659-666
- 11) G. Pelosi, *The Open Crystallography Journal*, **2010**, 3, 16-28
- 12) French F.A, Blanz E.J.J, *Cancer Res*, **1965**, 25, 1454-8
- 13) Sartorelli A.C, Agrawal K.C, Moore B.C, *Biochem. Pharm*, **1997**, 20, 3119-3123
- 14) Thelander L, Graslund A, *J. Biol. Chem*, **1983**, 258, 4063-4066

- 15) Kowol C.R, Trondl R, Heffeter P, Arion V.B, Jakupec M.A, Roller A, *J Med. Chem*, **2009**, 52, 5023-5043
- 16) Nitiss J., *Nature Reviews Cancer*, |**2009**, 9, 327-337
- 17) Junnan Chen, Yue-wern Huang, Guanshu Liu, Zahra Afrasiabi, Ekkehard Sinn, Subhash Padhye, Yinfa Ma, *Toxicology and Applied Pharmacology*, **2004**, 197, 40–48
- 18) Hancock , *Free Radical Biology & Medicine*, **2011**, 50, 110-121
- 19) Gòmez-Saiz P, Gil-García R, Maestro M.A, Pizarro J.L, Arriortua M.I, Lezama L *et al. J. Inorg. Biochem*, **2008**,102, 1910-1920
- 20) Persidis A, *Nature Biotechnology*, **1999**, 17, 94-95
- 21) Leslie E, *Toxicology and Applied Pharmacology* **2005**, 204, 216– 237
- 22) Leslie E.M, Deeley R.G, Cole S.PC, *Toxicology and Applied Pharmacology*, **2005**, 204, 216-237
- 23) Dean M, *The Human ATP-Binding Cassette (ABC) Transporter Superfamily*, NCBI, November 18, **2002**.
- 24) Gottesman M.M, Ambudkar S.V, *Journal of Bioenergetics and Biomembranes*, **2001**, 33(6), 453-458
- 25) Ludwig J.A, Szakacs G, Martin S.E, Chu B.F, Cardarelli C, Sauna Z.E, Caplen N.J, Fales M. H, Ambudkar S.V, Weinstein J.N, Gottesman M.M, *Cancer Res*, **2006**, 66(9), 4808–4815.
- 26) Wu Chung-Pu, Shukla S, Calcagno A.M, Hall M.D, Gottesman M.M, Ambudkar S.V, *Mol. Cancer Ther.* **2007**,6(12), 3287-3296

Chapter 2

Relationship between structure and biological activity of variously functionalized thiosemicarbazones and their copper(II) and nickel(II) metal complexes.

2.1 Introduction

Given the overwhelming but disorganized amount of information found in the literature I have decided to start from scratch and to plan a series of molecules with a common thiosemicarbazone core but possessing different characteristics. The parameters I chose for my research are: the influence of the aromatic/aliphatic nature of the aldehyde/ketone from which the thiosemicarbazone is synthesized, the overall hydrophobicity/hydrophilicity of the thiosemicarbazone modulated by adding on the terminal amino group hydrophilic fragments and the role of divalent metal ions of the first transition row (in particular copper(II) and nickel(II) for reasons explained below) and, as a starting point, to focus my studies on the effects on a single cell line (leukemia cell line U937). The aldehydes chosen to prepare the basic thiosemicarbazones are citronellal, vanillin and pyridoxal (Fig. 2.1).

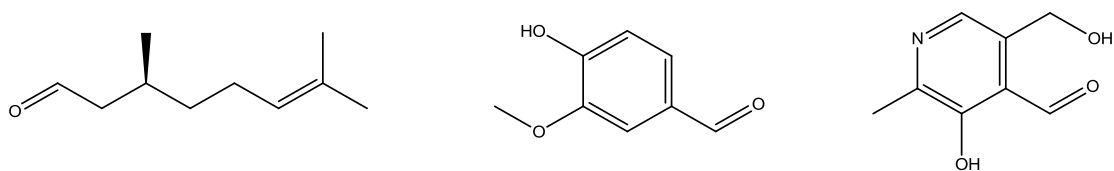


Figure 2.1 – S-citronellal, vanillin and pyridoxal

The first two were chosen as representative of aliphatic and aromatic derivatives, while pyridoxal allows us to explore also the role of the chelation mode on the activity of these compounds since this thiosemicarbazone can bind as tridentate.

Since the scarce water solubility is a notorious feature which afflicts thiosemicarbazone usage in biological media^{1,2}, on the other extreme of the thiosemicarbazide fragment, on the amino nitrogen, other fragments have been added to tune the hydrophobicity/hydrophilicity of the whole molecule: N-ethylmorpholine and glucose. Glucose was chosen to give the molecule a marked hydrophilicity and also in the hope that the molecule could be possibly internalized through glucose transport proteins. This substituent, being highly polar, should also help cast light on a putative internalization mechanism that assigns to these thiosemicarbazones a role in the transport of metal ions through the cell membrane. According to this model, thiosemicarbazones would act by wrapping the metal ion with their polar heads and exposing the hydrophobic part to the exterior making these complexes prone to cross the hydrophobic lipid bilayer of the cell membrane. The presence of polar groups should prevent this mechanism. Of the first row divalent metals, copper(II) and nickel(II) have been chosen to evaluate the influence of a metal ion on the activity of the relative complexes. Zinc, cobalt and iron have been initially excluded based on previous experiences of inactivity of zinc and cobalt derivatives, due probably to their tendency to form tetrahedral and octahedral complexes, and because of the instability of iron(II) complexes. Unfortunately, due to their very limited solubility, formation constants of metal complexes with thiosemicarbazones are rarely found in the literature and the values reported are rather unreliable³⁻⁵ and copper(II) and nickel(II), according to the Irving Williams series,

should also possess, given a ligand, the highest formation constants that give us a certain confidence that the complexes do not dissociate into their constituents in water. Altogether nine compounds have been synthesized and for each of them also their copper(II) and nickel(II) complexes have been used for the biological tests. Eventually it has also been decided to carry out the preliminary biological tests on proliferation inhibition using cell line U937. This cell line was chosen because it was used for citronellal thiosemicarbazone studies that were carried out previously.

2.2 Ligands

The mentioned aldehydes were condensed with three thiosemicarbazides: thiosemicarbazide, N4-ethyl-thiosemicarbazide and N4-glycosyl thiosemicarbazide (Fig. 2.2) giving a total of nine ligands (Tab. 2.1).

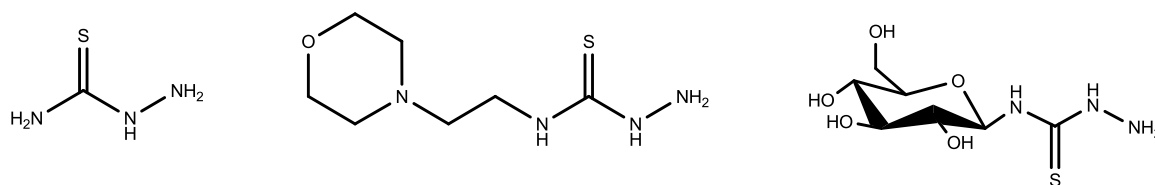


Figure 2.2

The former two were commercially available while the latter was *de novo* synthesized using D-glucose as starting reagent. Tab. 2.1 summarizes the synthesized ligands and the acronyms used from here on.

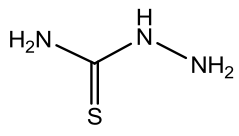
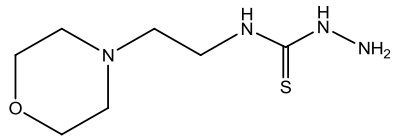
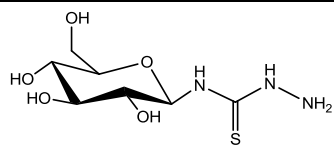
	Citronellal	Vanillin	Pyridoxal
	CitrTSC	VanTSC	PyrTSC
	CitrMor	VanMor	PyrMor
	CitrGlu	VanGlu	PyrGlu

Table 2.1

D-glucose was acetylated with pyridine and 4-dimethylaminopyridine in acetic anhydride and then halogenated with HBr 33% in dichloromethane under nitrogen atmosphere to obtain α -acetobromo-D-glucose (Fig. 2.3).

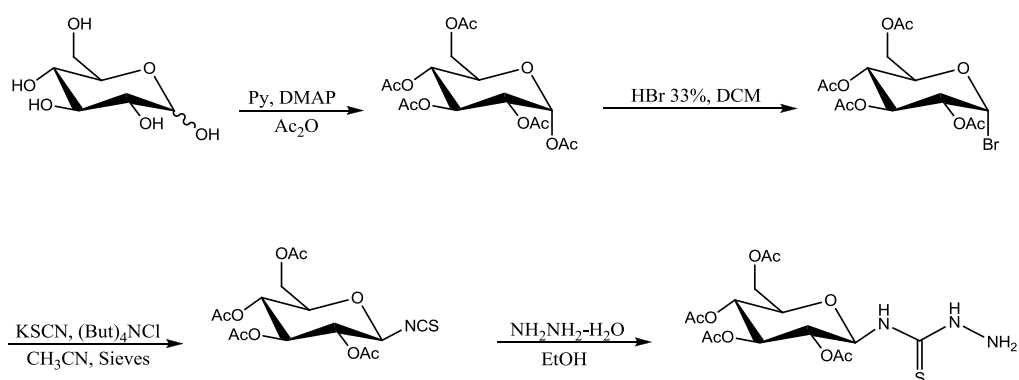


Figure 2.3 – Synthesis of acetylated glucosyl thiosemicarbazide

In the presence of potassium thiocyanate and tetrabutyl ammonium chloride, following a S_N2 mechanism, bromide was substituted with a isothiocyanate group⁶ giving the precursor of the thiosemicarbazide and its structure was determined by X-ray analysis (see experimental section).

Glucosyl thiosemicarbazide was obtained as a white solid by dropping a solution of glucosyl isothiocyanate in ethanol into a cooled solution of hydrated hydrazine in ethanol⁷.

All the condensation reactions between the functionalized thiosemicarbazide and the selected aldehydes to obtain thiosemicarbazones were carried out refluxing for several hours the reagents in ethanol. Acetylated glucosyl thiosemicarbazones were then deprotected following the Zemplen procedure (MeONa/MeOH dry).

2.2.1 Partition coefficient (P)

Octanol/water partition coefficient (P) is the ratio between the concentration of a compound in octanol and its concentration in water ($P = \frac{[\text{analyte}]_{\text{Octanol}}}{[\text{analyte}]_{\text{Water}}}$).

Partition coefficient is very used in pharmaceutical sciences to evaluate the distribution of a molecule in the two phases of a mixture of two immiscible solvents at equilibrium.

Hence the partition coefficient is a measure of how hydrophilic or hydrophobic a chemical substance is. In medical practice, partition coefficients are useful for example in estimating distribution of drugs within the body.

Drugs with partition coefficients > 2 are preferentially distributed to hydrophobic compartments such as lipid bilayers of cells while drugs with partition coefficients < 1.5 preferentially are found in hydrophilic compartments such as blood serum.

	logP		logP		logP
CitrTSC	3.3	CitrMor	3.2	CitrGlu	1.5
PyrTSC	1.2	PyrMor	1.2	PyrGlu	-0.5
VanTSC	0.2	VanMor	0.2	VanGlu	-1.4

Table 2.2 – Comparison between polarity (logP) of new thiosemicarbazones

LogPs were calculated with ALOGPS 2.1 software⁸. The values reported in Tab. 2.2 show that the ligands synthesized for the assays possess a wide variety of values that extend from 3.3 (maximum hydrophobicity) to -1.4 (minimum hydrophobicity).

2.3 Complexes

Copper(II) and nickel(II) complexes were obtained by refluxing an ethanol solution of the parent thiosemicarbazone to which the inorganic salts were added and the reaction products were separated by filtration. A few compounds were obtained in crystalline form by slow evaporation of the reaction solvent. The complexes were characterized by elemental analysis, ES-MS, X-ray diffraction.

2.4 Biological assays

U937 cells were grown until a concentration of 20×10^4 /mL was reached. Thiosemicarbazones and their metal complexes were then administered at different

concentrations (1 up to 100 μM) to establish the maximum concentration necessary to inhibit, after 24 h, cellular proliferation by 50%.

To evaluate inhibition, a colorimetric assay (XTT) was performed using ProCheck™ cell viability assay (Itergen). This technique is based on the spectrophotometric revelation of the cellular reduction of a tetrazole (2,3-bis-(2-methoxy-4-nitro-5-sulfophenyl)-2H-tetrazolium-5-carboxanilide) to a formazan (Fig. 2.4).

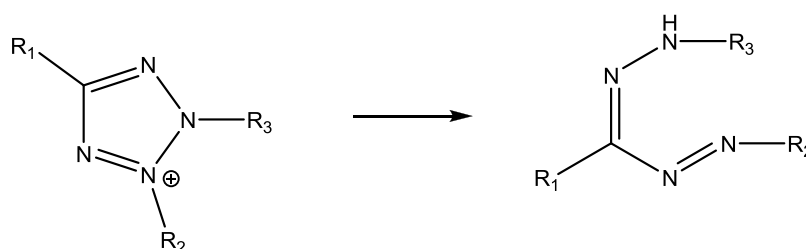


Figure 2.4 – Reduction of tetrazole to formazan

After treatment with the compounds, cells were distributed in a volume of 100 μL in a microtiter plate with 96 plates, then 20 μL of reagent cell viability ProCheck™ were added to a final volume of 120 μL . After 1 – 4 hours of incubation optical density was measured with ELX800 (Packard) spectrophotometer, in this way information about cell vitality are gained and it is possible to determine the maximum concentration necessary to inhibit cellular proliferation by 50% (IC_{50}). Once determined the IC_{50} value further experiments were carried out to determine cellular vitality after an incubation of 24h using Trypan blue to colour dead cells and a hemocytometer to count cells.

2.4.1 Cell growth inhibition of ligands and complexes

All the ligands have shown no significant antiproliferative activity on cell line U937, at least up to 100 μM , with the exception of CitrGlu that shows a 40% inhibition at 100 μM . Differently from the ligands, most of their metal complexes possess remarkable activity. From Tab. 2.3 it is apparent that copper derivatives are more active than those of nickel but while the non substituted thiosemicarbazones present activities of the same order of magnitude we observe remarkably low GI_{50} values for the ethylmorpholine copper derivatives. The most striking difference is observable between the copper glucosylated thiosemicarbazones for which the GI_{50} values pass from a 18 μM for the citronellal derivative to a >50 μM for the vanillin and the pyridoxal thiosemicarbazone derivatives.

	Complexes	GI_{50} (μM)	Complex	GI_{50} (μM)	Complex	GI_{50} (μM)
Tsc	$\text{Cu}(\text{CitrTSC})_2$	14.7	$\text{Cu}(\text{VanTSC})_2$	17	$\text{Cu}(\text{PyrTSC})\text{Cl}_2$	14.4
	$\text{Ni}(\text{CitrTSC})_2$	10	$\text{Ni}(\text{VanTSC})_2$	40	$\text{Ni}(\text{PyrTSC})\text{Cl}_2$	-
Mor	$\text{Cu}(\text{CitrMor})_2$	6.3	$\text{Cu}(\text{VanMor})_2$	9	$\text{Cu}(\text{PyrMor})\text{Cl}_2$	-
	$\text{Ni}(\text{CitrMor})_2$	7.8	$\text{Ni}(\text{VanMor})_2$	19.5	$\text{Ni}(\text{PyrMor})\text{Cl}_2$	-
Glu	$\text{Cu}(\text{CitrGlu})_2$	18	$\text{Cu}(\text{VanGlu})_2$	>50	$\text{Cu}(\text{PyrGlu})\text{Cl}_2$	83
	$\text{Ni}(\text{CitrGlu})_2$	44	$\text{Ni}(\text{VanGlu})_2$	>50	$\text{Ni}(\text{PyrGlu})\text{Cl}_2$	>100

Table 2.3 - GI_{50} of Cu and Ni of citronellal, vanillin and pyridoxal thiosemicarbazones

Besides testing the antiproliferative activity on cell lines U937 (histiocytic lymphoma) it has also been possible to extend the biological assays to cell line HT-29 (colon carcinoma). As an antiproliferative reference substance has been used cis-platin.

According to the NCI (National Cancer Institute) approach for the “60 human tumor cell line anticancer drug screen” (NCI60), growth inhibiting concentrations at 50% (GI_{50} , 50 % Growth Inhibition), growth inhibiting at 100% (TGI, Total Growth Inhibition) and lethal at 50% of the cells (LC_{50} , 50 % Lethal Concentration) have been determined. Evaluation has been carried out on a wide range of concentrations (0.5 ÷ 50 μ M).

All citronellal and vanillin ligands present no antiproliferative activity up to a concentration of 50 μ M. From the reported tables (Tab.2.4 and Tab.2.5) it is apparent that this activity is strongly influenced by metal complexation.

In particular, compounds with $GI_{50} < 20 \mu$ M on cell line U937 are nickel (II) complexes of CitrTSC, CitrMor, VanMor ($Ni(CitrTSC)_2$, $Ni(CitrMor)_2$, $Ni(VanMor)_2$) and copper(II) complexes of CitrTSC, CitrGlu, CitrMor, VanTSC and VanMor ($Cu(CitrTSC)_2$, $Cu(CitrGlu)_2$, $Cu(CitrMor)_2$, $Cu(VanTSC)_2$, $Cu(VanMor)_2$). Among them the only complexes of Cu (II) having a $GI_{50} < 20 \mu$ M on cell line HT29 are $Cu(CitrTSC)_2$ and $Cu(CitrMor)_2$. The glycosylation of the ligand seems to reduce the antiproliferative activity.

U937			
Compound	GI₅₀ (μM)	TGI (μM)	LC₅₀ (μM)
CitrTSC	>50	> 50	> 50
Ni(CitrTSC)₂	10	50	> 50
Cu(CitrTSC)₂	14,7	> 50	> 50
CitrGlu	>50	> 50	> 50
Ni(CitrGlu)₂	44	> 50	> 50
Cu(CitrGlu)₂	18	38	> 50
CitrMor	>50	> 50	> 50
Ni(CitrMor)₂	7,8	20	39,5
Cu(CitrMor)₂	6,3	8,2	10
VanTSC	> 50	> 50	> 50
Ni(VanTSC)₂	40	> 50	> 50
Cu(VanTSC)₂	17	40,5	> 50
VanGlu	> 50	> 50	> 50
Ni(VanGlu)₂	> 50	> 50	> 50
Cu(VanGlu)₂	> 50	> 50	> 50
VanMor	> 50	> 50	> 50
Ni(VanMor)₂	19,5	50	> 50
Cu(VanMor)₂	9	35	> 50

Table 2.4 – Ligand and complex concentrations inhibiting growth at 50% (GI₅₀, 50 % Growth Inhibition), growth at 100% (TGI, Total Growth Inhibition) and lethal at 50% (LC₅₀, 50 % Lethal Concentration) for cell line U937 (histiocytic lymphoma).

HT-29			
Compound	GI50 (μM)	TGI (μM)	LC50 (μM)
CitrTSC	>50	> 50	> 50
Ni(CitrTSC)₂	47	> 50	> 50
Cu(CitrTSC)₂	10	24,5	40,5
CitrGlu	>50	> 50	> 50
Ni(CitrGlu)₂	>50	> 50	> 50
Cu(CitrGlu)₂	>50	> 50	> 50
CitrMor	>50	> 50	> 50
Ni(CitrMor)₂	>50	> 50	> 50
Cu(CitrMor)₂	7,5	20,5	37
VanTSC	>50	> 50	> 50
Ni(VanTSC)₂	>50	> 50	> 50
Cu(VanTSC)₂	>50	> 50	> 50
VanGlu	>50	> 50	> 50
Ni(VanGlu)₂	>50	> 50	> 50
Cu(VanGlu)₂	>50	> 50	> 50
VanMor	>50	> 50	> 50
Ni(VanMor)₂	>50	> 50	> 50
Cu(VanMor)₂	34	> 50	> 50

Table 2.5 – Ligand and complex concentrations inhibiting growth at 50% (GI₅₀, 50 % Growth Inhibition), growth at 100% (TGI, Total Growth Inhibition) and lethal at 50% (LC₅₀, 50 % Lethal Concentration) for cell line HT29 (colon carcinoma).

Histosensibility has been tested for two of the molecules that from a first screening resulted to be the most active: complex $\text{Ni}(\text{CitrTSC})_2$ and complex $\text{Cu}(\text{CitrMor})_2$.

Cells deriving from hematological and CNS (central nervous system) tumors seem to be more sensitive to the nickel complex. These cells present a GI_{50} generally lower than $10\mu\text{M}$. In particular this complex induces a strong cytotoxic affect (LC_{50}) at concentrations lower than $50\mu\text{M}$ only on U266 lines (multiple myeloma), SH-SY5Y and SK-N-MC (CNS). The most resistant lines ($\text{IG}_{50} > 40\mu\text{M}$) are from colon (HT-29), prostate (PC-3), skin (A-375) and connective tissue (HT-1080) (Fig. 2.6).

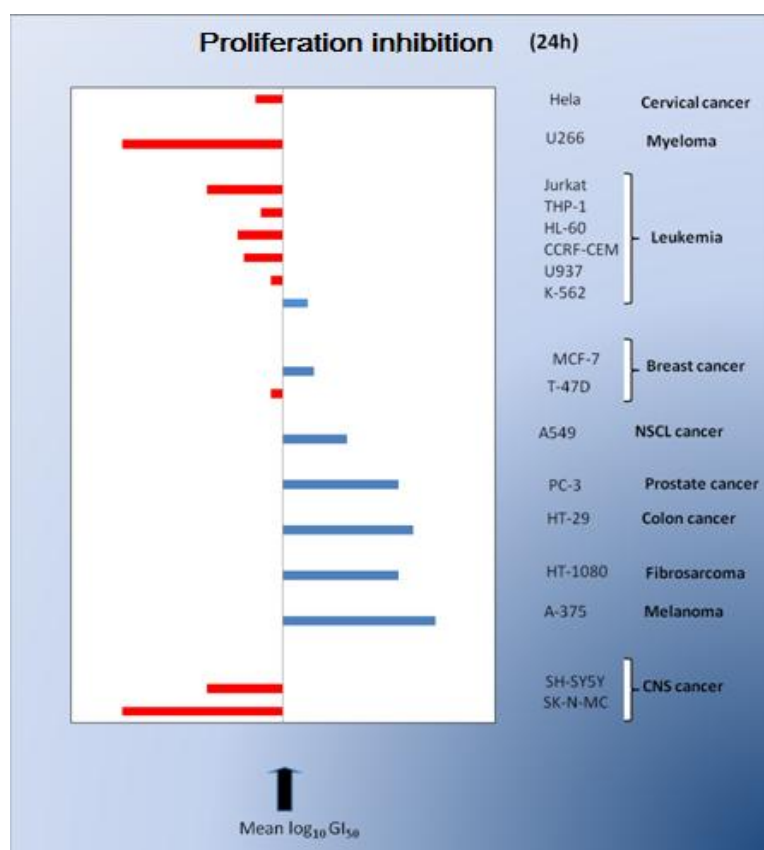


Figure 2.6 – Histosensitivity to complex $\text{Ni}(\text{CitrTSC})_2$ of the analyzed cell lines. In red are represented the most sensitive lines, in blue the less sensitive.

All tested cell lines have shown a mild sensitivity to complex $\text{Cu}(\text{CitrMor})_2$ with a $\text{GI}_{50} < 10 \mu\text{M}$, a strong cytotoxic effect (LC_{50}) at concentrations lower than $10 \mu\text{M}$ has been observed on cell lines U937 and Jurkat. Cell lines HeLa (cervix cancer); Jurkat (leukemia) and SK-N-MC (CNS) (Fig. 2.7).

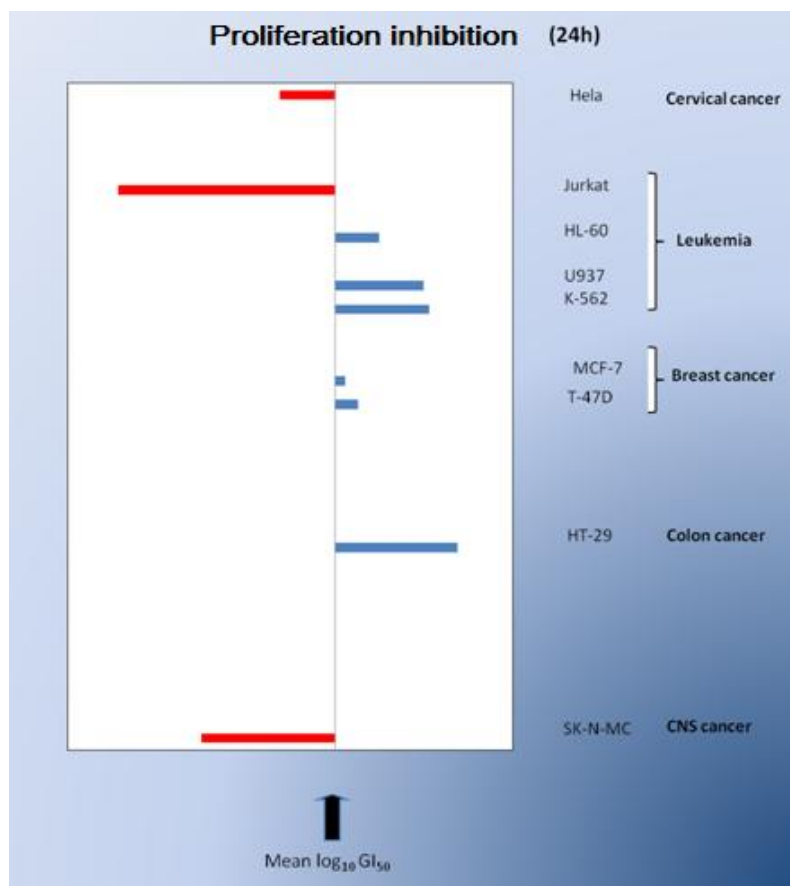


Figure 2.7 – Histosensitivity to complex $\text{Cu}(\text{CitrMor})_2$ of the analyzed cell lines. In red the more sensitive lines, in blue the less sensitive.

2.5 Conclusions

New thiosemicarbazones were synthesized with the aim to study how substituent groups in position N4 and coordination to copper(II) and nickel(II) influence their biological activity. The free ligands do not show significant biological activity independently from the presence of a substituent on N4. On the contrary, metal complexes show marked biological activity. Copper complexes present a general higher proliferation inhibition activity. In particular the copper complexes with the morpholine derivatives present higher activities than the non-substituted and the glycosylated thiosemicarbazones. Worth of note is that morpholine ligands are those with the partition coefficient closer to the values required for an effective lipid membrane crossing and this would confer them an easier way to diffuse into the cytoplasm. Nevertheless subsequent biological studies (unpublished results) have revealed that their activity is not proportional to the concentration as it is to be expected if the limiting process were diffusion.

The activity of vanillin and citronellal thiosemicarbazones was then extended to cell line HT-29 (colon carcinoma). Also in this case citronellal and vanillin ligands present no antiproliferative activity up to a concentration of 50 μ M and also in this case the glycosylation of the ligand seems to reduce the antiproliferative activity.

Histosensibility has been tested for two of the molecules that from a first screening resulted to be the most active: Ni(CitrTSC)₂ and Cu(CitrMor)₂. Cells deriving from hematological and CNS (central nervous system) tumors seem to be more sensitive to the nickel complex. In particular this complex induces a strong cytotoxic affect (LC₅₀) at concentrations lower than 50 μ M only on U266 lines (multiple myeloma), SH-SY5Y and SK-N-MC (CNS).

All tested cell lines have shown a mild sensitivity to complex $\text{Cu}(\text{CitrMor})_2$ with a $\text{GI}_{50} < 10 \mu\text{M}$, a strong cytotoxic effect (LC_{50}) at concentrations lower than $10 \mu\text{M}$ has been observed on cell lines Hela(cervix cancer), Jurkat (leukemia) and SK-N-MC (CNS).

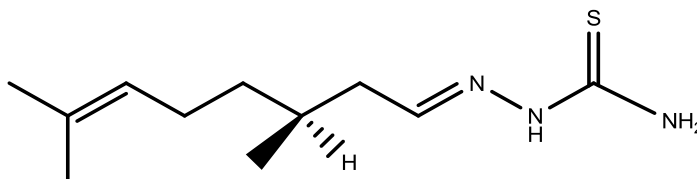
2.6 Experimental

Dry methanol were prepared according to standard procedures and stored over molecular sieves. TLC were performed on Silica gel Merck 60 F₂₅₄ aluminium sheets. Flash chromatography was performed on MP Silica 63-200 mesh 60Å (EchoChrom™), ¹H and NMR spectra were recorded on Bruker 300 Avance and Bruker 400 Avance spectrometers, at 300 K. The reported *J* values are referred to H,H coupling constants. Chemical shifts are reported as δ values in ppm using the solvent residual peak as internal standard. Elemental analysis were recorded on Flash 1112 Series Analyser (CE Instruments) Mass spectra by electrospray ionization (ESI) methods were recorded on LTQ ORBITRAP XL Thermo.

2.6.1 Synthesis of the ligands

[CitrTSC]

(S-citronellal thiosemicarbazone)



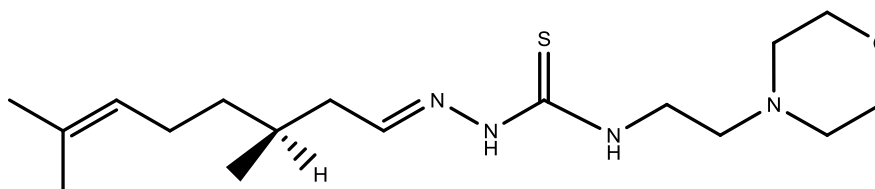
A solution of S-citronellal (0.40 mL, 2.22 mmol) and thiosemicarbazide (0.21 g, 2.22 mmol) in EtOH (10 mL) was refluxed for 60 min under stirring, the mixture was then cooled and the product was isolated as a white powder.

Yield : 95%

$^1\text{H NMR}$ (300MHz, CDCl_3): δ_{H} (ppm) 9.05 (s, 1H, *NH*), 7.27 (t, 1H, $J = 6.0$ Hz, $\text{CH}=\text{N}$), 7.08 (2br s, 1H each, *NH*), 5.04 (m, 1H, $\text{CH}=\text{C}(\text{CH}_3)_2$), 2.20 (2m, 2H, CH_2CHCH_3), 1.94 (m, 2H, $\text{CH}_2\text{CH}=\text{C}(\text{CH}_3)_2$), 1.76 (m, 1H, CH_2CHCH_3), 1.64 and 1.56 (2s, 6H, 3H each, $\text{CH}(\text{CH}_3)_2$), 1.34 (m, 1H, CH_2CHCH_3), 1.34 - 1.28 (2m, 2H, 1H each, $\text{CH}_3\text{CHCH}_2\text{CH}_2$), 0.94 (3H, d, $J = 7.0$, CHCH_3).

[CitrMor]

(S-citronellal-4-[2-(4-morpholinyl)ethyl]-3-thiosemicarbazone)



A solution of S-citronellal (0.35 mL, 1.95 mmol) in EtOH 95% (10 mL) was added to a stirred solution of N4 ethyl morpholine thiosemicarbazide (398 mg, 1.95 mmol) in EtOH 95% (10 mL).

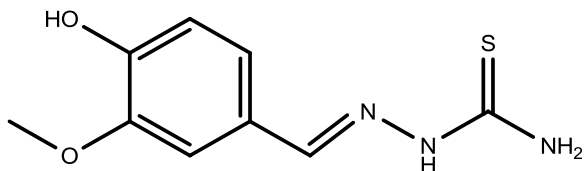
The mixture was refluxed until TLC (AcOEt/C₆H₁₂ 1:3) revealed starting material consumption.

After concentration under reduced pressure a pale yellow oil was obtained.

Yield: 96%

¹H NMR (300MHz, CDCl₃): δ_H (ppm) 8.78 (s, 1H, CH₂NHC=S), 7.88 (bs, 1H, NHN=C), 7.15 (t, 1H, CH=N), 5.04 (m, 1H, CH=C(CH₃)₂), 3.74 (2m, 4H, OCH₂CH₂N + CH₂NHCS), 2.65 (t, 2H, OCH₂CH₂N), 2.52 (m, 2H, NHCH₂CH₂N_{Mor}), 2.27 (m, 1H, C₃H₂, H-a), 2.0 (m, 4H, OCH₂CH₂N), 1.94 (m, 2H, CH₂CH=C(CH₃)₂), 1.76 (m, 1H, CH₂CHCH₃), 1.70 and 1.62 (2s, 6H, 3H each, CH(CH₃)₂), 1.4 - 1.25 (2m, 2H, 1H each, CH₃CHCH₂CH₂), 0.94 (d, 3H, J = 7.0, CHCH₃).

[VanTSC]
(Vanillin thiosemicarbazone)



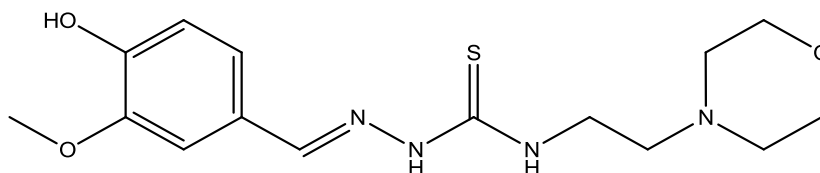
A stirred solution of vanillin (0.2 g, 1.31 mmol) and thiosemicarbazide (0.11 g, 1.31 mmol) in EtOH (20 mL) was refluxed. After 60 min under stirring at reflux temperature, the mixture was cooled and by slow solvent evaporation the product was isolated as yellow crystals

Yield: 92%

$^1\text{H NMR}$ (300MHz, CDCl_3): δ_{H} (ppm) 11.38 (s, 1H, NHN), 9.72 (s, 2H, NH_2), 7.96 (s, 1H, $\text{CH}=\text{N}$), 7.33 (d, $J = 1.59$ Hz, 1H, H_5van), 7.13 (dd, $J = 8.20, 1.59$ Hz, 1H, H_2van), 6.81 (d, $J = 8.20$ Hz, 1H, H_3van), 3.83 (s, 3H, OCH_3).

[VanMor]

(Vanillin-4-[2-(4-morpholinyl)ethyl]-3-thiosemicarbazone)



A stirred solution of vanillin (0.20 g, 1.31 mmol) and N4 ethyl morpholine thiosemicarbazide (0.26 g, 1.31 mmol) in EtOH (15 mL) was refluxed. After 3 h the mixture was poured into a crystallizer and the solvent was slowly evaporated to obtain the product as white crystals.

Yield: 90%

¹H NMR (300MHz, CDCl₃): δ_H (ppm) 11.38 (s, 1H, *NHN*), 8.29 (t, J = 5.29 Hz, 1H, *NH*), 7.96 (s, 1H, *CH=N*), 7.33 (d, J = 1.59 Hz, 1H, H₅van), 7.13 (dd, J = 8.20, 1.59 Hz, 1H, H₂van), 6.81 (d, J = 8.20 Hz, 1H, H₃van), 3.83 (s, 3H, OCH₃), 3.68 (m, 2H, CH₂NH), 3.56 (t, 2H, OCH₂CH₂N), 2.51 (t, J = 4.84 Hz, 1H, CH₂ CH₂NH), 2.44 (m, 2H, OCH₂CH₂N)

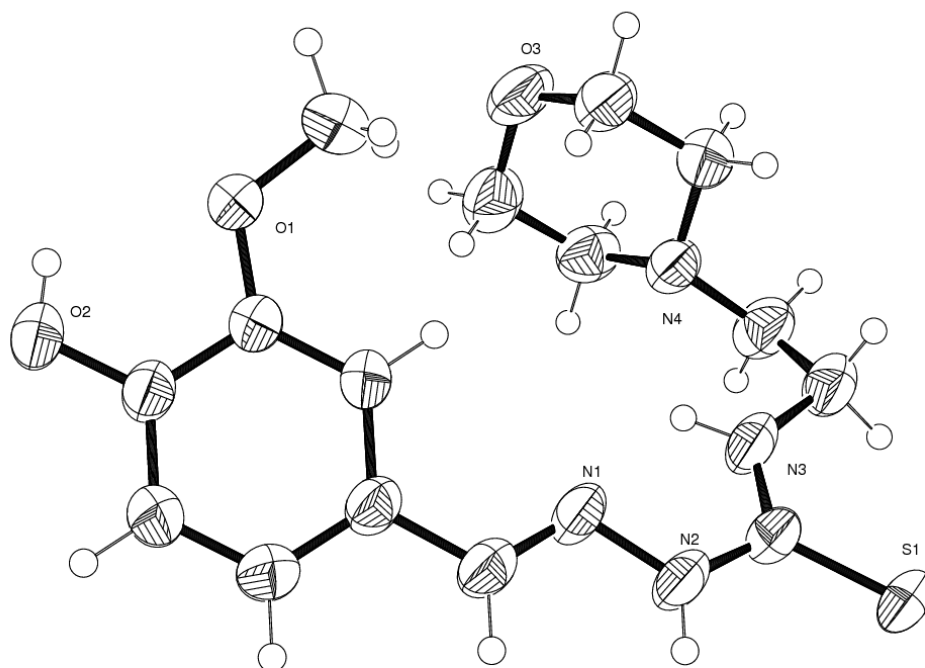
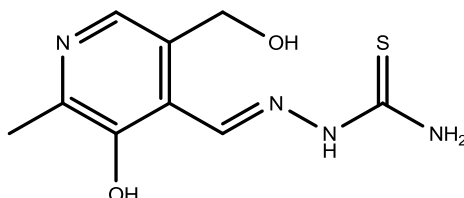


Figure 2.5. ORTEP drawing of VanMor (50% probability plot).

The X-ray structure was solved from data collected on a Bruker-Siemens SMART AXS 1000 diffractometer equipped with a CCD detector. Mo-K α ($\lambda = 0.71069 \text{ \AA}$) The structure was solved by direct methods and refined using SHELXL97. The drawing was plotted using ORTEPIII. Crystallographic data: C₁₅H₂₂N₄O₃S₁, Mr = 338., triclinic, space group P-1, a = 7.051(2) , b = 8.119(2), c = 15.798(4) \AA , $\alpha = 82.014(3)$, $\beta = 79.889(3)$, $\gamma = 86.463(4)^\circ$; V = 881.1(4) \AA^3 , Z = 2, $\rho_{\text{calc}} = 1.276 \text{ Mgm}^{-3}$, T = 298.15 K, F(000) = 210, crystal size = 0.50x0.40x0.30 mm, index range = $-9 < h < 9$, $-10 < k < 10$, $-20 < l < 20$, collected reflections = 11561, unique reflections = 4037, refined parameters = 208, goodness-of-fit = 1.043, final R factor = 0.0407, wR2 = 0.1235, electronic density residues = 0.19 and -0.16 e\AA^{-3} .

[PyrTSC]
(Pyridoxal thiosemicarbazone)



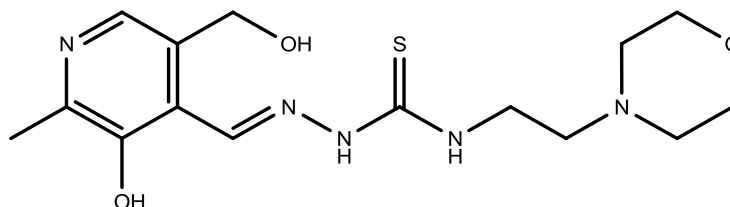
A stirred solution of pyridoxal (0.2 g, 1.31 mmol) and thiosemicarbazide (0.11 g, 1.31 mmol) in EtOH (10 mL) was refluxed. After 2 h under stirring at reflux temperature, the mixture was cooled and the product was isolated as a yellow powder.

Yield: 92%

¹H NMR (300MHz, DMSO-d₆): δ_H ppm 11.60 (br s, 1 H, *NH*), 9.65 (br s, 1H, *OH*), 8.57 (s, 3H, *CHN*_{py} + *NH*₂), 7.99 (s, 1H, *CHN*), 5.25 (s, 1H, *OH*), 4.57 (s, 2H, *CH*₂*O*), 1.76 (s, 3H, *CH*₃).

[PyrMor]

(Pyridoxal-4-[2-(4-morpholinyl)ethyl]-3-thiosemicarbazone)



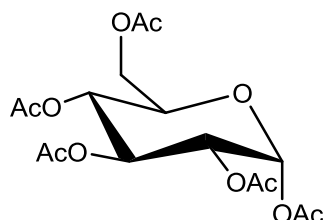
A stirred solution of pyridoxal (0.40 g, 2.39 mmol) and thiosemicarbazide (0.48 g, 2.39 mmol) in EtOH (30 mL) was refluxed. During the reflux a precipitate appeared and after 3 h the solution was filtered and the product collected.

Yield: 90%

¹H NMR (300 MHz, DMSO-d₆) : δ_H ppm 11.72 (br s, OH), 8.58 (s, 1H, CH_{pyr}), 8.30 (br m, 1H, NH), 8.01 (s, 1H, HC=N), 5.27 (t, J = 5.32 Hz, 1H, CH₂OH), 4.61 (d, J = 5.00 Hz, 1H, CH₂OH), 3.68 (m, 1H, CH₂NH), 3.64-3.59 (m, 1H, CH₂CH₂O), 2.53 (t, J = 4.71 Hz, 1H, CH₂N), 2.44 (m, 1H, CH₂N_{mor}), 2.41 (s, 3H, CH₃).

[GluOAc]

Glucose pentaacetate



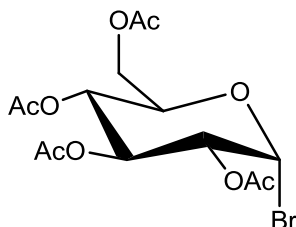
To a round flask containing D-glucose (1g, 9.24 mmol) in AcO₂ (7 mL) were added pyridine (7mL) and a small amount of 4- dimethylaminopyridine. The solution was stirred in an ice-cold bath for 5h and than at room temperature for 18h. Dichlorometane (20mL) and water (20mL) were added to the solution, the organic phase was then separated and consecutively washed with a sat. aq. CuSO₄ until the dark blue color disappeared and then with water (20mL). Then dried over Na₂SO₄ and concentrated under reduced pressure to give an oil which crystallizes.

Yield: 93%

¹H NMR (300MHz, CDCl₃): δ_H(ppm) 6.34 (d, J = 3.68 Hz, H-1), 5.47 (t, J = 10.30, 1H, H-3), 5.15 (m, 1H, H-4), 5.10 (dd, J = 10.30, 3.68 Hz, 1H, H-2), 4.28 (dd, J = 12.58, 4.22 Hz, 1H, H-7), 4.11 (m, 2H H-5, H-6), 2.18 (s, 3H, OAc), 2.10 (s, 3H, OAc), 2.04 (s, 3H, OAc), 2.03 (s, 3H, OAc), 2.02 (s, 3H, OAc).

[GluOAcBr]

Acetobromo- α -D-glucose



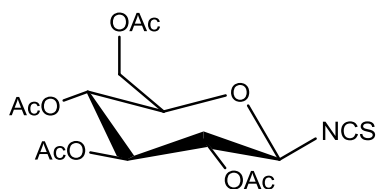
HBr in acetic acid (33%) was added dropwise to a solution of pentaacetylglucose (1 gr, 2.56 mmol) in dichloromethane (5 mL) under nitrogen atmosphere. The reaction mixture was stirred at room temperature for 2h, then ice-cold water (10 mL) was added and the mixture was extracted with CH_2Cl_2 (3·20 mL). The combined CH_2Cl_2 layers were washed with a saturated NaHCO_3 solution, H_2O , and brine, and the filtrate was evaporated in vacuo to give a thick oil which crystallizes.

Yield: 95%

$^1\text{H NMR}$ (300MHz, CDCl_3): δ_{H} (ppm) 6.63 (d, $J = 4.00$ Hz, 1H, $H-1$), 5.58 (t, $J = 9.72$ Hz, 1H, $H-3$), 5.18 (t, $J = 9.85$ Hz, $H-4$), 4.85 (dd, $J = 9.99, 4.05$ Hz, 1H, $H-2$), 4.39-4.27 (m, 1H, $H-5$), 4.13 (m, 2H, $H-6$), 2.08 (4s, 12H, OAc)

[GluOAcNCS]

2,3,4,6-Tetra-O-acetyl- β -D-glucose isothiocyanate



A mixture of potassium thiocyanate (0.200 g, 2 mmol), tetrabutylammonium chloride (0.285 g, 1 mmol) and molecular sieves (4Å, 1.5 g) in acetonitrile is stirred at room temperature for 3 h. Then acetobromo- α -D-glucose (0.423 g, 1 mmol) is added and the mixture refluxed until the reaction is complete as detected by TLC (AcOEt/ C₆H₁₂ 2:3). Then solution is filtered and concentrated under pressure to afford a residue, which is purified by flash chromatography (silica gel, AcOEt/ C₆H₁₂ 2:3).

Yield : 80%

¹H NMR (300MHz, CDCl₃): δ _H (ppm) 5.13 (m, 4H, *H*-1, *H*-2, *H*-3, *H*-4), 4.27 (dd, *J* = 12.45, 4.66 Hz, 1H, *H*-6), 4.17 (dd, *J* = 12.45, 2.27 Hz, 1H, *H*-6), 3.77 (ddd, *J* = 10.14, 4.66, 2.27 Hz, 1H, *H*-5), 2.13-2.05 (4s, 12H, OAc)

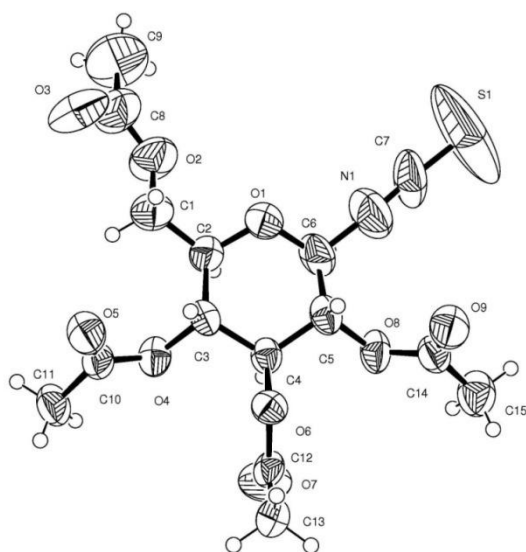
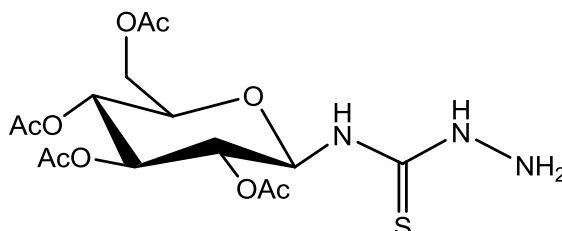


Figure 2.6. ORTEP drawing of 2,3,4,6-tetra-O-acetyl- β -D-glucose isothiocyanate (50% probability plot).

The X-ray structure was solved from data collected on a Bruker-Siemens SMART AXS 1000 diffractometer equipped with a CCD detector. Mo-K α ($\lambda = 0.71069 \text{ \AA}$) The structure was solved by direct methods and refined using SHELXL97. The drawing was plotted using ORTEPIII. Crystallographic data: C₁₅H₁₉N₁O₉S₁, Mr = 389.37, orthorhombic, space group P212121, a = 5.543(1), b = 14.113(2), c = 25.078(4) \AA , V = 1961.8(5) \AA^3 , Z = 4, $\rho_{\text{calc}} = 1.318 \text{ Mg m}^{-3}$, T = 298.15 K, F(000) = 816, crystal size = 0.40x0.30x0.30 mm, index range = $-6 < h < 6$, $-17 < k < 16$, $-31 < l < 23$, collected reflections = 11673, unique reflections = 3939, refined parameters = 255, goodness-of-fit = 0.952, final R factor = 0.0739, wR2 = 0.2415, electronic density residues = 0.51 and -0.47 e\AA^{-3} .

[GluOAcTSC]

2,3,4,6-Tetra-O-aceto- β -D-glucose thiosemicarbazide



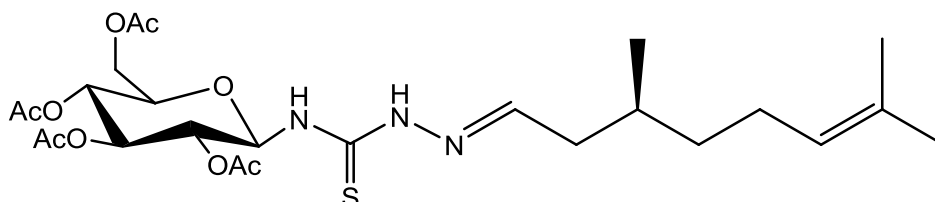
To a stirred solution of hydrazine monohydrate (86 μ L, 1.76 mmol) in EtOH (25 mL) at 0 °C, a solution of 2,3,4,6-tetra-O-acetyl- β -D-glucose isothiocyanate (0.67 g, 1.73mmol) in EtOH (40 mL) was slowly added dropwise. During the addition a white precipitate appeared. After the addition the solution was stirred for additional 5' and the precipitate was collected by filtration.

Yield: 76%

¹H NMR (300MHz, d₆DMSO): δ _H (ppm) 9.28 (s, 1H, NHC=S), 8.20 (s, 1H, NHNH₂), 5.78 (t, *J* = 9.35 Hz, 1H, *H*-1), 5.39 (t, *J* = 9.35 Hz, 1H, *H*-3), 5.11 (t, *J* = 9.35 Hz, 1H, *H*-2), 5.09 (t, *J* = 9.35 Hz, 1H, *H*-4), 4.33 (dd, *J* = 12.42, 4.41 Hz, 1H, *H*-6), 4.14 (dd, *J* = 12.42, 2.07 Hz, 1H, *H*-6), 3.89 (ddd, *J* = 9.35, 4.41, 2.07 Hz, 1H, *H*-5), 2.00 (m, 12H, OAc).

[CitrGluOAc]

(1-S-Citronellal-4-(2,3,4,6-tetra-O-aceto-β-D-glucosyl)-3-thiosemicarbazone)



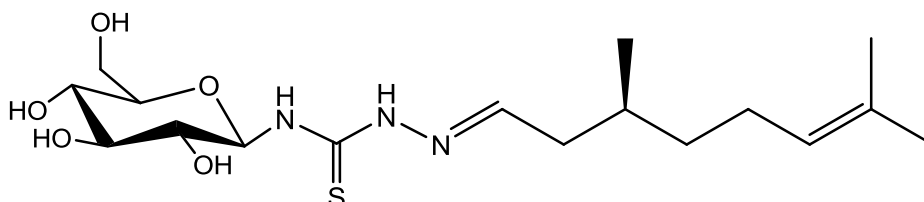
A stirred solution of citronellal (0.26 mL, 1.48 mmol) and glucosyl-thiosemicarbazide (0.62 g, 1.48 mmol) in EtOH (25 mL) was refluxed. After 24 min under stirring at reflux temperature, the mixture was cooled, the solution concentrated under reduced pressure and the product purified by flash chromatography (AcOEt/C₆H₁₂ 1:3).

Yield: 86%

¹H NMR (300MHz, CDCl₃): δ_H (ppm) 8.86 (s, 1H, NH), 7.13 (t, *J* = 8.39 Hz, 1H, HC=N), 5.95 (t, *J* = 8.89 Hz, 1H, H-1), 5.38 (t, *J* = 9.37 Hz, 1H, H-3), 5.15-5.02 (m, 2H, H-2, H-4) H_{4,2}, 4.33 - 4.03 (m, 2H, H-6, H-6'), 3.87 (m, 1H, H-5), 2.17 (m, 1H, CH₂CHN), 2.02 - 1.98 (m, 12H, OAc), 1.7 (m, 1H CHCH₃), 1.65 - 1.57 (2s, 6H, (CH₃)₂C=), 1.23 (m, 1H, CH₂CHCH₃), 0.9 (d, 3H, CHCH₃)

[CitrGlu]

(1-S-Citronellal-4-(β -D-glucosyl)-3-thiosemicarbazone)



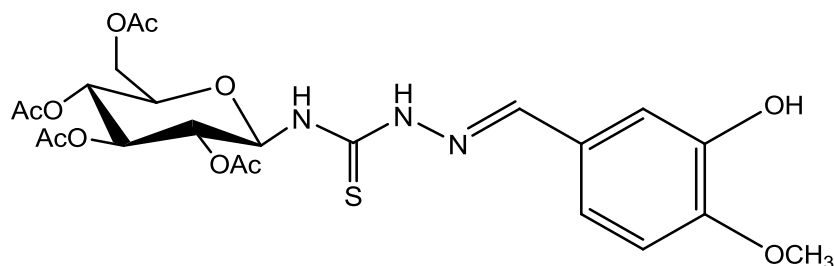
A solution of CitrGluOAc (0.37g, 2.35mmol) in dry methanol (50 mL) was heated to 50°C in a schlenck tube for 8 h in presence of a catalytic quantity of sodium methoxyde. Neutralization of the methoxyde by Dowex 50WX4 acid ion-exchange resin, followed by filtration and evaporation of the filtrate afforded a pure material by ^1H NMR.

Yield: 98%

^1H NMR (300MHz, CDCl_3): δ_{H} (ppm) 8.46 (s, 1H, NH) , 8.06 (d, $J = 8.76$ Hz, 1H, NH), 7.46 (t, $J = 5.84$ Hz, 1H, HC=N), 5.27 (t, $J = 8.74$ Hz, 1H, H-1), 5.08 (t, $J = 7.01$ Hz, 1H, HC=C(CH₃)₂) 3.70-3.00 (m, 6H, H-2, H-3, H-4, H-5, H-6, H-6'), 2.23 – 2.05 (2m, 1H, CH₂CHN), 1.97 (m, 1H, CH₂CH=C) 1.64 (m, 1H, CHCH₃) 1.64 – 1.57 (2s, 6H, (CH₃)₂C=), 1.21 (m, 1H, CH₂CHCH₃), 0.88 (d, 3H, CHCH₃)

[VanGluOAc]

(1-Vanillin-4-(2,3,4,6-tetra-O-aceto- β -D-glucosyl)-3-thiosemicarbazone)



A solution of glucosylthiosemicarbazide (1 g, 2.35 mmol) and vanillin (0.37g, 2.35mmol) in ethanol (50 mL) was refluxed for 12 h. Then the solution was cooled to room temperature concentrated under reduced pressure and purified by flash chromatography (AcOEt/C₆H₁₂ 2:3).

Yield: 81%

¹H NMR (300MHz, CDCl₃): δ_{H} (ppm) 9.88 (s, 1H, NH), 8.37 (d, $J = 8.45$ Hz, 1H, HC=N), 7.75 (s, 1H, NH), 7.52 (m, 1H, H_{van}), 7.03 (dd, $J = 8.14, 1.63$ Hz, 1H, CH_{van}), 6.93 (d, $J = 8.10$ Hz, 1H, CH_{van}), 5.67 (t, $J = 8.95$ Hz, 1H, H-1), 5.44 (t, $J = 9.49$ Hz, 1H, H-3), 5.18 (td, $J = 11.91, 9.58$ Hz, 2H, H-2, H-4), 4.43-4.15 (m, 2H, H-6, H-7), 4.04 (s, 3H, CH₃), 3.95 (m, 1H, H-5), 2.2-2.0 (m, 12H, OAc).

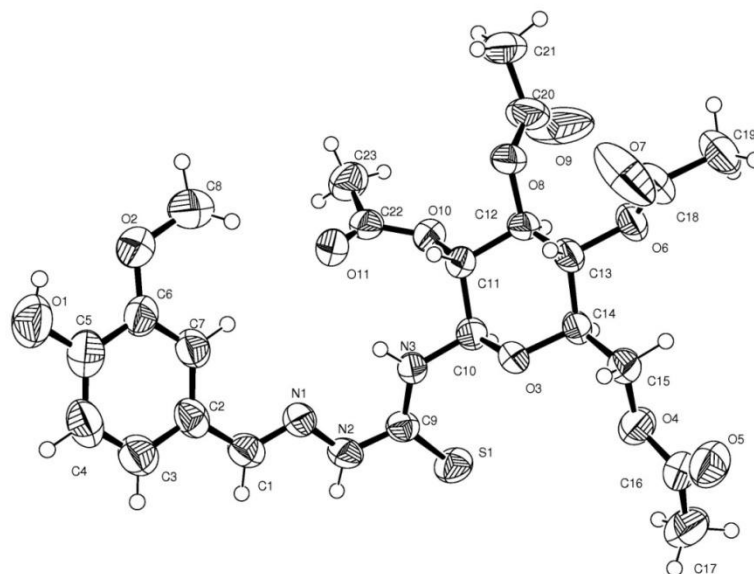
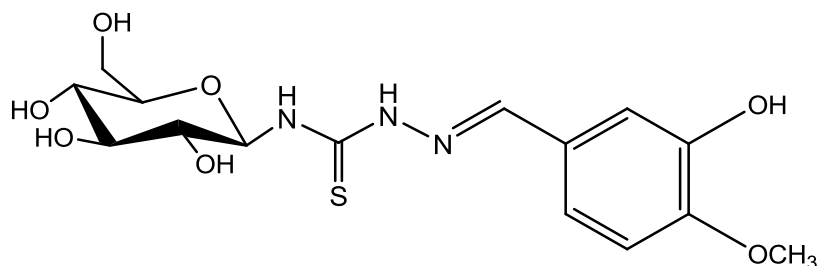


Figure 2.7. ORTEP drawing of VanGluOAc (50% probability plot).

The X-ray structure was solved from data collected on a Bruker-Siemens SMART AXS 1000 diffractometer equipped with a CCD detector. Mo-K α ($\lambda = 0.71069 \text{ \AA}$) The structure was solved by direct methods and refined using SHELXL97. The drawing was plotted using ORTEPIII. Crystallographic data: C₂₃H₂₉N₃O₁₁S₁, Mr = 553.54, orthorhombic, space group P212121, a = 9.015 (2), b = 15.221(3), c = 19.882(4) \AA , V = 2728.2(10) \AA^3 , Z = 4, $\rho_{\text{calc}} = 1.353 \text{ Mgm}^{-3}$, T = 298.15 K, F(000) = 1168, crystal size = 0.60x0.40x0.20 mm, index range = $-11 < h < 11$, $-18 < k < 19$, $-25 < l < 19$, collected reflections= 16954, collected reflections = 6297, refined parameters = 343, goodness-of-fit = 0.856, final R index = 0.0418, wR2 = 0.0898, electronic density residues = 0.25 and -0.16 e\AA^{-3} .

[VanGlu]

(1-Vanillin-4-(β -D-glucosyl)-3-thiosemicarbazone)



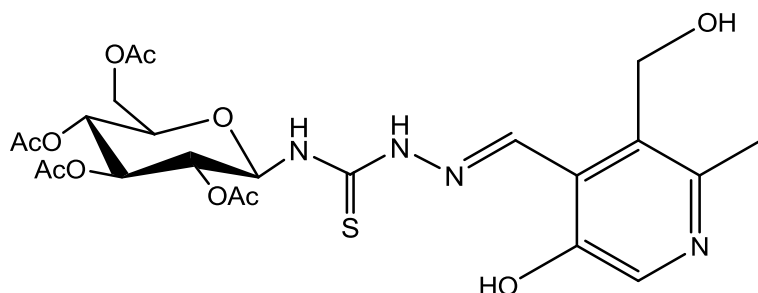
A solution VanGluOAc (0.37g, 2.35mmol) in dry methanol (50 mL) was refluxed for 8 h in the presence of a catalytic quantity of sodium methoxyde. Neutralization of the methoxyde by Dowex 50WX4 acid ion-exchange resin, followed by filtration and evaporation of the filtrate afforded a pure material by ¹H NMR.

Yield: 98%

¹H NMR (300MHz, D₂O): δ_{H} (ppm) 8.50 (s, 1H, NH), 8.25 (d, $J = 9.11$ Hz, 1H, NH), 7.92 (s, 1H, CHN), 7.22 (d, $J = 1.57$ Hz, 1H, CHvan), 6.97 (dd, $J = 8.24, 1.71$ Hz, 1H, CHvan), 6.51 (d, $J = 8.19$ Hz, 1H CHvan), 5.36 (t, $J = 9.07$ Hz, 1H, H-1), 3.76 (s, 3H, OCH₃), 3.70-3.00 (m, 6H, H-2-6).

[PyrGluOAc]

(1-(Pyridoxal)-4-(2,3,4,6-tetra-O-aceto-β-D-glucosyl)-3-thiosemicarbazone)



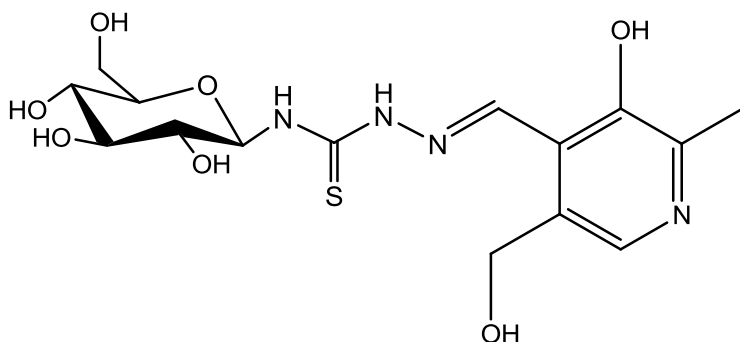
A solution of tetra-acetyl glucosylthiosemicarbazide (1 g, 2.3 mmol) and pyridoxal (0.39g, 2.3 mmol) in ethanol (50 mL) was refluxed for 12 h. Then the solution was cooled to r.t. concentrated under reduced pressure and purified by flash chromatography (AcOEt/C₆H₁₂ 10:1).

Yield: 81%

¹H NMR (300MHz, CDCl₃): δ_H (ppm) 8.61 (s, 1H, CH_{pyr}), 7.99 (s, 1H, HC=N), 5.98 (t, *J* = 9.13 Hz, 1H, H-1), 5.41 (t, *J* = 9.50 Hz, 1H, H-3), 5.31 (t, *J* = 5.30 Hz, 1H, H-2), 5.22 (d, *J* = 8.96 Hz, 1H, NH), 4.96 (t, *J* = 9.75 Hz, 1H, H-4), 4.58 (d, *J* = 5.26 Hz, 1H, CH₂Pyr), 4.11 (d, *J* = 9.99 Hz, 1H, H-5), 4.15 (m, 2H, H-6, H-7), 2.42 (s, 1H, CH₃), 2.01-1.91 (m, 12H, OAc)

[PyrGlu]

(1-Pyridoxal-4-(β -D-glucosyl)-3-thiosemicarbazone)



A solution of PyrGluOAc (0.37g, 2.35mmol) in dry methanol (50 mL) was refluxed for 8 h in the presence of a catalytic quantity of sodium methoxyde. Neutralization of the methoxyde by Dowex 50WX4 acid ion-exchange resin, followed by filtration and evaporation of the filtrate afforded a pure material by ^1H NMR.

Yield: 97%

^1H NMR (300MHz, CDCl_3): δ_{H} (ppm) 8.48 (s, 1H, *NH*), 7.89 (d, $J = 9.32$ Hz, 1H, *NH*), 7.48 (s, 1H, *CH*_{pyr}), 7.24 (s, 1H, *HC=N*), 5.41-5.19 (m, 1H, *H-1*), 4.55 (s, 1H, *CH*₂OH), 3.70-3.00 (m, 6H, *H-2*, *H-3*, *H-4*, *H-5*, *H-6*, *H-6'*) 2.37 (s, 3H, *CH*₃).

2.6.2 Synthesis of the complexes

[Cu(CitrTSC)₂]

A solution of Cu(OAc)₂·H₂O (0.05 mg, 0.25 mmol) in H₂O (10 mL) was added dropwise to a solution of CitrTSC (0.11 g, 0.5 mmol) in EtOH (20 mL), at room temperature. The complex was isolated as dark red solid by slow solvent evaporation.

Yield: 90%

Elem. An. C₂₂H₄₀CuN₆S₂: C, 51.68%; H, 7.88%; N, 16.42%; S, 12.53%. Found: C, 51.70%; H, 7.89%; N, 16.42%; S, 12.53%

[Ni(CitrTSC)₂]

A solution of Ni(OAc)₂·4H₂O (0. mg, 0.044 mmol) in H₂O (10 mL) was added dropwise to a solution of CitrTSC (19.98 mg, 0.088 mmol) in EtOH (20 mL), at room temperature. The complex was isolated as dark green crystals suitable for X-ray crystallography.

Yield: 92%

¹H NMR (300MHz, CDCl₃): δ_H (ppm) 6.81 (t, 1H, J = 6.0, C2H), 6.20 and 6.17 (2s, 2H, 1H each, N1H2), 5.14 (m, 1H, C7H), 2.07 (m, 2H, 3H2), 1.93 (m, 2H, C6H2), 1.65 and

1.61 (2s, 6H, 3H each, C₉H₃ and C₁₀H₃), 1.31 (m, 1H, C₄H), 1.22 (m, 2H, C₅H₂),
0.90 (d, 3H, J = 7.0, C₁₁H₃)

Elem. An. C₂₂H₄₀N₆NiS₂: C, 51.68%; H, 7.88%; N, 16.42%; S, 12.53%. Found: C,
51.60%; H, 7.82%; N, 16.57%; S, 12.58%

[Cu(CitrMor)₂]

To a solution of ligand CitrMor (0.40 g, 0.13 mmol) in EtOH (50 mL), at room temperature with stirring, was added Cu(OAc)₂·H₂O (0.13 g, 0.06 mmol). The resulting clear solution reddish first and brown after a while was left at room temperature and stirred for one hour. The complex was isolated as dark red crystals suitable for X-ray crystallography after slow evaporation of the solvent.

Yield: 90%

Elem. An. C₂₂H₄₀CuN₆S₂: C, 51.67%; H, 7.88%; N, 16.43%; S, 12.54%. Found: C,
51.60%; H, 7.81%; N, 16.58%; S, 12.59%.

[Ni(CitrMor)₂]

To a solution of ligand CitrMor (0.40 g, 0.11 mmol) in EtOH (50 mL), at room temperature with stirring, solid Ni(OAc)₂·4H₂O (0.10 g, 0.05 mmol) was added. The resulting clear reddish first and brown after a while, was left at room temperature and

stirred for one hour. The complex was isolated as green crystals suitable for X-ray crystallography after slow evaporation of the solvent.

Yield: 90%

$^1\text{H NMR}$ (300MHz, CDCl_3): δ_{H} (ppm) 6.85 (t, 1H, $\text{CH}=\text{N}$), 5.39 (bs, 1H, CH_2NHCS), 5.08 (m, 1H, $\text{CH}=\text{C}(\text{CH}_3)_2$), 3.74 (m, 4H, $\text{OCH}_2\text{CH}_2\text{N} + \text{CH}_2\text{NHCS}$), 3.31 (t, 2H, $\text{NCH}_2\text{CH}_2\text{NH}$), 2.52 (m, 2H, $\text{NHCH}_2\text{CH}_2\text{N}_{\text{Mor}}$), 2.45 (t, 2H, $\text{NCH}_2\text{CH}_2\text{NH}$), 2.31 (m, 4H, $\text{OCH}_2\text{CH}_2\text{N}$), 1.94 (2H, m, $\text{CH}_2\text{CH}=\text{C}(\text{CH}_3)_2$), 1.60 (1H, m, CH_2CHCH_3), 1.70 and 1.62 (6H, 2s, 3H each, $\text{CH}(\text{CH}_3)_2$), 1.4-1.2 (m, 2H, $\text{CH}_3\text{CHCH}_2\text{CH}_2$), 0.92 (d, 3H, CHCH_3).

Elem. An. $\text{C}_{34}\text{H}_{62}\text{N}_8\text{NiS}_2\text{O}_2$: C, 55.35 %; H, 8.47 %; N, 15.19 %; S, 8.69 % Found: C, 54.98 %; H, 8.36 %; N, 15.28 %; S, 8.50 %.

[Cu(CitrGlu)₂]

To a solution of ligand CitrGlu (0.40 g, 1.02 mmol) in EtOH (50 mL), at room temperature with stirring, was added $\text{Cu}(\text{OAc})_2 \cdot \text{H}_2\text{O}$ (0.1 g, 0.51 mmol). After 3 h the solution was poured into a crystallizer and the product was obtained as brown powder after slow evaporation of the solvent.

$\text{Cu}(\text{CitrGlu})_2$ was obtained as amorphous solid.

Yield: 90%

Elem. An: C₃₄H₆₀CuN₆O₁₀S₂ C=48,59%; H=7,18%; N=10,00% Found C=47,96%;
H=7,12%; N=10.10%.

Esi-MS : m/z 840,55 [ML₂+H]⁺

[Ni(CitrGlu)₂]

To a solution of ligand CitrGlu (0.30 g, 0.77 mmol) in EtOH (50 mL), at room temperature with stirring, was added Ni(OAc)₂·4H₂O (0.068 g, 0.38 mmol). After 3 h of stirring the solution was poured into a crystallizer and the solvent let to slowly evaporate. Ni(CitrGlu)₂ was obtained as amorphous solid.

Elem. An: C₃₄H₆₀N₆NiO₁₀S₂ C=37,85%; H=7,21%; N=7,02% Found C=37,88%;
H=7,12%; N=7.03%.

ESI-MS : m/z = 835.32 [ML₂+H]⁺

[Cu(VanTSC)₂]

To a stirred solution of VanTSC (0.300 g, 1.33 mmol) in EtOH (40mL) was added Cu(OAc)₂·H₂O (0.13 g, 0.66 mmol) and immediately the color turned to green/yellow and a precipitate appeared.

The solution was refluxed for 3 h then was cooled to r.t. and the green precipitate collected by filtration.

Yield: 62%

Elem. An. $C_{18}H_{20}CuN_6O_4S_2$ C=42,22%; H=3,94%; N=16,41% Found C=42,85%;
H=3,92%; N=16.40%.

[Ni(VanTSC)₂]

To a stirred solution of VanTSC (0.350 g, 1.55 mmol) in EtOH (40mL) was added Ni(OAc)₂·4H₂O (0.137 g, 0.77 mmol) and immediately the color turned to. The solution was refluxed for 3 h then was cooled to r.t. and green crystals were obtained by slow solvent evaporation.

Yield: 70%

Elem. An. $C_{18}H_{20}N_6NiO_4S_2$ C=42,22%; H=3,94%; N=16,41% Found C=42,51%;
H=3,79%; N=16.53%.

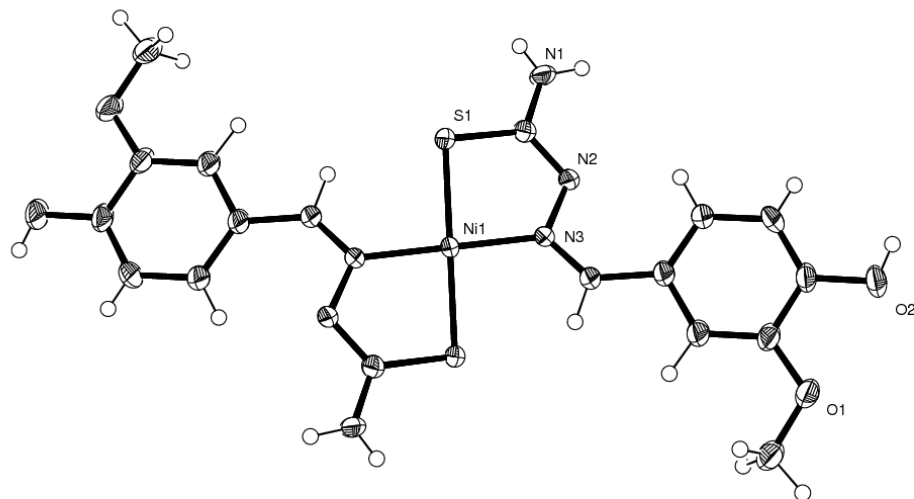


Figure 2.8 - ORTEP drawing of $[\text{Ni}(\text{VanTSC})_2]$ (50% probability plot).

The X-ray structure was solved from data collected on a Bruker-Siemens SMART AXS 1000 diffractometer equipped with a CCD detector. Mo-K α ($\lambda = 0.71069 \text{ \AA}$) The structure was solved by direct methods and refined using SHELXL97. The drawing was plotted using ORTEPIII. Crystallographic data: $\text{C}_{26}\text{H}_{44}\text{N}_6\text{O}_8\text{S}_2$, Mr = 691.50, triclinic, space group P-1, $a = 6.859(2)$, $b = 10.644(4)$, $c = 11.797(4) \text{ \AA}$, $\alpha = 72.869(6)$, $\beta = 78.656(6)$, $\gamma = 84.751(6)^\circ$; $V = 806.5(5) \text{ \AA}^3$, $Z = 2$, $\rho_{\text{calc}} = 1.423 \text{ Mg m}^{-3}$, $T = 298.15 \text{ K}$, $F(000) = 732$, crystal size = $0.30 \times 0.30 \times 0.30 \text{ mm}$, index range = $-8 < h < 8$, $-13 < k < 13$, $-15 < l < 15$, collected reflections = 9823, unique reflections = 3712, refined parameters = 220, goodness-of-fit = 1.018, final R factor = 0.0605, $wR_2 = 0.1736$, electronic density residues = 1.19 and -1.15 e \AA^{-3} .

[Cu(VanMor)₂]

To a stirred solution of VanMor (0.20 g, 0.56 mmol) in EtOH (40mL) was added Cu(OAc)₂·H₂O (0.055 g, 0.28 mmol) and immediately the color turned to brown and a precipitate appeared.

The solution was stirred at r.t. for 3 h then the precipitate was collected by filtration.

Yield: 64%

Elem. An. C₃₀H₄₂CuN₈O₄S₂ C=49,12%; H=5,77%; N=15,28% Found C=49,19%; H=5,78%; N=15.4%.

[Ni(VanMor)₂]

To a stirred solution of VanMor (0.20 g, 0.56 mmol) in EtOH (40mL) was added Ni(OAc)₂·4H₂O (0.05 g, 0.28 mmol) and immediately the color turned to green and a precipitate appeared.

The solution was refluxed for 3 h, then was cooled to r.t. and the precipitate collected by filtration.

Yield: 70%

Elem. An. C₃₀H₄₂N₈NiO₄S₂ C=49,12%; H=5,77%; N=15,28% Found C=49,21%; H=5,77%; N=15.3%.

ESI-MS : m/z 732,579 [ML₂ + H]⁺

[Cu(VanGlu)₂]

To a stirred solution of VanGlu (0.30 g, 0.77 mmol) in EtOH (40mL) was added Cu(OAc)₂·H₂O (0.75 g, 0.38 mmol). After 3 h of stirring the solution was poured into a crystallizer and was let slowly evaporate.

Yield: 65%

Elem. An. C₃₀H₄₀CuN₆O₁₄S₂ C=42,22%; H=3,94%; N=16,41% Found C=42,51%; H=3,79%; N=16.53%.

ESI-MS : m/z = 835,12267 [ML₂ + H]⁺

[Ni(VanGlu)₂]

To a stirred solution of VanGlu (0.350 g, 1.55 mmol) in EtOH (40mL) was added Ni(OAc)₂·4H₂O (0.137 g, 0.77 mmol) After 3 h of stirring the solution was poured in a crystallizer and was let slowly evaporate and the Ni(VanGlu)₂ compound was collected.

Yield: 70%

Elem. An. C₃₀H₄₀N₆NiO₁₄S₂ C=37,88%; H=7,20%; N=7,02% Found C=37,89%; H=7,31%; N=7.05%.

ESI-MS : m/z = 835,32751 [ML₂+H]⁺

[Cu(PyrTSC)Cl₂]

To a stirred solution of PyrTSC (0.15 g, 0.62 mmol) in EtOH (40mL) was added CuCl₂·2H₂O (0.106 g, 0.62 mmol) and immediately the color turned to green

The solution was refluxed for 3 h then was cooled to r.t. poured into a crystallizer and the product obtained for slow solvent evaporation.

Yield: 46%

Elem. An. C₉H₁₆Cl₂CuN₄O₄S, C=26,32%; H=3,93%; N=13,64% Found C=26,83%; H=4.11%; N=13.56%.

[Ni(PyrTSC)Cl₂]

To a stirred solution of PyrTSC (0.15 g, 0.62 mmol) in EtOH (40mL) was added NiCl₂·6H₂O (0.14 g, 0.62 mmol) and immediately the color turned to orange and an orange precipitate appeared. The solution was refluxed for 3 h then was cooled to r.t. and the brown/orange precipitate was collected by filtration.

Yield: 57%

Elem. An. C₉H₁₁Cl₂N₄NiO₂S C=32,42%; H=3,33%; N=16,80% Found C=39,89%; H=4.09%; N=20.68%.

[Cu(PyrMor)Cl₂]

To a solution of ligand PyrMor (0.10 g, 0.28 mmol) in EtOH (25 mL), at room temperature with stirring, was added CuCl₂·2H₂O (0.048 g, 0.28 mmol). The solution turned immediately dark. After 3 h of stirring at r.t. the solution was poured into a crystallizer and the solvent slowly evaporated to obtain a green powder.

Yield: 57%

Elem. An. C₁₅H₂₂Cl₂CuN₅O₃S: C, 39.91%; H, 4.91%; N, 15.51%;. Found: C, 41.1%; H, 4.8%; N, 16.57%;

[Ni(PyrMor)Cl₂]

To a solution of ligand PyrMor (0.20 g, 0.44 mmol) in EtOH (25 mL), at room temperature with stirring, solid NiCl₂·6H₂O (0.10 g, 0.44 mmol) was added. The resulting brown solution, was stirred at r.t., and a precipitate appeared. After 2h the brown/orange solid was collected by filtration.

Yield: 61%

Elem. An. C₁₅H₂₂Cl₂N₅NiO₃S: C, 40.34 %; H, 4.97%; N,15.68 %; Found: C, 39.98 %; H, 4.6 %; N, 15.28 %;

[Cu(PyrGlu)Cl₂]

CuCl₂·2H₂O (0.12 g, 0.74mmol) was added to a solution of PyrGlu (0.300 g, 0.74 mmol) in MeOH (20 mL). The resulting solution was stirred at r.t. for 4h and a dark brown precipitate appeared. The precipitate was collected by filtration.

Yield 40 %

Elem. An. . C₁₅H₂₂Cl₂CuN₄O₇S C=33,7%; H=3,94%; N=10,44% found C=33,43%; H=4,47%; N=10,36%.

ESI-MS : m/z = 464.03 [ML+H]⁺

[Ni(PyrGlu)Cl₂]

NiCl₂·6H₂O (0.17 g, 0.74mmol) was added to a solution of PyrGlu (0.300 g, 0.74 mmol) in MeOH (20 mL). The resulting solution was stirred at r.t. and an orange precipitate appeared. After 4 h the solid was collected by filtration.

Yield: 44%

Elem. An. C₁₅H₂₂Cl₂N₄NiO₇S C=33,93%; H=3,97%; N=10,55%. found C=33,84%; H=3,93%; N=10,61%.

ESI-MS: m/z = 491,07388 [ML+H+MeOH]⁺.

2.7 References

- 1) Agrawal, K. C.; Sartorelli, A. C. *Prog. Med. Chem.* **1978**, *15*, 321–356.
- 2) Matthew D. Hall, *et al.* *J. Med. Chem.* **2009**, *52*, 3191–3204.
- 3) Bhaskare, C. K., Hankare, P. P., Rampure, R. S. *J Indian Chem Soc* **1986**, *63*(3), 286-287.
- 4) Borges, R. H. U., Paniago, E., Beraldo H. *J Inorg Biochem* **1997**, *65*(4), 267-275
- 5) Seleem, H. S. M., El-Behairy, M., Mashaly, M. M., Mena, H. H. *J Serb Chem Soc* **2002**, *67*(4) 243-256.
- 6) Camarasa, M. J, Fernandez-Resa P, Garcia-Lopez M. T. H, Federico G. de las; Mendez-Castrillon, Paloma P, Felix A.S, *Synthesis*, **1984**, *6*, 509 - 510
- 7) Wu Peng, Ling-Hua C.A.O, *Chin. J. Org. Chem*, **2005**, *25*(9), 1121-1124
- 8) Tetko, I. V.; Gasteiger, J.; Todeschini, R.; Mauri, A.; Livingstone, D.; Ertl, P.; Palyulin, V. A.; Radchenko, E. V.; Zefirov, N. S.; Makarenko, A. S.; Tanchuk, V. Y.; Prokopenko, V. V. *J. Comput. Aid. Mol. Des.*, **2005**, *19*, 453-63

Chapter 3

Theoretical studies, synthesis and biological evaluation of glycosylated thiosemicarbazones

3.1 Ribonucleotide reductase

As already described in the introduction, ribonucleotide reductase (RNR, also known as ribonucleotide diphosphate reductase) is one of the putative targets of thiosemicarbazones. During my doctoral period, in collaboration with prof. E. Polverini of the Department of Physics in our University, a study aimed at evaluating the possible interactions of thiosemicarbazones with ribonucleotide reductase was carried out giving us a hint in the formulation of new thiosemicarbazones.

Ribonucleotide reductase is an enzyme which catalyzes the conversion of ribonucleotides (NTPs) to their corresponding deoxyribonucleotides (dNTPs), which are the building blocks for DNA replication and repair in all living cells¹. In this way this enzyme catalyzes the *rate limiting step* in DNA synthesis in the cell cycle². The activity of this enzyme is under strict control and this highlights the importance of a balanced supply of dNTPs for error-free DNA synthesis. Unbalanced dNTP pools lead to misincorporation of nucleotides into DNA, mutations and cell death³. Eukaryotic enzymes consist of two homodimeric proteins, R1 (α_2) and R2 (β_2) (Fig. 3.1).

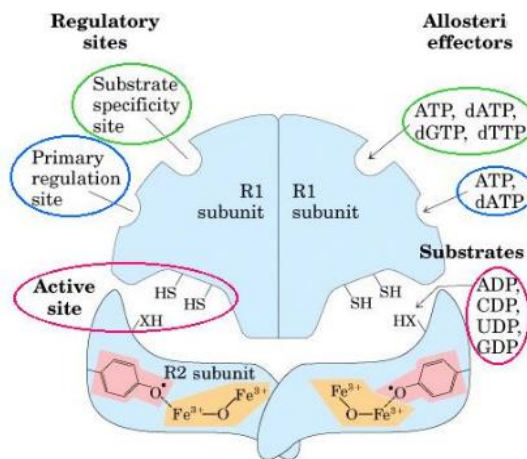


Figure 3.1 – Ribonucleotide reductase

The R1 (α_2) subunit harbors two allosteric sites, the catalytic site and redox active disulfide⁴ while the R2 (β_2) subunit contains an oxygen-linked diferric center and a stable tyrosyl radical¹. Depending on the allosteric configuration, one of the four ribonucleotides binds to the catalytic site¹.

3.1.1 Allosteric regulation

Allosteric regulation of RNR is a mechanism which allows the enzyme maintain balanced the pool of the four deoxynucleotides and to adapt rapidly to changes in the requirements for dNTPs⁵. Effectors bind to two separate sites (Fig. 3.1): the “activity site” which regulate the general activity of RNRs and the “specificity site” which regulate the substrate specificity. Nucleoside triphosphates are effectors, whereas nucleoside diphosphates are its substrates. The effectors induce conformational changes

of the protein structure providing the signal for the required adaptation at the catalytic site^{1,6}.

3.1.2 Docking

In the field of molecular modeling, docking is a method which predicts the preferred orientation of one molecule to a second when bound to each other to form a stable complex. Different couples effector-substrate modulate conformation of loop 2 (red in Fig. 3.2), for example dADP determine specificity for CDP substrate (see Fig. 3.2a). Once inside site S dATP, possessing an adenine which is a bicyclic system, occupies a bigger volume than the corresponding pyrimidine derivative, inducing a folding of loop 2 towards site C. As a consequence space inside site C become reduced and is favoured only the passage of pyrimidinic nucleotide as CDP.

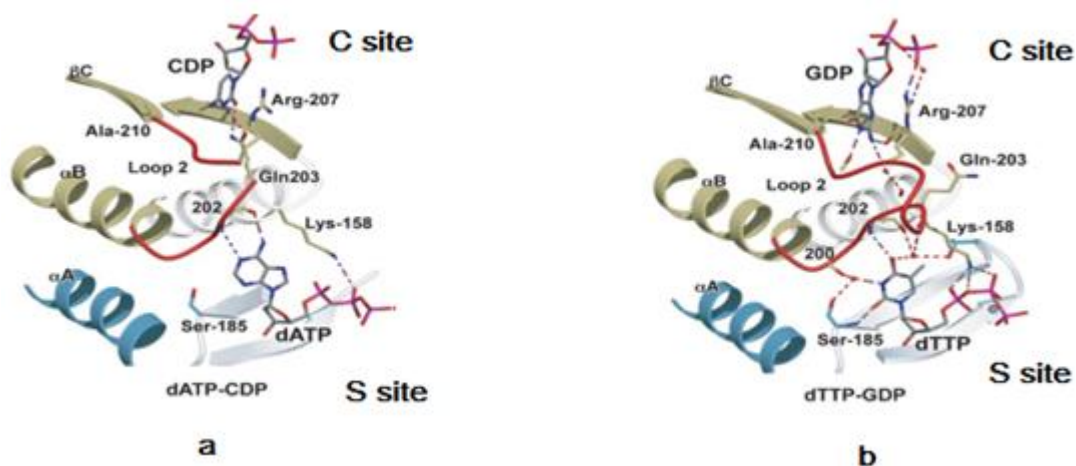


Figure 3.2

Opposite behaviour has the dTTP-GDP couple, because the effector possesses a pyrimidinic ring and this shifts loop 2 to site S, letting site C more accessible to an adenosinic nucleotide like GDP (see Fig. 3.2b).

For the reasons mentioned above and because during the docking simulation receptor stays rigid, two different structure were chosen, which possess different conformations of loop 2 and sites S and C. Docking simulation has been used to check the affinity of our exogenous ligands for these sites, their disposition inside them and if the binding energy is comparable with the energy of endogen ligands.

For the docking experiments two different ribonucleotide reductase structures were taken from the PDB (Protein data bank) *database*. For all these structures the protein source is *Homo sapiens* (RNR of class I).

The structure chosen are 2WGH and 3HND. 2WGH has site C occupied by CDP and site S by dATP while 3HND has site C occupied by GDP and site S by dTTP (Tab. 3.1).

	Site C	Site S
2WGH	CDP	dATP
3HND	GDP	dTTP

Table 3.1

The results of docking are clusters of conformations with a RMSD (root mean square deviation) below a threshold of 2 Å. RMSD is a measure of the average distance among atoms corresponding of overlapped structures; the lower is this value the more similar are structures. The larger a cluster is the higher probability the conformation with lowest

energy is favoured. In these docking experiments exogenous molecules evaluated are glycosylated thiosemicarbazones.

Looking at 2WGH table it is possible to note that exogenous molecules cannot compete with the specificity site but using as a model the acetylated glucose derivatives things change dramatically as can be seen from Tab. 3.2.

2WGH			
Molecule	Site S	Site C	
	(Kcal/mol)	(Kcal/mol)	
CDP	-9.23	- 6.44	
dATP	-11.75	-	
CitrGlu	-6.76	-6.53	
PyrGlu	-6.47	-3.64	
VanGlu	-	-6.66	

3HND			
Molecule	Site S	Site C	
	(Kcal/mol)	(Kcal/mol)	
GDP	-10.23	-7.69	
dTTP	-13.4	-8.05	
CitrGlu	-	-5.8	
PyrGlu	-5.0	-4.81	
VanGlu	-4.95	-5.36	

Table 3.2 – Binding energies for glycosylated thiosemicarbazones

As can be noticed the binding energies in the catalytic site for the acetylated glucose derivatives (gray background in Tab. 3.3) are of the same order of magnitude as the natural molecules and this has encouraged me in the synthesis of glycosylated thiosemicarbazones.

2WGH			3HND		
Molecule	Site S (Kcal/mol)	Site C (Kcal/mol)	Molecule	Site S (Kcal/mol)	Site C (Kcal/mol)
CDP	-9.23	- 6.44	GDP	-10.23	-7.69
dATP	-11.75	-	dTTP	-13.4	-8.05
CitrAcGlu	-6.02	-7.91	CitrAcGlu	-4.83	-7.35
PyrAcGlu	-	-6.66	PyrAcGlu	-4.7	-6.92
VanAcGlu	-	-6.59	VanAcGlu	-5.55	-7.23

Table 3.3 – Binding energies for acetylated glucosyl thiosemicarbazones

3.2 Synthesis of glycosylated thiosemicarbazones

Considering the interesting data obtained we decided to synthesize new glycosylated thiosemicarbazones employing not only glucose but galactose as well. The idea was to prepare tridentate ligands bearing the sugar moiety at N1 keeping free the N4 (Fig. 3.3)

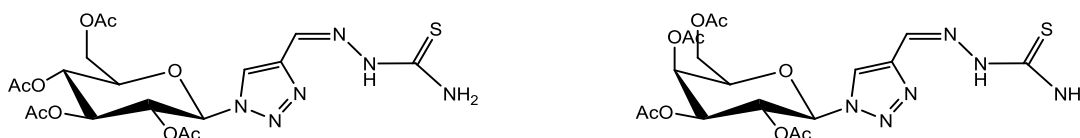


Figure 3.3 – Glucosyl (left) and galactosyl (right) thiosemicarbazones (GluOAcTriTSC and GalOAcTriTSC)

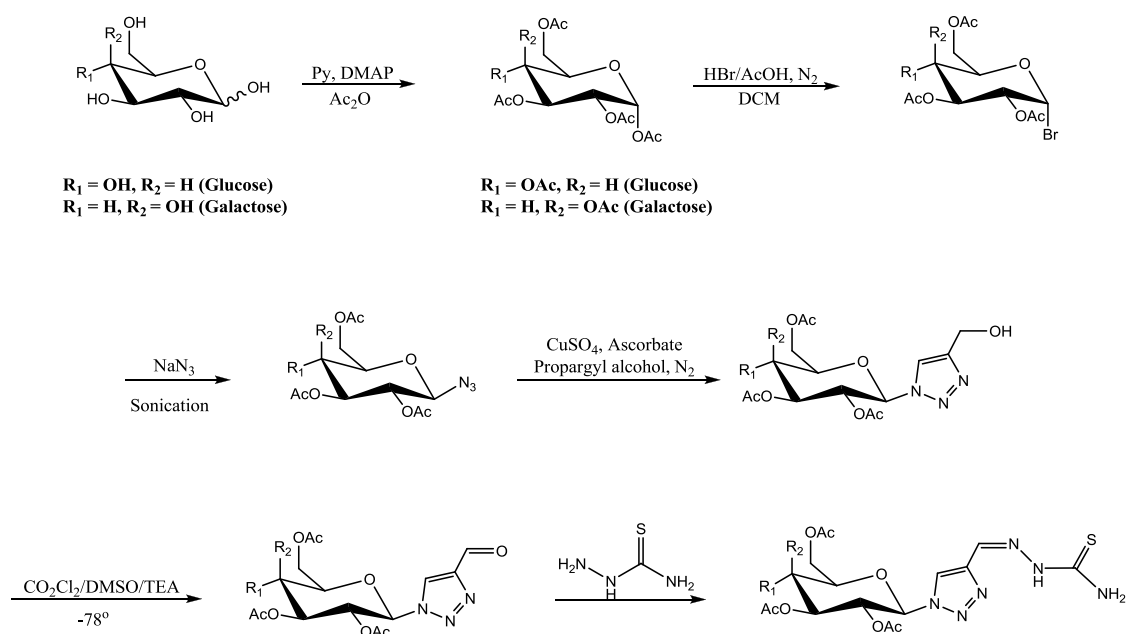


Figure 3.4 – Synthesis of GluOAcTriTSC and GalOAcTriTSC

The general synthesis of GluOAcTriTSC and GalOAcTriTSC (Fig. 3.4) was performed by brominating acetylated sugars (4- dimethylaminopyridine, Py, Ac₂O). Halogenated sugars were sonicated⁷ for 10' in presence of sodium azide to obtain a β-azo-sugar which subsequently underwent to Azide-Alkyne Huisgen Cycloaddition to give a hydroxy-glycosyl-triazole. To form a thiosemicarbazone the hydroxyl group was oxidized to aldehyde in presence of oxalyl chloride and dimethyl sulfoxide (Swern oxidation) at -80°C to avoid the occurring of side reactions. Once obtained, the aldehyde was condensed with the thiosemicarbazide to form the desired thiosemicarbazones.

As the complexes of glycosylated citronellal were the most active among the glycosylated series (Chapter 2) we decided to prepare and test the copper(II) and nickel(II) derivatives of acetylated CitrGlu. Ligand synthesis is reported in the

experimental section of chapter 2. The synthesis of both complexes was carried out in ethanol using a molar ratio metal-ligands 1:2, but the only compounds we were able to characterize was the nickel complex while all attempts to obtain the copper complex did not give to desired product.

3.3 Biological assays

Preliminary biological tests were done on Ni(CitrGluOAc)₂ and GalTriazTSC derivatives but U937 cells did not show any appreciable response even at concentrations of 100 and 50 μM respectively.

3.4 Conclusions

Interactions between a series of glycosylated thiosemicarbazones previously synthesized and two different structures of ribonucleotide reductase found in the Protein Data Bank were evaluated by docking studies. These studies revealed that these compounds have no affinity for the specificity site S and low affinity for the catalytic site C. Observing that the few interactions of the glucosyl moiety with the environment of the catalytic site C were due to its small size we attempted further docking studies using as a model the acetylated glucosyl derivatives. These molecules, presenting a larger steric hindrance and higher number of hydrogen acceptor atoms, gave promising results as potential inhibitors. In fact the binding energies of acetylated glucose derivatives are comparable with the energy associated to the natural ligands (CDP and GDP). Encouraged by these results two new glycosylated ligands were synthesized: a glucose and a galactose derivative.

As stated above, since the complexes of glycosylated citronellal were the most promising, we focused our experiments on the copper(II) and nickel(II) derivatives of the acetylated CitrGlu. The only compound we were able to fully characterize was the nickel complex while the expected copper complex was not obtained.

Biological assays were performed on three of the above mentioned compounds: the GalTriazTSC, the CitrAcGlu and its nickel complex $\text{Ni}(\text{CitrAcGlu})_2$ but we could not observe any activity even at high concentrations.

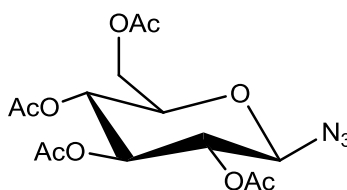
3.5 Experimental

TLC were performed on Silica gel Merck 60 F₂₅₄ aluminium sheets. Flash chromatography was performed on MP Silica 63-200 mesh 60Å (EchoChrom™), ¹H and NMR spectra were recorded on Bruker 300 Avance and Bruker 400 Avance spectrometers, at 300 K. The reported *J* values are referred to H,H coupling constants. Chemical shifts are reported as δ values in ppm using the solvent residual peak as internal standard. Elemental analysis were recorded on Flash 1112 Series Analyser (CE Instruments) Mass spectra by electrospray ionization (ESI) methods were recorded on LTQ ORBITRAP XL Thermo.

3.5.1 Ligands synthesis

[AzGluOAc]

1-Azido-1-deoxy-β-glucoopyranoside tetraacetate



A solution of aceto bromo- α -D-glucose (3 g, 7.29 mmol) and sodium azide (0.57 g, 8.76 mmol) in DMSO (35 mL) was sonicated for 10'. After that time the solution was diluted with water (100 mL) and extracted twice with chloroform (100 mL). The organic phase was anhydriified with Na₂SO₄

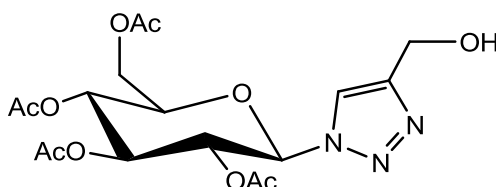
Anhydrous and concentrated under pressure to give a white solid which crystallize. If necessary the product was purified by flash chromatography (AcOEt/C₆H₁₂ 1:2).

Yield: 95%

¹H NMR (300 MHz, CDCl₃) : δ_H (ppm) 5.24 (t, *J* = 9.43 Hz, 1H). 5.13 (t, *J* = 9.67 Hz, 1H), 4.98 (t, *J* = 8.94 Hz, 1H), 4.67 (d, *J* = 8.84 Hz, 1H), 4.30 (dd, *J* = 12.48, 4.76 Hz, 1H), 4.19 (dd, *J* = 12.45, 2.33 Hz, 1H), 3.82 (ddd, *J* = 9.91, 4.73, 2.35 Hz, 1H), 2.10 (m, 12H, OAc),

[GluOAcTriOH]

4-Hydroxymethyl-1-(2',3',4'6'-tetra-O-acetyl-β-D-glucopyranosyl)-1,2,3-triazole



To a solution of glycosyl azide (1.1 g, 2.41 mmol) and propargyl alcohol (0.189 mL, 3.2 mmol) in acetone (10 mL) were added a solution of CuSO₄·5H₂O (0.124 g, 0.5 mmol) in water (5 mL) and ascorbic acid (0.88 g, 0.5 mmol) in water (5 mL). The solution was sonicated for 1h. After that time solvent was let slowly evaporate to obtain white crystals.

Yield: 65%

^1H NMR (300 MHz, CDCl_3) : δ_{H} (ppm) 7.85 (s, 1H, $\text{NCH}=\text{C}$), 5.92 (d, $J = 9.10$, 1H, $H-1$), 5.46 (m, 1H, $H-2$, $H-4$), 5.27 (t, $J = 9.10$ Hz, 1H, $H-3$), 4.80 (s, 2H, CH_2OH), 4.30 (dd, $J = 12.60$, 4.90 Hz, 1H, $H-6$), 4.16 (dd, $J = 12.60$, 2.06 Hz, 1H, $H-6$), 4.04 (ddd, $J = 10.08$, 4.90, 2.06 Hz, 1H, $H-5$), 2.90 (s, 1H, CH_2OH), 2.08 (s, 6H, OAc), 2.04 (s, 3H, OAc), 1.88 (s, 3H, OAc)

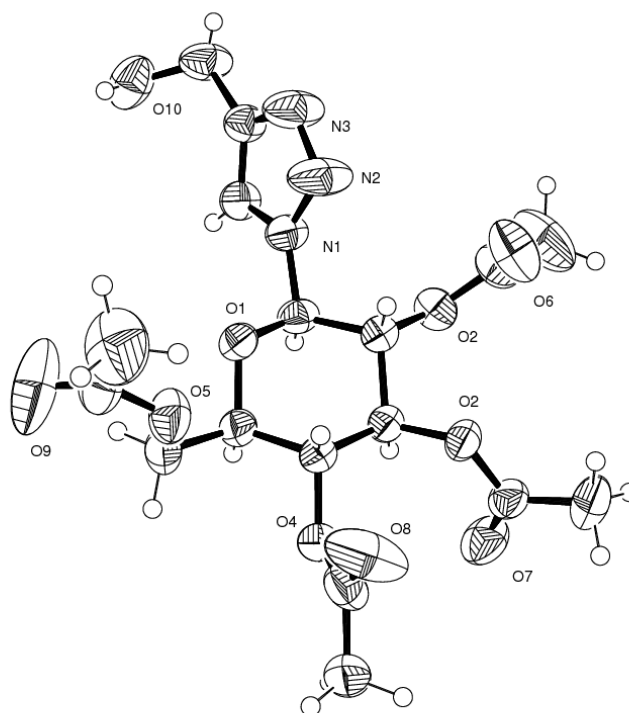
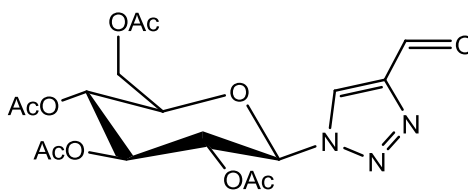


Figure 3.5. ORTEP drawing of 4-Hydroxymethyl-1-(2',3',4',6'-tetra-O-acetyl- β -D-glucopyranosyl)-1,2,3-triazole (50% probability plot).

The X-ray structure was solved from data collected on a Bruker-Siemens SMART AXS 1000 diffractometer equipped with a CCD detector. Mo-K α ($\lambda = 0.71069 \text{ \AA}$) The structure was solved by direct methods and refined using SHELXL97. The drawing was plotted using ORTEPIII. Crystallographic data: C₁₇H₂₃N₃O₁₀, Mr = 427.37, orthorhombic, space group P2₁2₁2₁, a = 8.134(1), b = 15.190(2), c = 17.002 (3) \AA ; V = 2100.7(5) \AA^3 , Z = 4, $\rho_{\text{calc}} = 1.335 \text{ Mgm}^{-3}$, T = 298.15 K, F(000) = 896, crystal size = 0.60x0.60x0.60 mm, index range = $-11 < h < 11$, $-21 < k < 21$, $-24 < l < 24$, collected reflections = 34084, unique reflections = 6423, refined parameters = 311, goodness-of-fit = 1.062, final R factor = 0.0517, wR2 = 0.1597, electronic density residues = 0.26 and -0.22 e\AA^{-3} .

[GluOAcTriO]

4-Formyl-1-(2',3',4'6'-tetra-O-acetyl- β -D-glucopyranosyl)-1,2,3-triazole



A stirred solution of oxalyl chloride (0.117 mL, 1.29 mmol) in dichloromethane (7 mL) was cooled to -78°C , after that a solution of dimethylsulfoxide (0.117 mL, 1.29 mmol) in dichloromethane (7 mL) was rapidly added and the temperature kept at -78°C . After 5' minutes was slowly (10') dropped a solution of glycosyl triazole (0.2 g, 0.46 mmol) in dichloromethane keeping the temperature constant (-78°C). The solution was stirred

for 15' and after that period of time triethylamine (4 mL, 30mmol) was added. Stirring was continued for 5' at -78°C and then temperature was let rise r.t. The solution was filtered, washed with water, the organic phase was then anhydricated with Na₂SO₄ anhydrous and finally concentrated under reduced pressure.

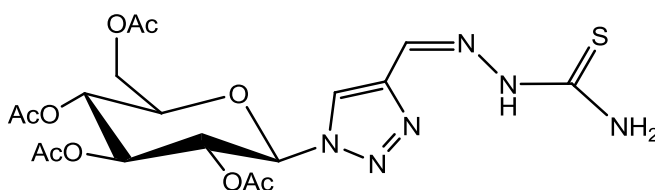
The product was purified by flash chromatography (AcOEt/C₆H₁₂ 1:2).

Yield: 80%

¹H NMR (300 MHz, CDCl₃) : δ_H ppm 10.18 (s, 1H, CHO), 5.95 (d, *J* = 10.06 Hz, 1H, *H*-1), 5.48 – 5.41 (m, 2H), 5.28 (t, *J* = 10.06, 1H), 4.34 (dd, *J* = 12.40, 4.85 Hz, 1H, *H*-6), , 4.20 (dd, *J* = 12.40, 2.30 Hz, 1H, *H*-6), 4.06 (ddd, *J* = 10.06, 4.85, 2.30 Hz, 1H, *H*-5), 2.12 (s, 3H, OAc), 2.10 (s, 3H, OAc), 2.06 (s, 3H, OAc), 1.94 (s, 3H, OAc)

[GluOAcTriTSC]

1-(2',3',4'6'-tetra-O-acetyl-β-D-glucopyranosyl)-1,2,3-triazo-4-Thiosemicarbazone



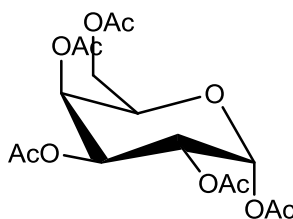
After dissolution of (0.820 g, 1.9 mmol) in ethanol (30 mL) thiosemicarbazide (0.190 g, 2.09 mmol) was added and the mixture was stirred at r.t. for 24 h resulting in a white precipitate which was filtered and washed with ethanol.

Yield : 94%

¹H NMR (300 MHz, DMSO-*d*₆) : δ_H ppm 10.38 (s, 1H, *NH*), 8.83 (s, 1H, *CH=N*), 7.91 (s, 1H, *CH=C*), 6.49 (s, 2H, *NH*₂), 6.40 (d, *J* = 9.20 Hz, 1H, *H-1*), 5.61 (t, *J* = 9.20 Hz, 1H, *H-3*), 5.51 (t, *J* = 9.20 Hz, 1H, *H-2*), 5.14 (t, *J* = 9.20 Hz, 1H, *H-4*), 4.40 (ddd, *J* = 9.20, 5.47, 2.33 Hz, 1H, *H-5*), 4.18 (dd, *J* = 12.31, 5.47 Hz, 1H, *H-6*), 4.08 (dd, *J* = 12.31, 2.33 Hz, 1H, *H-6*), 2.05 – 1.83 (4s, 12H, *OAc*)

[GalOAc]

Galactose pentaacetate



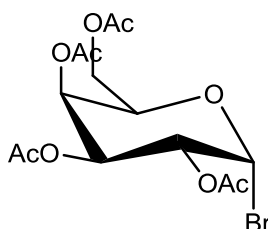
To a round flask containing D-Galactose (1g, 9.24 mmol) in AcO₂ (7 mL) were added pyridine (7mL) and a small amount of 4- dimethylaminopyridine. The solution was stirred in an ice-cold bath for 5h and than at r.t. for 18h. Dichlorometane (20mL) and water (20mL) were added to the solution, the organic phase was then separated and consecutively washed with a sat. aq. CuSO₄ until the dark blue color disappear, water (20mL), dried over Na₂SO₄ and concentrated under reduced pressure to give an oil which crystallize.

Yield: 92%

$^1\text{H NMR}$ (300 MHz, CDCl_3) : δ_{H} (ppm) 5.71 (d, 1H, *H-1*), 5.43 (m, 1H, *H-4*), 5.33 (t, 1H, *H-2*), 5.09 (dd, 1H, *H-3*), 4.16 (m, 1H, *H-6*), 4.17 (m, 1H, *H-7*), 4.07 (m, 1H, *H-5*), 2.17 – 2.00 (4s, 15H, 5 OAc)

[GalOAcBr]

Acetobromo- α -D-galactose



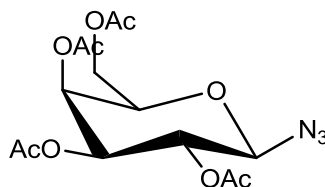
In un pallone a due colli contenente galattosio pentacetato (1 g, 2.56 mmol) in diclorometano (5 ml), mantenuto sotto atmosfera di azoto, è stato aggiunto HBr 33% (1.2 mL, 7.68 mmol). La soluzione risultante è stata agitata fino a quando la TLC ($\text{AcOEt}/\text{C}_6\text{H}_{12}$ 2:3) non ha mostrato la scomparsa del composto di partenza. Successivamente la soluzione è stata concentrata sotto pressione, sciolta in diclorometano (10 mL), lavata ripetutamente con NaHCO_3 aq. sat., acqua e infine la fase organica è stata anidrificata e concentrata sotto pressione per dare un olio che all'aria cristallizza. Se necessario il solido ottenuto è stato purificato tramite flash cromatografia con miscela ($\text{AcOEt} / \text{C}_6\text{H}_{12}$ 2:3)

Yield: 87%

$^1\text{H NMR}$ (300 MHz, CDCl_3) : δ_{H} (ppm) 6.69 (d, $J = 3.92$ Hz, 1H, $H-1$), 5.51 (d, $J = 3.12$ Hz, 1H, $H-4$), 5.39 (dd, $J = 10.67, 3.12$ Hz, 1H, $H-3$), 5.04 (dd, $J = 10.67, 3.92$ Hz, 1H, $H-2$), 4.48 (t, $J = 6.54$ Hz, 1H, $H-5$), 4.18 (dd, $J = 11.40, 6.54$ Hz, 1H, $H-6$), 4.10 (dd, $J = 11.40, 6.54$ Hz, 1H, $H-6$), 2.07 (4s, 12H, OAc)

[AzGalOAc]

1-Azido-1-deoxy- β -galactopyranosyl tetra acetate



A solution of aceto bromo- α -D-galactose (3 g, 7.29 mmol) and sodium azide (0.57 g, 8.76 mmol) in DMSO (35 mL) was sonicated for 10'. After that time the solution was diluted with water (100 mL) and extracted twice with chloroform (100 mL). The organic phase was anhydricated with Na_2SO_4 .

Anhydrous and concentrated under pressure to give a white solid which crystallize. If necessary the product was purified by flash chromatography ($\text{AcOEt}/\text{C}_6\text{H}_{12}$ 1:2).

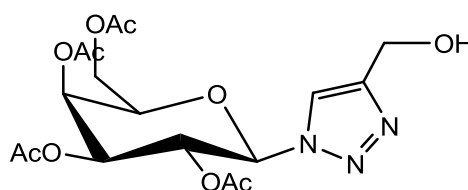
Yield : 93%

$^1\text{H NMR}$ (300 MHz, CDCl_3) : δ_{H} (ppm) 5.45 (dd, $J = 3.29, 1.09$ Hz, 1H, $H-4$), 5.19 (dd, $J = 10.39, 8.68$ Hz, 1H, $H-2$), 5.06 (dd, $J = 10.36, 3.34$ Hz, 1H, $H-3$), 4.62 (d, $J = 8.67$

Hz, 1H, *H-1*), 4.20 (dd, $J = 6.54, 2.39$ Hz, 2H, *H-6*), 4.04 (m, 1H, *H-5*), 2.09 (4 s, 12H, *OAc*).

[GalOAcTriOH]

4-Hydroxymethyl-1-(2',3',4'6'-tetra-O-acetyl- β -D-galactopyranosyl)-1,2,3-triazole



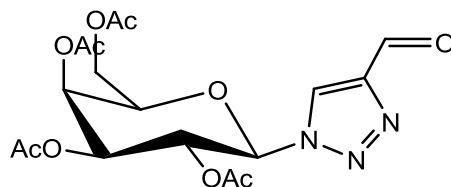
To a solution of 1-Azido-1-deoxy- β -galactopyranosyl tetra acetate (0.90 g, 2.41 mmol) and propargyl alcohol (0.170 mL, 2.9 mmol) in t-Butanol (10 mL) were added two aqueous solutions (5 mL) of $\text{CuSO}_4 \cdot 5\text{H}_2\text{O}$ (0.134 g, 0.54 mmol) and ascorbic acid (0.188 g, 1.07 mmol). The resulting solution was reflux under nitrose atmosphere and monitored by TLC (AcOEt/ C_6H_{12} 2:1). After 4 h water was added (100 mL) and the organic phase was extracted twice with ethyl acetate (100mL). The organic phase was anhydricated with Na_2SO_4 anhydrous and concentrated under reduced pressure. Finally the product was purified by flash chromatografia (AcOEt/ C_6H_{12} 1:2).

Yield: 77,2%

$^1\text{H NMR}$ (300 MHz, CDCl_3) : δ_{H} (ppm) 7.89 (bs, 1H, $\text{NCH}=\text{C}$), 5.87 (d, $J = 9.36$ Hz, 1H, *H-1*), 5.57 (m, 2H, *H-2*, *H-4*), 5.27 (dd, $J = 10.25, 3.37$ Hz, 1H, *H-3*), 4.84 (s, 2H, CH_2OH), 4.22 (m, 3H, *H-5*, *H-6*, *H-6'*), 2.25-2.03 (4s, 12H, *OAc*)

[GalOAcTriO]

4-Formyl-1-(2',3',4'6'-tetra-O-acetyl-β-D-galactopyranosyl)-1,2,3-triazole



A stirred solution of oxalyl chloride (0.117 mL, 1.29 mmol) in dichloromethane (7 mL) was cooled to -78°C , after that a solution of dimethylsulfoxide (0.117 mL, 1.29 mmol) in dichloromethane (7 mL) was rapidly added and the temperature kept at -78°C . After 5' minutes was slowly (10') dropped a solution of galctosyl triazole (0.2 g, 0.46 mmol) in dichloromethane keeping the temperature constant (-78°C). The solution was stirred for 15' and after that period of time triethylamine (4 mL, 30mmol) was added. Stirring was continued for 5' at -78°C and then temperature was let rise r.t. The solution was filtered, washed with water, the organic phase was then anhydricated with Na_2SO_4 anhydrous and finally concentrated under reduced pressure.

The product was purified by flash chromatography ($\text{AcOEt}/\text{C}_6\text{H}_{12}$ 1:2).

Yield: 74%

$^1\text{H NMR}$ (300 MHz, CDCl_3) : δ_{H} (ppm) 10.17 (s, 1H, CHO), 8.44 (s, 1H, NCH=C), 5.94 (d, $J = 9.15$ Hz, 1H, H-1), 5.59 (d, $J = 3.30$ Hz, 1H, H-4), 5.52 (t, $J = 9.15$, 1H, H-2), 5.31 (dd, $J = 9.15, 3.30$ Hz, 1H, H-3), 4.21 (m, 3H, H-5, H-6, H-6'), 2.24 (s, 3H, OAc) 2.06 (s, 3H, OAc), 2.03 (s, 3H, OAc), 1.93 (s, 3H, OAc)

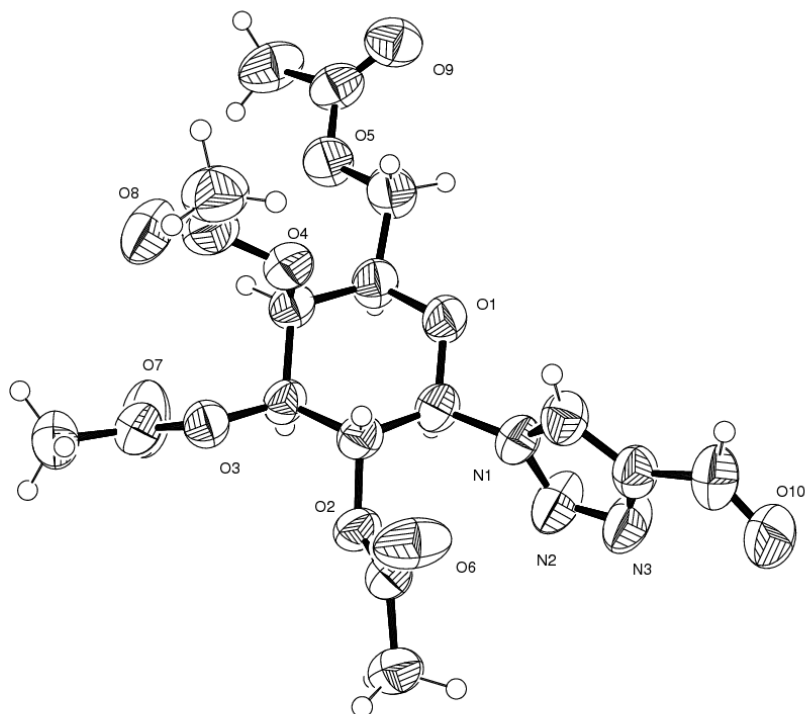


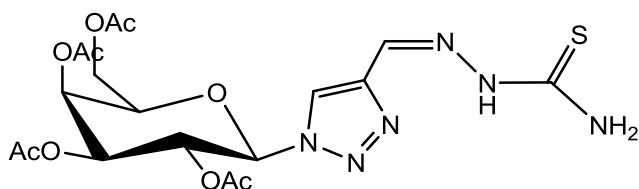
Figure 3.5. ORTEP drawing of 4-formyl-1-(2',3',4',6'-tetra-O-acetyl- β -D-galactopyranosyl)-1,2,3-triazole (50% probability plot).

The X-ray structure was solved from data collected on a Siemens AED diffractometer. Cu-K α ($\lambda = 1.54178 \text{ \AA}$) The structure was solved by direct methods and refined using SHELXL97. The drawing was plotted using ORTEPIII. Crystallographic data: C₁₇H₂₃N₃O₁₀, Mr = 427.37, orthorhombic, space group P2₁2₁2₁, a = 9.0621(5), b = 25.398(5), c = 9.0492(9) \AA ; V = 2082.8(5) \AA^3 , Z = 4, $\rho_{\text{calc}} = 1.363 \text{ Mg m}^{-3}$, T = 298.15 K, F(000) = 896, crystal size = 0.60x0.30x0.30 mm, index range = 0 < h < 11, 0 < k < 30, 0 < l < 11, collected reflections = 2289, unique reflections = 2258, refined parameters =

271, goodness-of-fit = 0.928, final R factor = 0.0456, wR2 = 0.1313, electronic density residues = 0.18 and $-0.14 \text{ e}\text{\AA}^{-3}$.

[GalOAcTriTSC]

4-Thiosemicarbazone-1-(2',3',4'6'-tetra-O-acetyl- β -D-galactopyranosyl)-1,2,3-triazole



After dissolution of formyl galacto triazole (0.820 g, 1.9 mmol) in ethanol (30 mL) thiosemicarbazide (0.190 g, 2.09 mmol) was added and the mixture was stirred at r.t. for 24 h resulting in a precipitate which was filtered and washed with ethanol.

Yield: 94%

$^1\text{H NMR}$ (300 MHz, $\text{DMSO-}d_6$) : δ_{H} (ppm) 11.54 (s, 1H, *NH*), 8.88 (s, 1H, *HC=N*), 8.12 (s, 1H, *HCNN*), 8.08 (s, 1H), 6.35 (d, $J = 8.78 \text{ Hz}$, 1H, *H-1*), 5.49 (m, 3H, *H-2*, *H-3*, *H-4*), 4.70 (m, 1H, *H-5*), 4.16 (dd, $J = 11.42, 4.91 \text{ Hz}$, 1H, *H-6*), 4.05 (dd, $J = 11.66, 7.27 \text{ Hz}$, 1H, *H-6'*), 2.1 – 1.8 (4s, 3H, *OAc*)

Complex synthesis

[Ni(CitrGluOAc)₂]

A solution of Ni(OAc)₂·4H₂O (0.33 g, 0.13 mmol) and CitrGluOAc (0.15 g, 0.26 mmol) in EtOH (35 mL) was refluxed for 4 h, then cooled to r.t. The solution was poured into a crystallizer and the solvent slowly evaporate to afford a dark green-brown solid.

Yield: 90%

Elem. An: C₅₀H₇₆N₆NiO₁₈S₂ C=51,24%; H=6,54%; N=7,17% Found C=51,28%; H=6,62%; N=7.03%.

ESI-MS : m/z = 1172.1 [ML₂+H]⁺

3.6 References

- 1) Jordan A, Reichard P, *Annu. Rev. Biochem.* **1998**, 67, 71–98
- 2) Raje N, S. Kumar S, Hideshima T, Ishitsuka K, Yasui H, Chhetri S, Vallet S, Vonescu E, Shiraishi N, Kiziltepe T, Elford H.L, Munshi N.C, Anderson K.C, *British Journal of Haematology*, **2006**, 135(1), 52-61
- 3) Thelander L, *Nature Genetics*, **2007**, 39, 6, 703
- 4) Shao J, Zhou B, Bernard Chu, Y. Yen, *Current Cancer Drug Targets*, **2006**, 6, 409-431
- 5) Larsson K.M, Jordan A, Eliasson R, Reichard P, Logan D.T, Nordlund P, *Nature Structural & Molecular Biology*, **2004**, 11(11), 1142-1149
- 6) Fairman W.J *et al*, *Nature Structural & Molecular Biology*, **2011**, 18(13), 316-323
- 7) Deng Schenglou, Gangadharmath U, Chang T. Cheng Wei, *J. Org. Chem*, **2006**, 71, 5179-5185

Chapter 4

Thiosemicarbazones as inhibitors of topoisomerase II α

4.1 Topoisomerase II α

Topoisomerase are a family of ubiquitous enzymes involved in regulation of supercoiling DNA¹. Type II topoisomerases are cellular enzymes involved in altering the supercoiled DNA, in segregation of newly replicated chromosome pairs and in chromosome condensation^{2,3}. The eukaryotic enzymes are dimers (170 k-Da) while prokaryotic are A2B2 tetramers.

Type II topoisomerases work by cleaving and opening one DNA duplex, passing a second duplex through the opening and then resealing the break^{4,5}. The DNA cleavage is a transesterification, mediated by magnesium, between a pair of tyrosyl residues and a pair of a DNA phosphodiester base³.

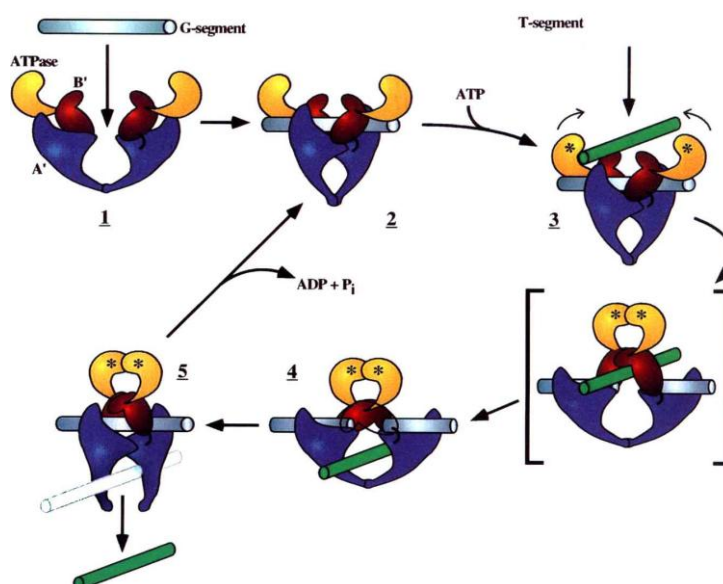


Figure 4.1 - Topoisomerase II model of catalytic reaction

In Fig. 4.1 is depicted the catalytic reaction cycle of topoisomerase II: the ATPase domain, B' and A' subfragments are coloured yellow, red and blue, respectively. The G-segment DNA (containing DNA gate) is grey and the transported T-segment is green. The catalytic cycle begins with the binding of DNA substrate by Topo-II (1). Once bound ATP (represented by asterisks) (2) and the T-segment a series of conformational changes occur causing the split of the G-segment by the A' subfragments. Concomitantly, the ATPase domains dimerize and the T-segment is transported through the break and into the central hole (4). Once the DNA is transported, the G-segments is resealed and the T-segment released from the enzyme through the opening of the dimer interface between A'(5). The interface between the two A' subfragments again dimerizes and ATP is hydrolyzed and released to regenerate the starting state (2)³.

4.1.1 Topoisomerase inhibition

Since the discovery that Topoisomerase II (Topo-II) was the target of active cancer drugs, in particular doxorubicin and etoposide, this enzyme has gained some attention. (Fig. 4.2)^{6,7}.

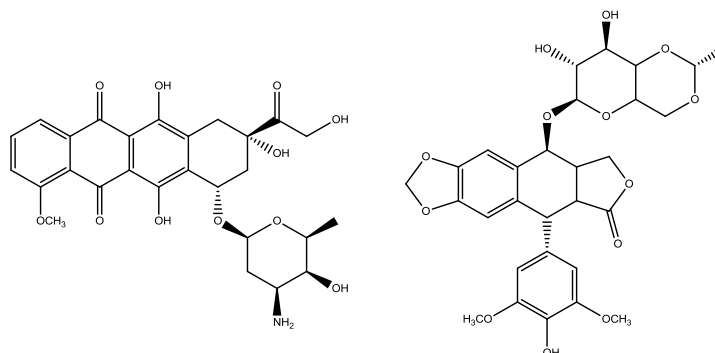


Figure 4.2 – Doxorubicin (left), etoposide (right)

Studies revealed that the most clinically active drugs that target Topo-II generate enzyme-mediated DNA damage^{7,8}. Drugs targeting Topo-II are classified in two groups, according to their effect on enzyme function (Fig. 4.3). The first group, which includes doxorubicin and etoposide is called Topo-II poisons. The mechanism of action of this class of drugs is to stabilize the cleavable complex forming a drug-enzyme-DNA complex which is toxic and can induce apoptosis. Drugs belonging to the second class, called catalytic inhibitors, interfere with Topo-II catalytic activity, preventing DNA-enzyme linkage or its release from DNA, leading to cell death⁹. Inhibition of Topo-II at several different points of the enzyme catalytic cycle entails different cellular and biochemical consequences.

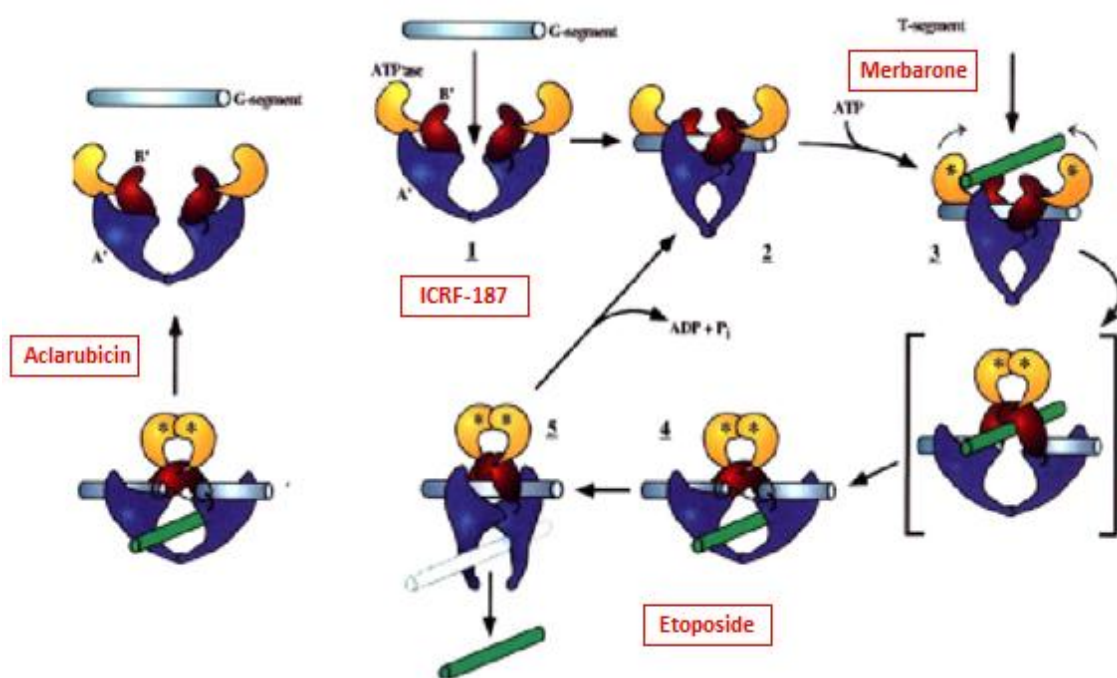


Figure 4.3 – Mode of action of different Topo-II inhibitors

Antibiotics belonging to the family of coumarins like novobiocin and coumermycin, known to inhibit nucleic acid synthesis in bacteria, compete with ATP for binding Topo-II¹⁰. Other drugs used in cancer therapy, which can inhibit Topo-II are aclarubicin, merbaron, etoposide. Aclarubicin, an anthracycline drug, used for the treatment of acute myelocytic leukemia, inhibits the binding of DNA to Topo-II, acting as an intercalating agent¹¹.

Another way to block the catalytic activity is to prevent the relegation of the cleaved DNA. This is the mechanism of action of etoposide, which stabilizes each of the two scissile bonds of the cleavage complex inducing in this manner cell death¹².

Topo-II α can also be inhibited after that the strand passage is completed but before ATP hydrolysis by bisdioxopiperazines, such as dexrazoxane (ICRF-187), which inhibits ATP hydrolysis and maintains the enzyme close around the DNA¹¹.

4.2 Thiosemicarbazones and topoisomerase II α

Several research groups have investigated thiosemicarbazones as antitumor agents and have shown that some of these compounds inhibit Topo-II, stabilizing the cleavable products formed by Topo-II and DNA¹³⁻¹⁵. A few papers have also been published regarding thiosemicarbazones^{16,17} and as metal complexes^{18,19}. Ashutosh Rao *et al.*¹⁶ showed that Dp44mT (Fig. 4.4), a molecule with antitumor activity used in mice xenografted with a range of human tumors, causes DNA damage and inhibition of Topo-II α activity. In their work they demonstrated that Dp44mT can selectively inhibit Topo-II α and not Topo-I nor Topo-II β .

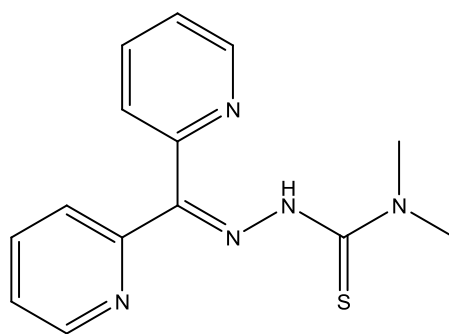


Figure 4.4 – Dp44mT a potent iron chelator

The Topo-II α -mediated activity of Dp44mT was observed using Nalm-6 leukemia cells that were heterozygous deficient for Topo-II α , in which Dp44mT had only half of the cytotoxic activity compared with wild-type cells. In addition, Dp44mT is able to induce the formation of stable cellular Topo-II α -DNA complexes, indicative of Topo-II α poisoning in cancer cells. In the same period Huang *et al.*¹⁷ discovered that, among a new series of α -heterocyclic TSCs, one compound (4,4'-N-Dimethyl quinoline thiosemicarbazone, TSC24) (Fig 4.5) exhibited broad antiproliferative activity in a panel of human tumor cells and suppressed tumor growth in mice.

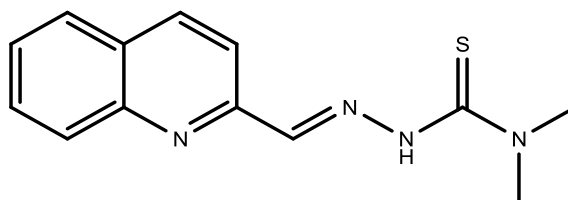


Figure 4.5 – 4,4'-N-Dimethyl quinoline thiosemicarbazone (TSC24)

Mechanism studies revealed that TSC24 acts as a topoisomerase II- α catalytic inhibitor. First, HL-60/MX2 cells, which are resistant to Topo-II poison such as etoposide phosphate (VP-16) were fully sensitive to TSC24. Second, TSC24 failed to trap Topo-IIA-DNA complexes but antagonized etoposide-stabilized cleavage complexes in the presence of ATP. Finally, TSC24 was unable to induce DNA damage but countered etoposide-mediated DNA damage in HT-29 cells. Further studies revealed that TSC24 inhibited Topo-II-mediated ATP hydrolysis. High affinity of TSC24 for HsATPase was revealed with SPR assay (surface plasma resonance spectroscopy). Molecular docking predicted that TSC24 act as an ATP competitor, binding to ATP-binding pocket in a planar conformation with the heterocyclic nitrogen, imine nitrogen, and sulfur forming a meridional tridentate coordination environment^{17,18}.

Recent discovery of the topoisomerase II α (Topo-II α) inhibition property of thiosemicarbazones and their metal complexes expanded the array of biochemical targets and reinforced the potential application of metal thiosemicarbazonato complexes in cancer research. Furthermore recent publications showed *in vivo* and *in vitro* inhibition of Topo-II α by α -heterocyclic thiosemicarbazones and their Cu(II) complexes at IC₅₀ below that of the widely employed Topo-II α poison etoposide (VP-16). The importance of Topo-II α in many forms of cancer and the great potential of thiosemicarbazones and their metal complexes as chemotherapeutics agents open new pathways of study¹⁸.

In 2006 Lihui Wei *et al*¹⁹ investigated the relationship between the *in vitro* and *in vivo* behavior of novel ⁶⁴Cu-TSC complexes (Fig. 4.6) and the expression of Topo-II activity. Small-animal PET of animals with L1210 tumors (high Topo-II expressing

cells) showed excellent tumor accumulation compared with that of animals with PC-3 tumors (low Topo-II expressing) and the L1210 tumor uptake was significantly reduced by coadministration of a Topo-II poison.

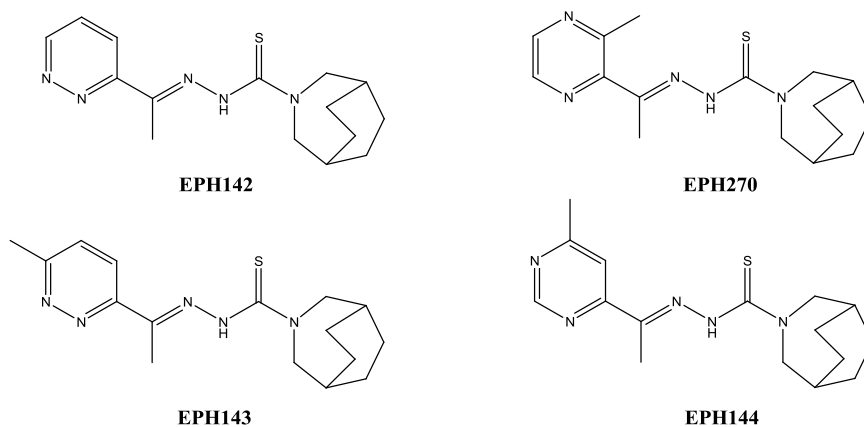


Figure 4.6 - Structures of ligands EPH142, EPH143, EPH144, and EPH270 used to prepare ^{64}Cu labeled complexes

Similar results appeared in a recent work¹⁸ where several copper (II) complexes of α -heterocyclic thiosemicarbazones of formyl pyridine and acetyl pyrazine (Fig. 4.7) were tested *in vitro* as Topo-II α inhibitors and as antiproliferative in SK-BR-3 and MCF-7 breast cancer cells, expressing respectively high and low levels of Topo-II α .

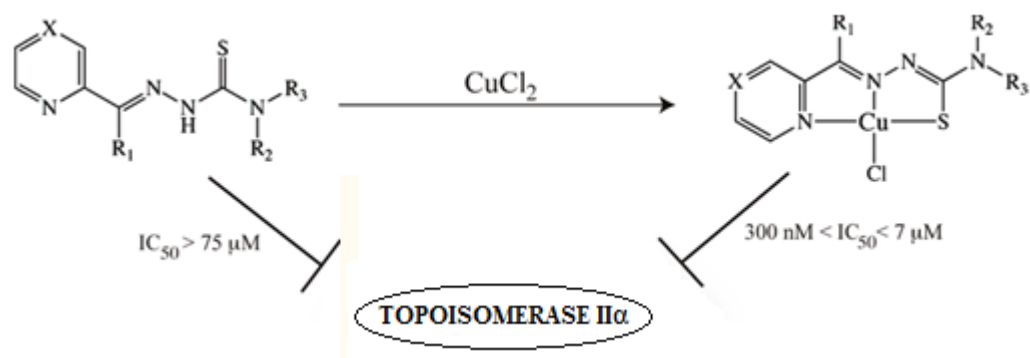


Figure 4.7 – Biological activity of α -heterocyclic thiosemicarbazones and their Cu(II) complexes.

Cu(TSC)Cl complexes resulted to inhibit Topo-II more strongly than the ligands alone and possess with respect to them a GI₅₀ in most cases lower by well over an order of magnitude. Gel electrophoresis experiments revealed that Cu(TSC)Cl complexes are catalytic inhibitors rather than poisons, even though the mechanism remains unknown. Considering copper complexes, noteworthy are their low GI₅₀ values from <1 to 6 μ M with SK-BR-3 cells and from 2 to 12 μ M with MCF-7 cells suggesting that Topo-II α inhibitions may play a role in antiproliferative effects of these complexes.

4.3 Project description

Taking into account the hypothesized action mechanism of these α -heterocyclic compounds, in particular TSCS24¹⁷, and the higher activity they show when bound to metals, I decided to synthesize tridentate derivatives using as starting aldehydes formyl quinoline and two substituted isatins (5-fluoro and sodium 5-sulfonate isatins - Fig. 4.8) to study how the presence of substituents on the thiosemicarbazide fragment and how

the coordination to copper(II) and nickel(II) can influence the biological activity of a this group of thiosemicarbazones. and also how the presence of a charge on the 5-sulfonate isatin can affect the internalization mechanism.

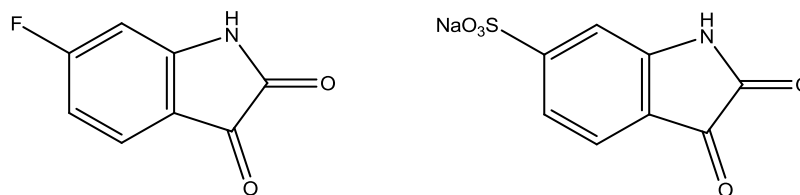


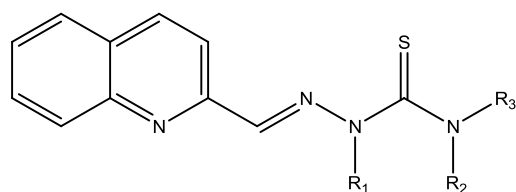
Figure 4.8 – 5-fluoro and sodium 5-sulfonate isatins

Isatin was chosen for two reasons: the first is that its thiosemicarbazones are known to possess biological activity²⁰ and the second is that once condensed with a thiosemicarbazide, the resulting thiosemicarbazone behaves as a tridentate ligand through the oxygen of the carbonyl group in β to the pyrrolidine nitrogen. Differently from my previous studies, besides checking the proliferation inhibition activity, I have also tried a different approach in an attempt to shed some light on the action mechanisms of these molecules by focusing my attention on the direct effect of thiosemicarbazones on one of the putative target enzymes: topoisomerase II α .

4.3.1 Ligands and complexes

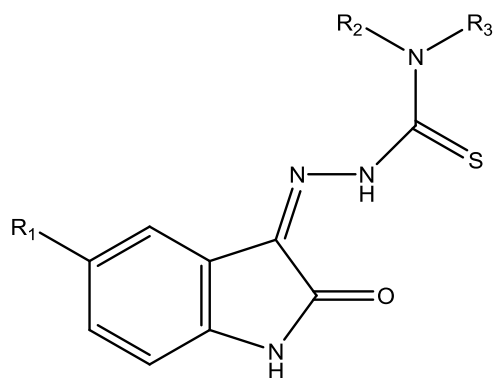
The thiosemicarbazone ligands were synthesized via the typical condensation route from their parent thiosemicarbazides and the appropriate ketone or aldehyde. N2 and N4

substituents were altered to provide a structurally systematic series of compounds. In the following tables (Tab. 4.1 and Tab. 4.2) is the list of the synthesized compounds.



	R1	R2	R3
QN42M	H	Me	Me
QN41M	H	H	Me
QN41E	H	H	Et
QN41Al	H	H	Allyl
QN41Ph	H	H	Phenyl
QN21M	Me	H	H
QN42H	H	H	H

Table 4.1 – Quinoline derivatives



	R1	R2	R3
FIN42M	F	Me	Me
FIN41M	F	H	Me
FIN41E	F	H	Et
FIN41Ph	F	H	Phenyl
SIN42M	SO ₃ Na	Me	Me
SIN41M	SO ₃ Na	H	Me
SIN41E	SO ₃ Na	H	Et
SIN41Ph	SO ₃ Na	H	Phenyl

Table 4.2 – Isatin derivatives

Subsequently, the copper and nickel complexes were prepared by heating a solution of the ligands with CuCl_2 and NiCl_2 respectively.

4.4 Proliferation inhibition assay

Due to the costs of the biological assays only part of the synthesized compounds were tested on cell line U937. To evaluate the IC_{50} of the complexes, stock solutions of the complexes were prepared dissolving the compounds in DMSO with a concentration of 10 mg/mL. U937 cells were cultured in RPMI-1640 medium with a density of $1.5 \cdot 10^5$ cell/mL. After 24h cells were transferred into a microtiter plate with 96 plates, treated with DMSO 0.1% (v/v) as control and with complex at different times. Cell proliferation was measured using Cell-Titer 96[®] Aqueous One Solution; an hour before the end of the treatment 20 μL of MTS solution were added in every plate. MTS becomes reduced from tetrazole to formazan. These reductions take place in mitochondria only when reductase enzymes are active and therefore conversion is used as a measure of viable (living) cells. Formazan is a colored compound with a maximum of absorbance at 490 nm. Using a particular spectrofluorimeter (Multiskan Acent, Thermo Labsystem, Helsinki, Finland) for microtiter plates it is possible to know the number of living cells. Every experiment was repeated three times to build a calibration curve. After 5 minutes cells were put in a hemocytometer and counted manually with an inverted microscope.

4.4.1 Cell growth inhibition of ligands and complexes

Looking at the biological activity table (Tab. 4.3) of these compounds it is possible to do some considerations.

Q	IC₅₀(μM)	FI	IC₅₀(μM)	SI	IC₅₀(μM)
QN42M	0.82				
CuQN42M	0.48	CuFIN42M	0.84		
NiQN42M	8.69				
QN41M	2.25	FIN41M	>100	SIN41M	>100
CuQN41M	2.25	CuFIN41M	2.62	CuSIN41M	>100
NiQN41M	12.05				
QN41Ph	12.05	FIN41Ph	>100	SIN41Ph	>100
CuQN41Ph	1.8	CuFIN41Ph	2.94	CuSIN41Ph	>100
QN21Me	>100				
CuQN21Me	16.2	CuFIN41E	2.74		
NiQN21Me	>100				
QN42H	55				
CuQN42H	4.1				
NiQN42H	42				

Table 4.3 – IC₅₀ values on U937 cell inhibition of free and complexed thiosemicarbazones

4.4.2 Quinolines derivatives

At first glance, it is apparent that substituents on the thiosemicarbazide nitrogens play an important role in the activity of these compounds. IC_{50} values extend over a range between $0.82\mu\text{M}$ to over $100\mu\text{M}$. The best activity ($0.82\mu\text{M}$) is shown by the derivative with two methyls on the terminal nitrogen and it already worsens for the monomethylated analogue ($2.25\mu\text{M}$). The phenyl substituted has an increase in the IC_{50} value ($12.05\mu\text{M}$) but for the free N terminal derivative the IC_{50} bounces to $55\mu\text{M}$. Methylation of N2 causes the worst effect and the molecule presents no significant activity below the $100\mu\text{M}$ concentration.

4.4.3 Quinoline metal complexes

Comparing ligands and their metal complexes it is noteworthy that all copper(II) complexes show the best IC_{50} values, from $0.48\mu\text{M}$ for CuQN42M to $16.2\mu\text{M}$ for CuQN21Me. The free ligand QN21M and its nickel complex NiQN21M have no effect for concentrations lower than $100\mu\text{M}$.

Efficacy of the compound is not only a matter of metal but also a matter of substituents, as noticed before, methyl substituent on N2 not only reduces the activity of the ligand but also that of the complexes in particular that of nickel derivatives ($>100\mu\text{M}$) while copper complexes is still appreciable ($16.2\mu\text{M}$).

4.4.4 Fluoro isatin

In the case of isatin derivatives we have unfortunately access to less assays but we can see that also in this case copper derivatives show a good activity with IC_{50} values in the

range 0.84 - 2.94 μM . These are a little bit lower than the copper quinoline analogues but higher than those of nickel. A remarkable case is the thiosemicarbazone with a methyl in position 2, which results to be much more active than both copper and nickel complexes of the quinoline series. Also this kind of derivatives follows the trend of an increase of biological activity passing from a N2 methylated to a N4 monomethylated and to N4 dimethylated. Although these difference are not so marked, the N4 dimethylated presents a noteworthy IC_{50} of 0.84 μM compared to 2.94 μM of the N2 methylated and 2.62 μM of the N4 monomethylated.

4.4.5 Sodium isatin-5-sulfonate

Isatin sulfonate derivatives independently from the nature of the substituents or metal complexes do not inhibit cellular proliferation up to concentrations of 100 μM . This is probably due to the presence of a negative charge of the sulfonate group and supports the hypothesis of passive diffusion through the cell membrane.

4.5 Topoisomerase II α inhibition assays

Inhibition assays were performed using a kit which uses eukaryotic topoisomerase-II α (TopoGen). 14 μ L of H₂O, 4 μ L of buffer solution, 1 μ L of supercoiled DNA and 1 μ L of topoisomerase-II α are mixed in a microcentrifuge tube (1.7 mL). The drug was added as a 2 μ L of a stock solution in DMSO and then water was added until a final volume of 20 μ L was reached. The reaction mixture was shaken with care, shortly centrifuged and incubated at 37°C for 30'. Subsequently 2 μ L of SDS 10% were added to quench the reaction, 2 μ L of proteinaseK to digest the remaining proteins. The reaction mixture was newly incubated at 37°C for 15'. After this second incubation 2.5 μ L of (10X) were loaded, the tube shaken and centrifuged. The resultant reaction solutions were loaded onto 1% agarose gel and electrophoresed for 5 h at 5 V/cm to separate the possible products: supercoiled DNA, linear DNA and relaxed DNA. The gel was incubated with a solution of TAE containing ethidium bromide (5 μ g/L). For visualization a BioRad Fluor-S MultiImagerTM was used.

4.5.1 Ligands and metal complexes topoisomerase II α inhibition

Concerning topoisomerase II α activity, we ran an electrophoresis gel (Fig. 4.9) for the most active ligand (the dimethylated quinoline thiosemicarbazone, QN42M, and its copper and nickel complexes CuQN42M and NiQN42M), CuQN21M, CuFIN41M and CuFIN41Ph . As an overall comment, it is noticeable that copper derivatives are effective Topo-II α inhibitors while the other two seem to have little effect on the enzyme.

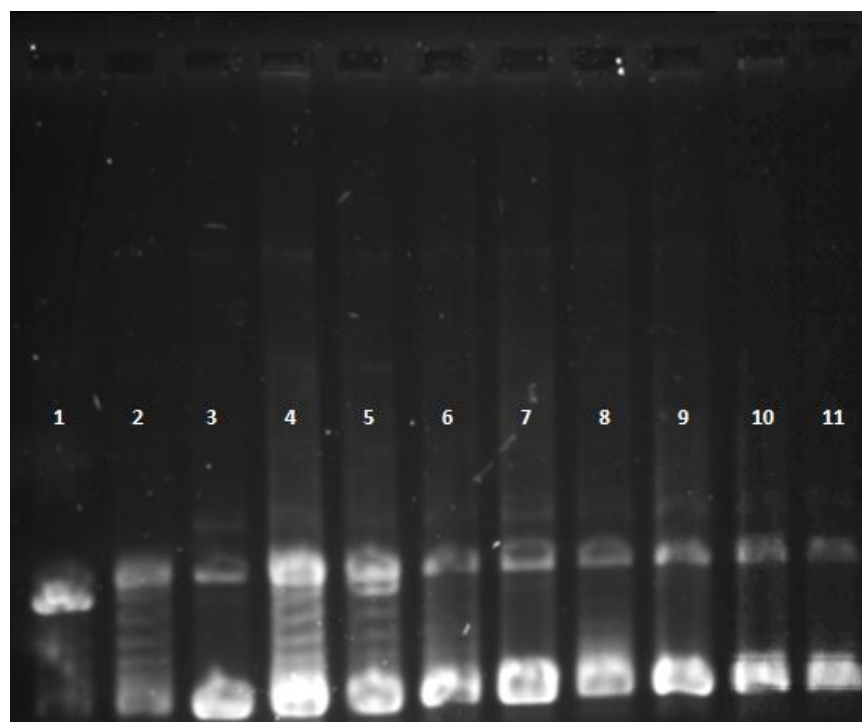


Figure 4.9 – 1. Linear DNA; 2. Plasmidic DNA + Topo-II without inhibitors (Topo-II positive); 3. Plasmidic DNA without Topo-II (Topo-II negative) (supercoiled); 4. DMSO; 5. RPMI 1640 medium; 6. QN42M; 7. CuQN42M; 8. NiQN42M; 9. CuQN21M; 10. CuFIN41M; 11. CuFIN41Ph. The concentration of the thiosemicarbazones used in this experiment was 50 μ M as required by the assay kit.

The third position is occupied by plasmidic DNA. In this experiment DMSO and RPMI 1640 medium were also tested to check if they can interfere with Topoisomerase II. The tested compounds are from lane 6 to lane 11. The concentration of thiosemicarbazones used in this experiment was 50 μ M according to the assay kit requirements.

4.5.2 Quinoline

All the compounds tested show activity against Topo-II isomerase exhibit inhibition of Topo-II isomerase. The most active ones are the copper thiosemicarbazones with methyl on N4. Ligands alone and nickel complex show inhibition but not at the same level of the other two, this can be seen looking at the electrophoresis. In fact in lanes with NiQN42M (lane 8) and QN42M (lane 6) we can observe topoisomers due to an incomplete inhibition of the enzyme while in the two copper complex lanes the ladder is not present.

4.5.3 Isatin

To study how the difference in steric hindrance on N4 affect the activity we chose two copper complexes bearing on the terminal nitrogen a methyl and a phenyl group respectively. Despite substantial differences in the functionalization, both complexes showed high inhibition of Topo-II isomerase.

4.6 Conclusions

Several thiosemicarbazones of quinoline and isatin have been prepared and these compounds have been used to synthesize copper and nickel derivatives.

X-ray studies revealed that copper quinoline derivatives tend to be square planar with a M:L ratio of 1:1 and nickel complexes octahedral with stoichiometry M:L 1:2.

Part of these compounds, ligands and complexes, were tested on leukemic cell line U937 to study proliferation inhibition. The presence of a charged ligand negatively

influences the biological activity: in fact neither ligands alone nor their copper complexes resulted to be active.

As far as the other compounds are concerned, also in this case copper complexes are more active than the corresponding ligands and nickel derivatives.

Substitution of N4 influences the biological activity, in particular among all the prepared compounds. Thiosemicarbazones with a dimethylated terminal nitrogen showed higher activity.

Some of these compounds were also tested as topoisomerase-II α inhibitors. Noteworthy is the higher activity of copper complexes and the very low activity of the simple ligand allows to exclude the role of thiosemicarbazones as simple chelators. The fact that the also the nickel derivative is inactive suggests the need for a redox metal, such as copper, to make the inhibitor more effective.

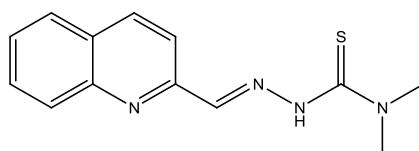
4.6 Experimental

TLC were performed on Silica gel Merck 60 F₂₅₄ aluminium sheets. Flash chromatography was performed on MP Silica 63-200 mesh 60Å (EchoChrom™), ¹H and NMR spectra were recorded on Bruker 300 Avance and Bruker 400 Avance spectrometers, at 300 K. The reported *J* values are referred to H,H coupling constants. Chemical shifts are reported as δ values in ppm using the solvent residual peak as internal standard. Elemental analysis were recorded on Flash 1112 Series Analyser (CE Instruments).

4.6.1 Syntheses of the quinoline-based ligands

[QN42M]

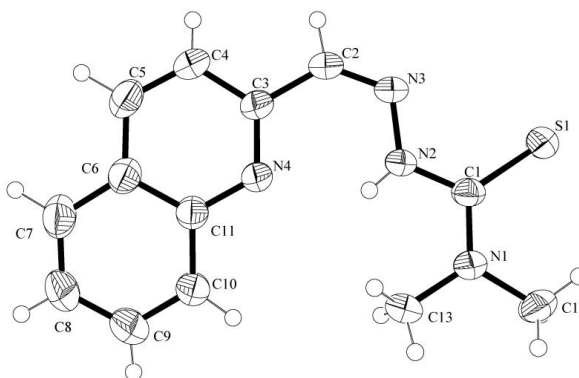
(N4-dimethyl-2-formylquinolinethiosemicarbazone)



To a stirred solution of 4,4-methyl-3-thiosemicarbazide (271 mg, 2.16 mmol) in methanol (60 ml) at r.t. was added formyl quinoline (351 mg, 2.16 mmol) and some drop of glacial acetic acid. After 1 h a precipitate appeared, the solution was stirred for 20 h then the solid was collected by filtration and washed with cold ethanol and dried.

Yield : 42%

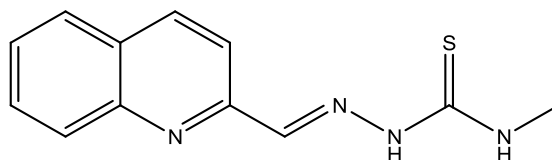
¹H NMR (330MHz, DMSO-*d*₆): δ_H (ppm) 8.67 (1H, m, CH arom.), 8.60 (2H, d, J = 8.7 Hz, NH₂), 8.39 (1H, d, J = 8.7 Hz, CH arom.), 8.02 (2H, m, CH arom.), 7.96 (1H, s, CH=N), 7.79 (1H, t, J = 7.5 Hz, CH arom.), 7.64 (1H, t, J = 7.5 Hz, CH arom.), 3.87 (3H, s, N-CH₃)



The X-ray structure was solved from data collected on a Siemens AED diffractometer. Cu-K α ($\lambda = 1.54178 \text{ \AA}$) The structure was solved by direct methods and refined using SHELXL97. The drawing was plotted using ORTEPIII. Crystal data: C₁₃H₁₄N₄S₁, Mr = 258.34, triclinic, space group P -1, a=9.3005(6), b=11.3588(7), c=6.3554(3) \AA , $\alpha=95.809(5)$ $\beta=96.883$ $\gamma=106.034(4)^\circ$, V=634.25(6) \AA^3 , Z=2, $\rho_{\text{calc}}=1.353 \text{ Mg m}^{-3}$, T=298.15 K, F(000)=272, crystal size=0.30x0.30x0.60 mm, index range = $0 < h < 11$, $-12 < k < 13$, $-7 < l < 7$, collected reflections =2396, unique reflections=2396, refined parameters=219, goodness-of-fit =1.214, final R index=0.0794, wR₂=0.2352, electronic density residues= 0.50 e -1.24 e\AA^{-3} .

[QN41M]

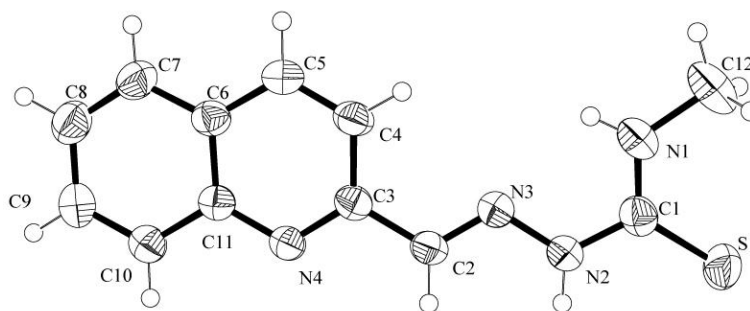
(N4-methyl-2-formylquinolinethiosemicarbazone)



To a stirred solution of 4,3-methyl-3-thiosemicarbazide (234.2 mg, 2.16 mmol) in ethanol (60 ml) at 0°C was added formyl quinoline (351 mg, 2.16 mmol) and some drop of glacial acetic acid. After 30' a precipitate appeared, the solution was stirred at r.t. for 24 h, then the solid was collected by filtration and washed with cold ethanol and dried. The compound was crystallized from acetonitrile.

Yield : 78%

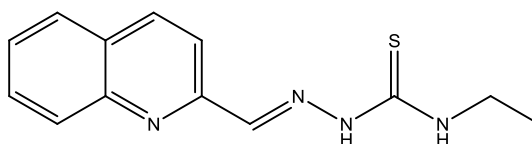
¹H NMR (330MHz, DMSO-*d*₆): δ_H (ppm) 11.87 (1H, s, C=N-NH), 8.81 (1H, q, J = 4.2 Hz, S=C-NH), 8.45 (1H, d, J = 8.7 Hz, CH arom.), 8.39 (1H, d, J = 8.7 Hz, CH arom.), 8.23 (1H, s, CH=N), 8.00 (2H, t, J = 7.5 Hz, CH arom.), 7.78 (1H, t, J = 7.8 Hz, CH arom.), 7.62 (1H, t, J = 7.5 Hz, CH arom.), 3.07 (3H, d, J = 4.5 Hz, NH-CH₃).



The X-ray structure was solved from data collected on a Siemens AED diffractometer. Cu-K α ($\lambda = 1.54178 \text{ \AA}$) The structure was solved by direct methods and refined using SHELXL97. The drawing was plotted using ORTEPIII. Crystal data: C₁₂H₁₂N₄S₁, Mr =244.32, orthorhombic, space group P 21 21 21, a=16.0279(6), b=10.1013(4), c=7.5821(3) \AA , $\alpha=90.00$ $\beta=90.00$ $\gamma=90.00$ $^\circ$, V=1227.56(8) \AA^3 , Z=4, $\rho_{\text{calc}}=1.322 \text{ Mg m}^{-3}$, T=298.15 K, F(000)=512, crystal size =0.50x0.50x0.70 mm, index range = $0 < h < 15$, $-10 < k < 10$, $0 < l < 8$, collected reflections =1221, unique reflections=1221, refined parameters=154, goodness-of-fit =1.351, final R index=0.1353, wR2= 0.2336, electronic density residues= 0.78 e -1.22 e\AA^{-3} .

[QN41E]

(N4-ethyl-2-formylquinolinethiosemicarbazone)



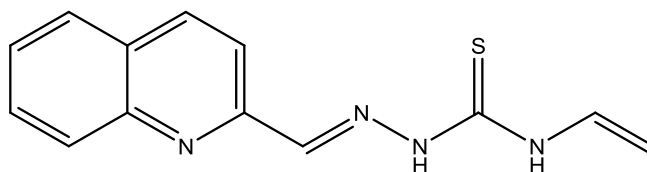
To a stirred solution of 4,3-methyl-3-thiosemicarbazide (234.2 mg, 2.16 mmol) in ethanol (60 ml) at 0°C was added formyl quinoline (351 mg, 2.16 mmol) and some drop of glacial acetic acid. After 30' a precipitate appeared, the solution was stirred at r.t. for 24 h, then the solid was collected by filtration and washed with cold ethanol and dried. The compound was crystallized from acetonitrile.

Yield : 42%

¹H NMR (330MHz, DMSO-*d*₆): δ_H (ppm) 11.82 (1H, s, C=N-NH), 8.87 (1H, t, J = 5.7 Hz, S=C-NH), 8.46 (1H, d, J = 8.7 Hz, CH arom.), 8.40 (1H, d, J = 8.7 Hz, CH arom.), 8.24 (1H, s, CH=N), 8.01 (2H, m, CH arom.), 7.78 (1H, t, J = 7.8 Hz, CH arom.), 7.63 (1H, t, J = 7.2 Hz, CH arom.), 3.65 (2H, m, NH-CH₂CH₃), 1.19 (3H, t, J = 7.2 Hz, NH-CH₂CH₃).

[QN41A1]

(N4-allyl-2-formylquinolinethiosemicarbazone)



To a stirred solution of 4,3-methyl-3-thiosemicarbazide (234.2 mg, 2.16 mmol) in ethanol (60 ml) at 0°C was added formyl quinoline (351 mg, 2.16 mmol) and some drop of glacial acetic acid. After 30' a precipitate appeared, the solution was stirred at r.t. for

24 h, then the solid was collected by filtration and washed with cold ethanol and dried.

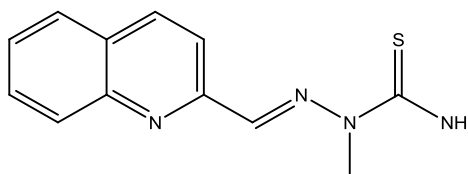
The compound was crystallized from acetonitrile.

Yield: 32%

¹H NMR (330MHz, DMSO-*d*₆): δ_H (ppm) 11.91 ppm (1H, s, C=N-NH), 9.02 ppm (1H, t, J = 6 Hz, NH-CH₂CH₃), 8.48 ppm (1H, d, J = 8.7 Hz, CH arom.), 8.39 ppm (1H, d, J = 8.7 Hz, CH arom.), 8.25 ppm (1H, s, CH=N), 8.01 ppm (2H, t, J = 7.5 Hz, CH arom.), 7.78 ppm (1H, t, J = 7.8 Hz, CH arom.), 7.63 ppm (1H, t, J = 7.5 Hz, CH arom.), 5.95 ppm (1H, m, NH-CH₂CH=CH₂), 5.17 ppm (2H, m, NH-CH₂CH=CH₂), 4.27 ppm (2H, t, J = 5.7 Hz, NH-CH₂CH=CH₂)

[QN21M]

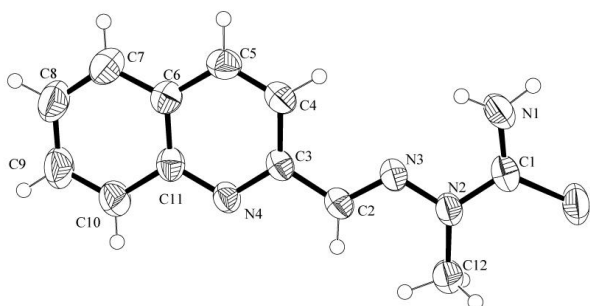
(N (2)-methyl-2-formylquinolinethiosemicarbazone)



To a stirred solution of 4,3-methyl-3-thiosemicarbazide (468 mg, 3.5 mmol) in ethanol (60 ml) at 0°C was added formyl quinoline (560.6 mg, 3.5 mmol) and some drop of glacial acetic acid. After 30' a precipitate appeared, the solution was stirred at r.t. for 24 h, then the solid was collected by filtration and washed with cold ethanol and dried. The compound was crystallized from acetonitrile.

Yield: 74%

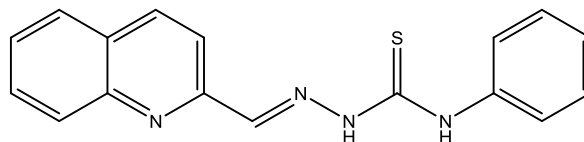
$^1\text{H NMR}$ (330MHz, $\text{DMSO-}d_6$): δ_{H} (ppm) 12.20 ppm (1H, s, C=N-NH), 10.39 (1H, s, S=C-NHPhe), 8.62 (1H, d, $J = 8.4$ Hz, CH arom.Quin), 8.40 (1H, d, $J = 8.7$ Hz, CH arom.Quin), 8.35 (1H, s, CH=N), 8.02 (2H, t, $J = 9$ Hz, CH arom.Quin), 7.79 (1H, t, $J = 7.5$ Hz, CH arom.Quin), 7.64 (1H, t, $J = 7.5$ Hz, CH arom.Quin), 7.57 (2H, d, $J = 8.1$ Hz, CH arom.Phe), 7.41 (2H, t, $J = 7.5$ Hz, CH arom.Phe), 7.26 (1H, t, $J = 7.5$ Hz, CH arom.Phe)



The X-ray structure was solved from data collected on a Siemens AED diffractometer. Cu-K α ($\lambda = 1.54178$ Å) The structure was solved by direct methods and refined using SHELXL97. The drawing was plotted using ORTEPIII. Crystal data: $\text{C}_{12}\text{H}_{12}\text{N}_4\text{S}_1$, $M_r = 244.32$, monoclinic, space group $P 2_1/n$, $a=10.3280(8)$, $b=10.713(2)$, $c=11.0160(10)$ Å, $\alpha=90.00$ $\beta=95.600(7)$ $\gamma=90.00$ °, $V=1213.0(3)$ Å 3 , $Z=4$, $\rho_{\text{calc}}=1.338$ Mg m^{-3} , $T=298.15$ K, $F(000)=512$, crystal size = $0.40 \times 0.40 \times 0.40$ mm, index range = $-12 < h < 12$, $0 < k < 13$, $0 < l < 13$, collected reflections = 2410, unique reflections = 2294, refined parameters = 154, goodness-of-fit = 1.175, final R index = 0.1128, $wR_2 = 0.2640$, electronic density residues = $0.59 \text{ e} - 1.00 \text{ e} \text{ \AA}^{-3}$.

[QN41Ph]

(N4-phenyl-2-formylquinolinethiosemicarbazone)



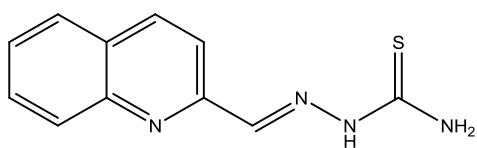
To a stirred solution of 4,3-methyl-3-thiosemicarbazide (412.5 mg, 3.9 mmol) in ethanol (60 ml) at 0°C was added formyl quinoline (616.5 mg, 3.9 mmol) and some drop of glacial acetic acid. After 30' a precipitate appeared, the solution was stirred at r.t. for 24 h, then the solid was collected by filtration and washed with cold ethanol and dried. The compound was crystallized from acetonitrile.

Yield: 52%

¹H NMR (330MHz, DMSO-*d*₆): δ_H (ppm) 8.67 (1H, m, CH arom.), 8.60 (2H, d, J = 8.7 Hz, NH₂), 8.39 (1H, d, J = 8.7 Hz, CH arom.), 8.02 (2H, m, CH arom.), 7.96 (1H, s, CH=N), 7.79 (1H, t, J = 7.5 Hz, CH arom.), 7.64 (1H, t, J = 7.5 Hz, CH arom.), 3.87 (3H, s, N-CH₃)

[QN42H]

(2-formylquinolinethiosemicarbazone)



To a stirred solution of 4,3-methyl-3-thiosemicarbazide (337.6 mg, 3.7 mmol) in ethanol (60 ml) at 0°C was added formyl quinoline (582.1 mg, 3.7 mmol) and some drop of glacial acetic acid. After 30' a precipitate appeared, the solution was stirred at r.t. for 24 h, then the solid was collected by filtration and washed with cold ethanol and dried. The compound was crystallized from acetonitrile.

Yield: 77%

¹H NMR (330MHz, DMSO-*d*₆): δ_H (ppm) 8.67 (1H, m, CH arom.), 8.60 (2H, d, J = 8.7 Hz, NH₂), 8.39 (1H, d, J = 8.7 Hz, CH arom.), 8.02 (2H, m, CH arom.), 7.96 (1H, s, CH=N), 7.79 (1H, t, J = 7.5 Hz, CH arom.), 7.64 (1H, t, J = 7.5 Hz, CH arom.), 3.87 (3H, s, N-CH₃)

4.7.2 Syntheses of the quinoline-based complexes

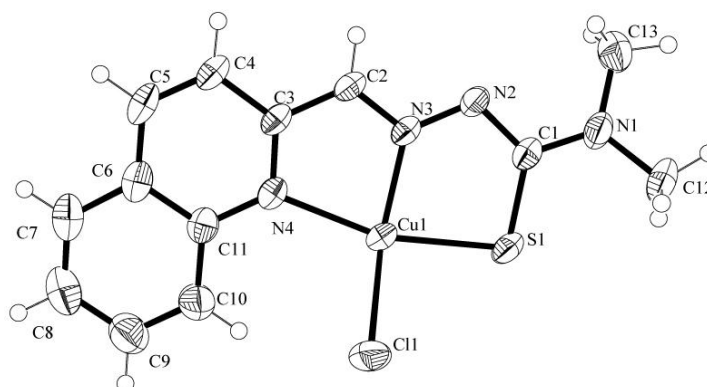
CuQN42M

[Cu(QN42M)Cl]

To a stirred solution of QN42M (0.62 mg, 0.23 mmol) in hot ethanol (20mL) was added an equimolar quantity of CuCl₂·2H₂O (0.40 mg, 0.23 mmol). The solution became immediately dark and a precipitate appeared. Stirring was continued for 2h under reflux then the solution was cooled at r.t and the precipitate collected by filtration and crystallized from ethanol

Yield: 46%

Elem. An. C₁₃H₁₃ClCuN₄S, C, 48.78%; H, 3.68%; N, 15.72%; found C, 43.41%; H, 3.43%; N, 17.35%



The X-ray structure was solved from data collected on a Bruker-Siemens SMART AXS 1000 diffractometer equipped with a CCD detector. Mo-K α ($\lambda = 0.71069 \text{ \AA}$) The structure was solved by direct methods and refined using SHELXL97. The drawing was

plotted using ORTEPIII. Crystal data: $C_{13}H_{13}Cl_1Cu_1N_4S_1$, $M_r = 356.32$, monoclinic, space group P 21/a, $a=8.443(2)$, $b=19.779(5)$, $c=8.638(2)$ Å, $\alpha=90.00$ $\beta=101.778(3)$ $\gamma=90.00$ °, $V=1412.1(6)$ Å³, $Z=4$, $\rho_{\text{calc}}=1.676$ Mgm⁻³, $T=298.15$ K, $F(000)=724$, crystal size =0.30x0.50x0.60 mm, index range = $-11 < h < 11$, $-27 < k < 27$, $-12 < l < 12$, collected reflections =18792, unique reflections=4055, refined parameters=181, goodness-of-fit =0.737, final R index=0.0747, $wR_2= 0.1651$, electronic density residues= 0.96 e -0.96 eÅ⁻³.

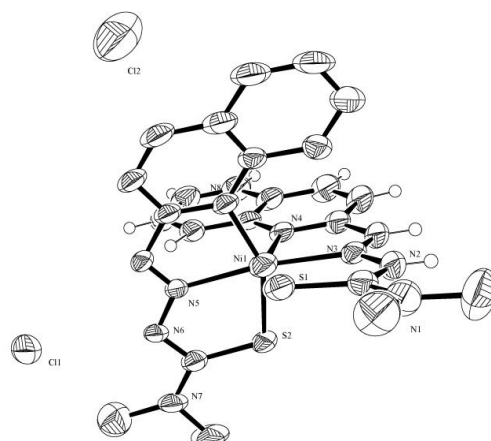
NiQN42M



To a stirred solution of QN42M (0.44 mg, 0.17 mmol) in hot methanol (35mL) was added an equimolar quantity of NiCl₂·6H₂O (0.41 mg, 0.17 mmol). The solution turn immediately to dark orange. Stirring was continued for 5h under reflux then the solution was cooled to r.t. After slow solvent evaporation a microcrystalline orange-brown solid was obtained which was recrystallized from methanol/ethanol (1:1)

Yield: 56%

Elem. An. $C_{26}H_{28}Cl_2 N_8NiS_2$, C, 48.32%; H, 4.38%; N, 17.33%; found C, 16.54%; H, 4.86%; N, 5.86%



The X-ray structure was solved from data collected on a Siemens AED diffractometer. Cu-K α ($\lambda = 1.54178 \text{ \AA}$) The structure was solved by direct methods and refined using SHELXL97. The drawing was plotted using ORTEPIII. Crystal data: C₂₆H₂₈Cl₂N₈Ni₁S₂, Mr =646.29, triclinic, space group P -1, a=9.8780(7), b=12.4010(8), c=12.8510(6) \AA , α =87.750(3) β =76.814(5) γ =74.760(5) $^\circ$, V=1478.45(16) \AA^3 , Z=2, ρ_{calc} =1.452 Mg m^{-3} , T=298.15 K, F(000)=668, crystal size =0.30x0.40x0.40 mm, index range = $0 < h < 12$, $-15 < k < 15$, $0 < l < 15$, collected reflections =5591, unique reflections=5591, refined parameters=348, goodness-of-fit =1.736, final R index=0.1443, wR₂= 0.3670, electronic density residues= 2.23 e -3.60 e\AA^{-3} .

CuQN41M

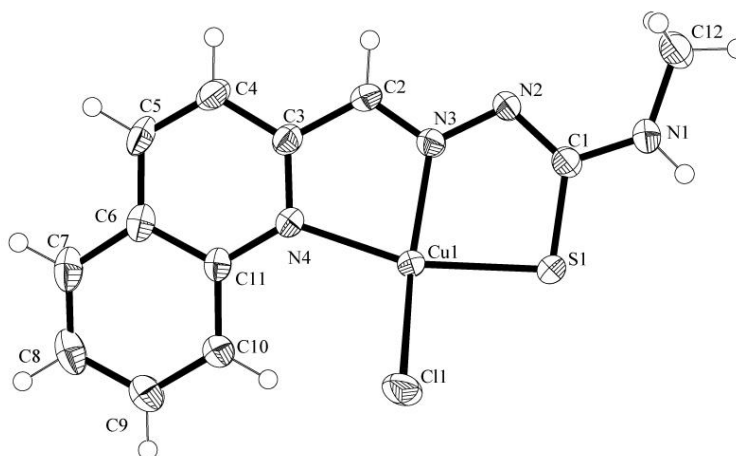
[Cu(QN41M)Cl]

To a stirred solution of QN41M (0.45 mg, 0.19 mmol) in hot acetonitrile (50mL) was added an equimolar quantity of CuCl₂·2H₂O (0.31 mg, 0.19 mmol). The solution

became immediately green and a precipitate appeared. Stirring was continued for 2h under reflux then the solution was cooled at r.t and the precipitate collected by filtration, the filtrate washed with acetonitrile and crystallized from ethanol/acetonitrile (1:2)

Yield: 39%

Elem. An. $C_{12}H_{11}ClCuN_4S$, C, 37.99%; H, 3.98%; N, 14.77%; found C, 38.21%; H, 3.84%; N, 14.64%



The X-ray structure was solved from data collected on a Siemens AED diffractometer. Cu-K α ($\lambda = 1.54178 \text{ \AA}$) The structure was solved by direct methods and refined using SHELXL97. The drawing was plotted using ORTEPIII. Crystal data: $C_{12}H_{11}ClCuN_4S$, Mr = 342.30, monoclinic, space group P 2 $_1$ /n, a=9.7210(5), b=10.1550(10), c=13.0880(10) \AA , $\alpha=90.00$ $\beta=103.410(7)$ $\gamma=90.00$ $^\circ$, V=1256.78(17) \AA^3 , Z=4, $\rho_{\text{calc}}=1.809 \text{ Mgm}^{-3}$, T=298.15 K, F(000)=692, crystal size=0.40x0.40x0.50 mm, index range = $0 < h < 11$, $-11 < k < 11$, $-15 < l < 15$, collected reflections =2460, unique reflections=2361, refined parameters=172, goodness-of-fit =1.035, final R index=0.0399, wR2=0.1058, electronic density residues= 0.52 e $-0.68 \text{ e}\text{\AA}^{-3}$.

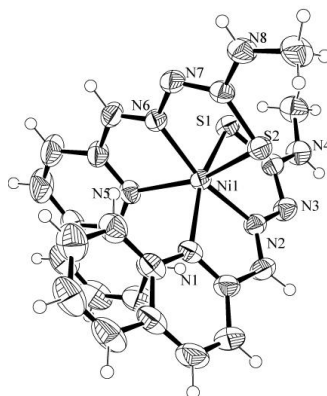
NiQN41M



To a stirred solution of QN41M (0.65 mg, 0.26 mmol) in hot ethanol (50mL) was added an equimolar quantity of $\text{NiCl}_2 \cdot 6\text{H}_2\text{O}$ (0.59 mg, 0.26 mmol). The solution turned immediately to dark red. Stirring was continued for 2h under reflux then the solution was cooled to r.t. After slow solvent evaporation a microcrystalline orange-brown solid was obtained which was recrystallized from methanol/ethanol (1:1).

Yield: 51%

Elem. An. $\text{C}_{26}\text{H}_{28}\text{Cl}_2\text{N}_8\text{NiS}_2$, C, 52.84%; H, 4.06%; N, 20.54%; found C, 44.64%; H, 3.84%; N, 16.76%



The X-ray structure was solved from data collected on a Bruker-Siemens SMART AXS 1000 diffractometer equipped with a CCD detector. Mo-K α ($\lambda = 0.71069 \text{ \AA}$) The structure was solved by direct methods and refined using SHELXL97. The drawing was plotted using ORTEPIII. Crystal data: $\text{C}_{24}\text{H}_{22}\text{N}_8\text{NiS}_2$, Mr=545.33, monoclinic, space group $P 2_1/c$, $a=16.3250(8)$, $b=9.8130(5)$, $c=16.5410(8) \text{ \AA}$, $\alpha=90.00$

$\beta=108.4460(10)$ $\gamma=90.00^\circ$, $V=2513.7(2)$ \AA^3 , $Z=4$, $\rho_{\text{calc}}=1.441$ Mgm^{-3} , $T=298.15$ K, $F(000)=1128$, crystal size = $0.50 \times 0.60 \times 0.60$ mm, index range = $-24 < h < 24$, $-14 < k < 14$, $-24 < l < 24$, collected reflections = 40762, unique reflections = 8305, refined parameters = 316, goodness-of-fit = 1.033, final R index = 0.0487, $wR_2 = 0.1140$, electronic density residues = 1.37 e -0.21 e \AA^{-3} .

CuQN41E

[Cu(QN41E)Cl]

To a stirred solution of QN41E (0.63 mg, 0.25 mmol) in hot methanol (50 mL) was added an equimolar quantity of $\text{CuCl}_2 \cdot 2\text{H}_2\text{O}$ (0.41 mg, 0.25 mmol). The solution became immediately dark green and a precipitate appeared. Stirring was continued for 2 h under reflux then the solution was cooled at r.t and the green precipitate collected by filtration, washed with methanol

Yield: 74%

Elem. An. $\text{C}_{13}\text{H}_{13}\text{ClCuN}_4\text{S}$, C, 39.80%; H, 4.37%; N, 14.28%; found C, 39.57%; H, 4.08%; N, 13.69%

NiQN41M



To a stirred solution of QN41E (0.57 mg, 0.22 mmol) in hot methanol (50mL) was added an equimolar quantity of NiCl₂·6H₂O (0.59 mg, 0.26 mmol). The solution turned immediately to dark red. Stirring was continued for 5h under reflux then the solution was cooled to r.t. After slow solvent evaporation a microcrystalline orange-brown solid was obtained.

Yield: 41%

Elem. An. C₂₆H₂₈N₈NiS₂, C, 54.46%; H, 4.57%; N, 19.54%; found C, 35.87%; H, 4.55%; N, 12.66%

CuQN41Al



To a stirred solution of QN41Al (0.76 mg, 0.28 mmol) in hot acetonitrile (30mL) was added an equimolar quantity of CuCl₂·2H₂O (0.48 mg, 0.28 mmol). The solution became immediately dark green and a precipitate appeared. Stirring was continued for 5h under reflux then the solution was cooled at r.t and the dark red precipitate collected by filtration, washed with acetonitrile.

Yield: 42%

Elem. An. $C_{14}H_{13}ClCuN_4S$, C, 38.21%; H, 4.81%; N, 12.73%; found C, 37.97%; H, 3.15%; N, 12.34%

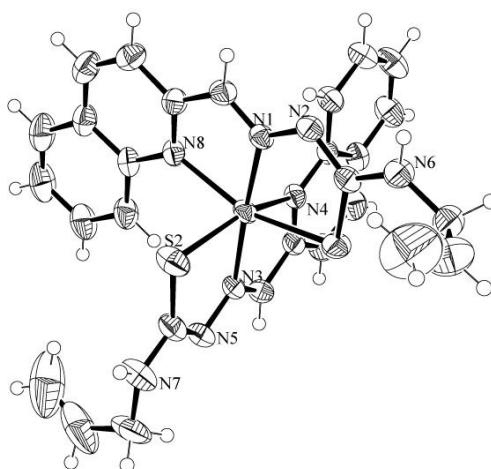
NiQN41AI



To a stirred solution of QN41AI (0.62 mg, 0.23 mmol) in methanol (50mL) was added an equimolar quantity of $NiCl_2 \cdot 6H_2O$ (0.55 mg, 0.23 mmol). The solution turn immediately to dark red. The solution was then refluxed for 5h then cooled to r.t. After slow solvent evaporation a microcrystalline orange-brown solid was obtained, which was recrystallized from methanol

Yield: 41%

Elem. An. $C_{26}H_{28}N_8NiS_2$, C, 54.46%; H, 4.57%; N, 19.54%; found C, 35.87%; H, 4.55%; N, 12.66%



The X-ray structure was solved from data collected on a Bruker-Siemens SMART AXS 1000 diffractometer equipped with a CCD detector. Mo-K α ($\lambda = 0.71069 \text{ \AA}$) The structure was solved by direct methods and refined using SHELXL97. The drawing was plotted using ORTEPIII. Crystal data: C₂₈H₂₈N₈Ni₁O₁S₂, Mr=615.41, triclinic, space group P -1, a=10.3360(13) b=11.9400(14) c=13.3360(16) \AA , α =105.9110(18) β =108.7620(18) γ =99.6060(19) $^\circ$, V=1438.7(3) \AA^3 , Z=2, ρ_{calc} =1.421 Mg m^{-3} , T=298.15 K, F(000)=640, crystal size =0.30x0.30x0.60 mm, index range = -14 < h < 14, -16 < k < 16, -18 < l < 18, collected reflections =22296, unique reflections=8333, refined parameters=360, goodness-of-fit =0.840, final R index=0.0738, wR₂= 0.1498, electronic density residues= 0.69 e -0.44 e \AA^{-3} .

CuQN41Ph

[Cu(QN41Ph)Cl]

To a stirred solution of QN41Ph (0.45 g, 0.15 mmol) in hot methanol (40mL) was added an equimolar quantity of CuCl₂·2H₂O (0.48 g, 0.15 mmol). The solution became immediately dark and a precipitate appeared. Stirring was continued for 4h under reflux then the solution was cooled at r.t and the dark red precipitate collected by filtration, washed with acetonitrile.

Yield: 68%

Elem. An. C₁₇H₁₃ClCuN₄S, C, 50.49%; H, 3.24%; N, 13.85%; found C, 49.89%; H, 3.22%; N, 13.67%

NiQN41Ph

[Ni(QN41Ph)₂]

To a stirred solution of QN41Ph (0.58 mg, 0.23 mmol) in methanol (80mL) were first added some drops of a solution of NaOH 1N and then an equimolar quantity of NiCl₂·6H₂O (0.45 g, 0.19 mmol). The solution turn immediately to dark red. The solution was then refluxed for 5h then cooled to r.t. After slow solvent evaporation a microcrystalline orange-brown solid was obtained.

Yield: 48%

Elem. An. C₃₄H₂₈N₈NiS₂, C, 61.00%; H, 3.91%; N, 16.74%; found C, 38.60%; H, 3.13%; N, 10.15%

CuQN21M

[Cu(QN21M)Cl]

To a stirred solution of QN21M (0.80 g, 0.33 mmol) in hot acetonitrile (70mL) was added an equimolar quantity of CuCl₂·2H₂O (0.56 g, 0.33 mmol). The solution became immediately dark green and a precipitate appeared. Stirring was continued for 6h under reflux then the solution was cooled at r.t and the dark red precipitate collected by filtration, washed with acetonitrile.

Yield: 42%

Elem. An. $C_{18}H_{16}ClCuN_4S$, C, 38.21%; H, 4.11%; N, 12.25%; found C, 38.21%; H, 3.78%; N, 12.56%

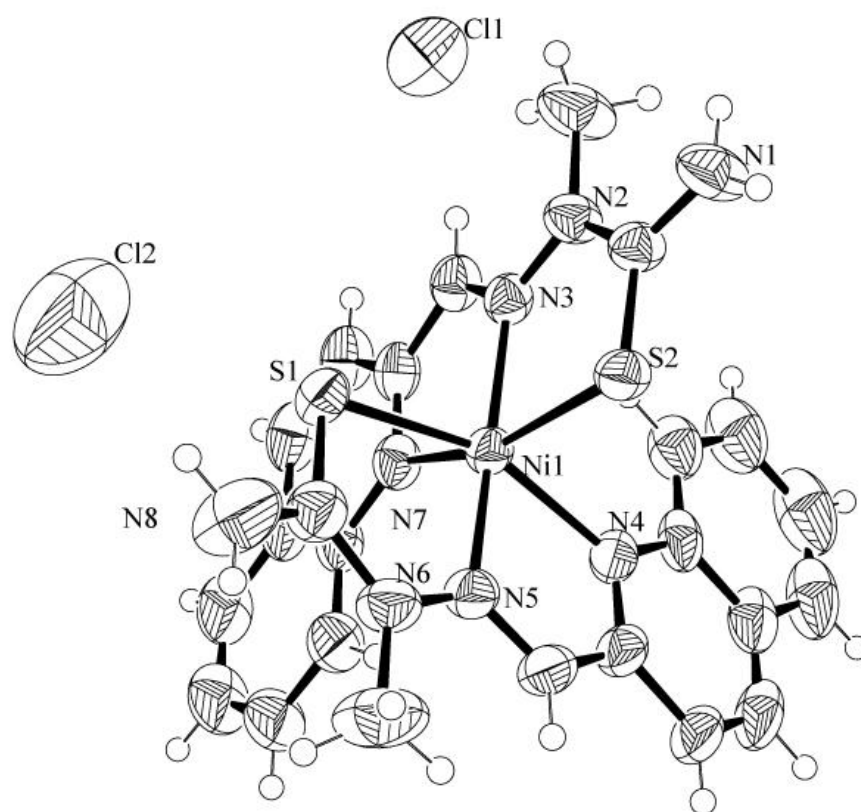
NiQN21M



To a stirred solution of QN41A1 (0.88 g, 0.23 mmol) in methanol (50mL) was added an equimolar quantity of $NiCl_2 \cdot 6H_2O$ (0.55 g, 0.23 mmol). The solution turn immediately to dark red. The solution was then refluxed for 20 h then cooled to r.t. After slow solvent evaporation a microcrystalline orange-brown solid was obtained, which was recrystallized from methanol

Yield: 41%

Elem. An. $C_{24}H_{23}N_8NiS_2$, C, 46.10%; H, 4.99%; N, 17.92%; found C, 28.14%; H, 4.82%; N, 10.53%



The X-ray structure was solved from data collected on a Bruker-Siemens SMART AXS 1000 diffractometer equipped with a CCD detector. Mo-K α ($\lambda = 0.71069 \text{ \AA}$) The structure was solved by direct methods and refined using SHELXL97. The drawing was plotted using ORTEPIII. Crystal data: C₂₄H₃₁Cl₂N₈Ni₁O_{3.5}S₂, Mr=625.26, monoclinic, space group C 2/c, a=24.5390(13) b=13.9800(8) c=19.4900(11) Å, $\alpha=90.00$ $\beta=113.1240(8)$ $\gamma=90.00$ °, V=6149.0(6)Å³, Z=4, $\rho_{\text{calc}}=0.675 \text{ Mg m}^{-3}$, T=298.15 K, F(000)=1300, crystal size =0.40x0.40x0.40 mm, index range = -30 < h < 30, -17 < k < 17, -24 < l < 24, collected reflections =36973, unique reflections=6320, refined parameters=402, goodness-of-fit =0.986, final R index=0.0681, wR₂= 0.1981, electronic density residues= 0.54 e -1.36 eÅ⁻³.

CuQN42H

[Cu(QN42H)Cl]

To a stirred solution of QN41Ph (0.104 g, 0.45 mmol) in hot acetonitrile (30mL) was added an equimolar quantity of CuCl₂·2H₂O (0.77 g, 0.45 mmol). The solution became immediately dark green and a precipitate appeared. Stirring was continued for 5h under reflux then the solution was cooled at r.t and the dark red precipitate collected by filtration, washed with acetonitrile.

Yield: 58%

Elem. An. C₁₄H₁₃ClCuN₄S·4H₂O, C, 38.21%; H, 4.81%; N, 12.73%; found C, 37.97%; H, 3.15%; N, 12.34%

NiQN42H

[Ni(QN42H)₂]

To a stirred solution of QN41Al (0.88 g, 0.38 mmol) in methanol (50mL) was added an equimolar quantity of NiCl₂·6H₂O (0.91 g, 0.38 mmol). The solution turn immediately to dark red. The solution was then refluxed for 5h then cooled to r.t. After slow solvent evaporation a microcrystalline orange-brown solid was obtained, which was recrystallized from methanol

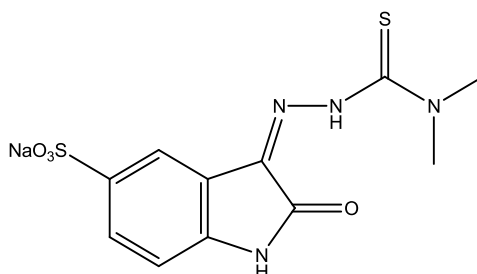
Yield: 44%

Elem. An. $C_{26}H_{28}N_8NiS_2$, C, 54.46%; H, 4.57%; N, 19.54%; found C, 35.87%; H, 4.55%; N, 12.66%

4.7.3 Syntheses of the isatin-based ligands

[ISN42M]

(1-(isatin 5'- sulfonic acid sodium salt)-4-(4'-dimethyl)-3-thiosemicarbazone)

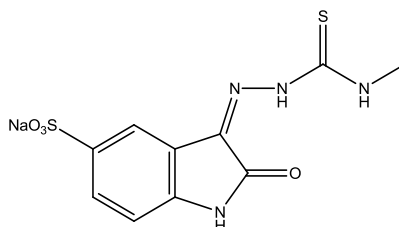


A stirred solution of 4,4 dimethyl-thiosemicarbazide (97.8 g, 0.8 mmol) and isatin-5-sulfonic acid sodium salt dehydrate (229.7 g, 0.8 mmol) in MeOH (100 mL) was refluxed for 24h. Solution was cooled to r.t. and poured into a crystallizer and the solvent was let slowly evaporate.

$^1\text{H NMR}$ (300MHz, $\text{DMSO-}d_6$): δ_{H} (ppm) 13.32 (s, 1H, *NHN*), 11.35 (s, 1H, *NH*), 7.75 (d, $J = 1.78$ Hz, 1H, *CHar*), 7.60 (dd, $J = 8.07, 1.78$ Hz, 1H, *CHar*), 6.90 (d, $J = 8.07$ Hz, 1H, *CHar*), 3.39 (s, 6H, CH_3).

[ISN41M]

(1-(isatin 5'- sulfonic acid sodium salt)-4-(4'-methyl)-3-thiosemicarbazone)



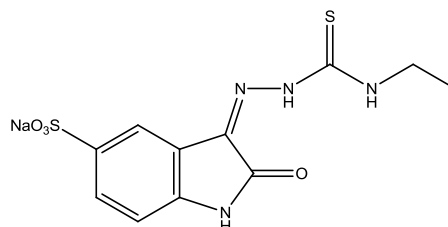
A stirred solution of 4-Methyl-thiosemicarbazide (130.4 g, 1.25mmol) and isatin-5-sulfonic acid sodium salt dihydrate (350g, 1.22mmol) in EtOH (50 mL) was refluxed for 16 h, during this time a precipitate appeared. After this time the solution was cooled at r.t. and filtered, the orange solid washed with EtOH several times and dried.

Yield: 80%

¹H NMR (300MHz, DMSO-*d*₆): δ_H (ppm) 12.55 (s, 1H), 9.43 (s, 1H), 8.01 (d, *J* = 1.38 Hz, 1H), 7.59 (s, 1H), 6.86 (d, *J* = 7.87 Hz, 1H), 3.07 (d, *J* = 4.55 Hz, 3H)

[ISN41E]

(1-(isatin 5'- sulfonic acid sodium salt)-4-(4'-ethyl)-3-thiosemicarbazone)



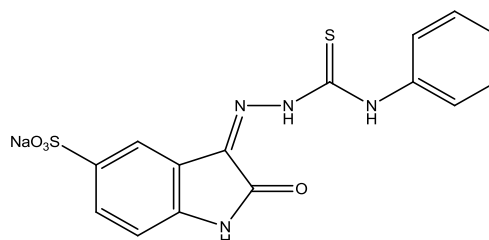
A solution of 4-ethyl thiosemicarbazide (258.4 g, 0.87 mmol) and isatin-5-sulfonic acid sodium salt dihydrate (250g, 0.87 mmol) in MeOH (150 mL) was cooled to 0°C and stirred for overnight. After that the solution was cooled at r.t., poured into a crystallizer and the solvent slowly evaporated to obtain yellow crystals which were harvested and recrystallized from EtOH/MeOH (3:1).

Yield: 76.4%

¹H NMR (300MHz, DMSO-*d*₆): δ_H (ppm) 12.53 (s, 1H, *NH*), 11.29 (s, 1H *NH*), 9.50 (m, 1H, *NH*), 8.02 (m, 1H, *CHar*), 7.57 (m, 1H, *CHar*), 6.87 (d, 1H, *CHar*), 3.67 (d, *J* = 7.28 Hz, 2H, *CH*₂*CH*₃), 1.18 (m, 3H, *CH*₃).

[ISN41Ph]

(1-(isatin 5'- sulfonic acid sodium salt)-4-(4'-phenyl)-3-thiosemicarbazone)



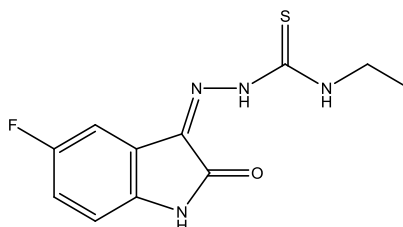
A solution of 4-phenyl thiosemicarbazide (118.6 g, 0.87 mmol) and isatin-5-sulfonic acid sodium salt dihydrate (250g, 0.87 mmol) in MeOH (150 mL) was cooled to 0°C and stirred for overnight. After that the solution was cooled at r.t., poured into a crystallizer and the solvent slowly evaporated to obtain yellow crystals which were harvested and recrystallized from EtOH/MeOH (3:1).

Yield: 76.4%

¹H NMR (300MHz, DMSO-*d*₆): δ_H (ppm) 12.79 (s, 1H, *NH*), 11.39 (d, 1H *NH*), 11.02 (m, 1H, *NH*), 8.23 (d, Arom), 7.72-7.63 (m, Arom), 7.54-7.47 (dd, Arom), 7.42-7.33 (m, Arom), 7.29-7.24 (m, Arom), 6.89-6.87 (m, Arom).

[IFN41E]

(1-(5'-fluoro isatin)-4-(4'-ethyl)-3-thiosemicarbazone)



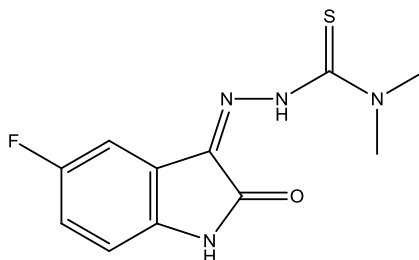
A stirred solution of 4-ethyl thiosemicarbazide (258.4 g, 2.16 mmol) and 5-fluoro isatin (254g, 2.16 mmol) in MeOH (150 mL) was refluxed for 6h. After that the solution was cooled at r.t., poured into a crystallizer and the solvent slowly evaporated to obtain yellow crystals which were harvested and recrystallized from EtOH/MeOH (3:1).

Yeld: 76.4%

$^1\text{H NMR}$ (300MHz, DMSO- d_6): δ_{H} (ppm) 12.46 (s, 1H, NH), 11.22 (s, 1H NH), 9.37 (m, 1H, NH), 7.50 (m, 1H, CHar), 7.25 (m, 1H, CHar), 6.95 (d, $J = 4.16$ Hz, 1H, CHar), 3.92 (d, $J = 7.28$ Hz, 2H, CH_2CH_3), 1.18 (m, 3H, CH_3).

[IFN42M]

(1-(5'-fluoro isatin)-4-(4'-dimethyl)-3-thiosemicarbazone)



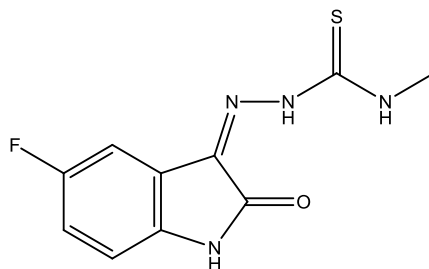
A stirred solution of 4,4-methyl thiosemicarbazide (181 g, 1.51 mmol) and 5-fluoro isatin (250.4g, 1.51 mmol) in MeOH (125 mL) was refluxed for 24h cooled at r.t., poured into a crystallizer and the solvent slowly evaporated to obtain orange crystals which were harvested and recrystallized from EtOH/MeOH (3:1).

Yield: 87.2%

¹H NMR (300MHz, DMSO-*d*₆): δ_H (ppm) 13.41 (s, 1H, *NH*), 11.33 (s, 1H *NH*), 7.36 (dd, *J* = 8.16, 2.58 Hz, 1H, *CHar*), 7.21 (m, 1H, *CHar*), 6.96 (dd, *J* = 8.7, 4.19 Hz, 1H, *CHar*), 3.39 (s, 6H, 2CH₃)

[IFN41M]

(1-(5'-fluoro isatin)-4-(4'-methyl)-3-thiosemicarbazone)



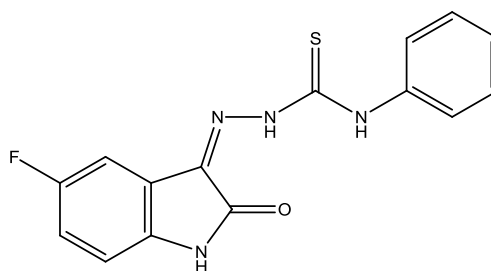
A solution of 4-methy-thiosemicarbazide (350 g, 3.22 mmol) and 5-fluoro isatin (391.9 g, 3.22 mmol) in EtOH (70 mL) was cooled to 0°C and stirred 24 h

Yield:

¹H NMR (300MHz, DMSO-*d*₆): δ_H (ppm) 12.50 (s, 1H, *NH*), 9.33 (bm, 1H, *NHCH*₃), 7.45 (dd, *J* = 8.25, 2.74 Hz, 1H, *CHar*), 7.20 (m, 1H, *CHar*), 6.93 (dd, *J* = 8.25, 4.30 Hz, 1H, *CHar*), 3.09 (d, *J* = 4.05 Hz, 3H, CH₃)

[IFN42Ph]

(1-(5'-fluoro isatin)-4-(4'-phenyl)-3-thiosemicarbazone)



A solution of 4-methy-thiosemicarbazide (206.7 g, 1.22 mmol) and 5-fluoro isatin (201.6 g, 1.22 mmol) in EtOH (75 mL) was cooled to 0°C and stirred 24 h, during that time a yellow precipitate appeared. After 24 h the precipitate was collected by filtration and washed with MeOH.

Yield: 51%

¹H NMR (300MHz, DMSO-*d*₆): δ_H (ppm) 12.77 (s, 1H, *NH*), 11.31 (s, 1H, *NH*), 11.05 (s, 1H, *NH*), 8.14 (d, *J* = 1.44 Hz, 1H), 7.63 (dd, *J* = 8.10, 1.73 Hz, 1H), 7.58 (dd, *J* = 8.43, 1.03 Hz, 2H), 7.42 (m, 2H), 7.27 (m, 1H)

4.7.4 Syntheses of the isatin-based complexes

CuIFN41M

[Cu(IFN41M)Cl]

A solution of IFN41M (0.09 g, 0.35 mmol) and CuCl₂·2H₂O (61.02 g, 0.35 mmol) in MeOH (55 mL) was refluxed for 2 h. During the reaction time a dark green solid appeared. The precipitate was collected by filtration.

Yield: 74%

Elemental analysis : calcd. for C₁₀H₈ClCuFN₄OS C, 34.29%; H, 2.30%; N, 16.10%, found C, 35.11%; H, 2.33%; N, 16.06%,

CuISN41M

[Cu(ISN41M)Cl]

A solution of ISN41M (0.10 g, 0.32 mmol) and CuCl₂·2H₂O (0.05 g, 0.32 mmol) in MeOH (50 mL) was refluxed for 8 h. During that time a solid appeared. After that time the precipitate was collected by filtration, washed with methanol and dried.

Yield: 42%

Elemental analysis : calcd. for C₁₀H₈ClCuN₄NaO₄S₂, C, 27.57; H, 1.85; N, 12.87; found C, 27.85%; H, 2.11%; N, 12.50%

CuIFN41E

[Cu(IFN41E)Cl]

A stirred solution of IFN41E (0.074 g, 0.28 mmol) and CuCl₂·2H₂O (0.048 g, 0.28 mmol) in MeOH (50 mL) was refluxed for 8h, during which time a green solid precipitate appeared. After 8 h the solution was cooled to r.t. and the precipitate collected by filtration.

Yield: 59%

Elemental analysis : calcd. for C₁₁H₁₀ClCuFN₄OS₂, C, 36.27%; H, 2.77%; N, 15.38%; found C, 35.89%; H, 3.42%; N, 14.01%

Cu(ISN41E)

[Cu(ISN41E)Cl]

To a stirred solution of IFN41E (0.080 g, 0.22 mmol) in MeOH (50 mL) was added CuCl₂·2H₂O (0.038 g, 0.22 mmol). Then the solution was refluxed, during which time a green solid precipitate appeared. After 8 h the solution was cooled to r.t. and the precipitate collected by filtration.

Yield: 97%

Elemental analysis : calcd. for C₁₁H₁₀ClCuN₄NaO₄S₂, C, 29.47%; H, 2.25%; N, 12.50%;
found C, 28.34%; H, 2.47%; N, 11.49%

CuIFN41Ph

[Cu(IFN4Ph)Cl]

A stirred solution of IFN4Ar (0.052 g, 0.16 mmol) and CuCl₂·2H₂O (0.028 g, 0.16 mmol) in MeOH (50 mL) was refluxed for 8 h, during this period of time a brown/green precipitate appeared. After 8 h the precipitate was collected by filtration.

Yield: 39%

Elemental analysis : calcd. for C₁₅H₁₀ClCuFN₄OS, C, 43.69%; H, 2.44%; N, 13.59%;
found C, 43.67%; H, 2.34%; N, 13.26%

CuISN41Ph)

[Cu(ISN41Ph)Cl]

To a stirred solution of ISN4Ar (0.1 g, 0.56 mmol) in MeOH (50 mL) were added some drops of NaOH 5M monitoring the pH (8-9) after that was added CuCl₂·2H₂O (0.42 g, 0.56 mmol) and the colour turned dark. Then the solution was refluxed for 8 h, cooled to r.t. and poured into a crystallizer and the solvent slowly evaporate to obtain a red crystals.

Yield: 78.2

Elemental analysis : calcd. for C₁₅H₁₀ClCuN₄NaO₄S₂, C, 33.84%; H, 2.65%; N, 10.52%;
found C, 30.58%; H, 2.67%; N, 8.74 %

CuIFN42M

[Cu(IFN42M)Cl]

To a stirred solution of IFN42M (0.071 g, 0.26 mmol) in MeOH (50 mL) were added some drops of NaOH 5M monitoring the pH (8-9) after that was added CuCl₂·2H₂O (0.044 g, 0.26 mmol) and the colour turned dark. Then the solution was refluxed for 8 h, cooled to r.t. and the precipitate collected by filtration.

Yield: 18.3%

Elemental analysis : calcd. for $C_{11}H_{10}ClCuFN_4OS$, C, 36.27%; H, 2.77%; N, 15.38%;
found C, 36.17%; H, 2.68%; N, 14.93%

CuISN42M

[Cu(ISN42M)Cl]

To a stirred solution of ISN42M (0.058 g, 0.15 mmol) in MeOH (50 mL) were added some drops of NaOH 5M monitoring the pH (8-9) after that was added $CuCl_2 \cdot 2H_2O$ (0.026 g, 0.15 mmol) and the colour turned red-orange. Then the solution was refluxed for 8 h, cooled to r.t., poured into a crystallizer and the solvent slowly evaporated.

Yield: 53%

Elemental analysis : calcd. for $C_{11}H_{10}ClCuNaN_4O_4S_2$, C, 36.27%; H, 2.77%; N, 15.38%;
found C, 36.17%; H, 2.68%; N, 14.93%

4.8 References

- 1) McClendon A.K., Osheroff N., *Mutation Research*, **2007**,623(1-2), 83-97
- 2) Gellert, M.A. *Rev. Biochem.* **1981**, 50, 879-910
- 3) Berger J. M., Gamblin S.J., Harrison S.C., Wang J.C. *Nature* **1996**, 379, 225-232
- 4) Brown P.O., Cozzarelli N.R., *Science*, **1979**, 206, 1081-1083
- 5) Liu L. F., Alberts B.M., *Cell*, **1980**, 19, 697-707
- 6) Liu, L. F. *Annu. Rev. Biochem.* **1989**, 58, 351–375.
- 7) Nitiss J.L. *Nature Reviews*, **2009**, 9, 338-350
- 8) Chen, G. L. *et al. J. Biol. Chem.* **1984**, 259, 13560–13566.
- 9) Lehmann M., de Souza Prudente Vilar K., Franco A., Reguly M. L., Rodriguez de Andreade H.H., *Environmental and Molecular Mutagenesis*, **2004**, 43, 250-257
- 10) Maxwell A., *Trends in microbiology*, **1997**, 5(3), 102-109
- 11) Larsen A.K., Escargueil A. E., Skladanowski A. *Pharmacology & Therapeutics*, **2003**, 99, 167-181
- 12) Bromberg D. K., Burgin A.B., Osheroff *J. Biol. Chem.*, **2003**, 278(9), 7406-7412
- 13) Lihui W. *et al. The Journal of Nuclear Medicine* **2006**, 47(12), 2034
- 14) Easmon J, Puerstinger G, Heinisch G, *et al. J. Med. Chem.* **2001**, 44, 2164–2171.
- 15) Easmon J, Puerstinger G, Roth T, *et al. Int. J. Cancer.* **2001**, 94, 89–96.
- 16) Rao, V. A.; Klein, S. R.; Agama, K. K.; Toyoda, E.; Adachi, N.; Pommier, Y.; Shacter, E. B, *Cancer Res.* **2009**, 69 (3), 948–957.

- 17) Huang, H.; Chen, W.; Ku, X.; Meng, L.; Lin, L.; Wang, X.; Zhu, C.; Wang, Y.;
Chen, Z.; Li, M.; Jiang, H.; Chen, K.; Ding, J.; Liu, H. *J. Med. Chem.* **2010**, *53*,
3048–3064.
- 18) Zeglis B.M., Divilov V. and Lewis J.L., *J. Med. Chem.* **2011**, *54*, 2391–2398
- 19) Wei L., Easmon J., Nagi R.K., Muegge B.D., Meyer L.A. and Lewis J.L., *J.*
Nucl. Med. **2006**, *47*, 2034–2041
- 20) Matthew D. Hall, *et al. J. Med. Chem.* **2009**, *52*, 3191–3204.

Acknowledgments

I wish to thank prof. P. Tarasconi, prof. G. Pelosi, prof. F. Bisceglie and prof. M. Belicchi Ferrari, for their kindness and assistance, dr. Silvana Pinelli, dr. Rossella Alinovi, prof. Annamaria Buschini, dr. Francesca Mussi, dr. Susanna Franzoni, dr. Barbara Montali for the biological experiments. The lab mates Anastasia, Cecilia, Simone, Francesco, Erica, Chiara Chiara, Gianluca and Maria Chiara a.k.a. Mary. The super-technicians Beppe & Marco that eventually will be happy for the conclusion of my doctoral period and last but not least my family for their support in these years.